# Integrated optimal design for hybrid electric vehicles

*Document status and date:*
Published: 30/11/2015

*Document Version:*
Publisher's PDF, also known as Version of Record (includes final page, issue and volume numbers)

*Please check the document version of this publication:*

• A submitted manuscript is the version of the article upon submission and before peer-review. There can be important differences between the submitted version and the official published version of record. People interested in the research are advised to contact the author for the final version of the publication, or visit the DOI to the publisher's website.
• The final author version and the galley proof are versions of the publication after peer review.
• The final published version features the final layout of the paper including the volume, issue and page numbers.

[Link to publication](#)

# Integrated

# Optimal Design

## for Hybrid Electric Vehicles

Emilia Silvaş

# Integrated Optimal Design for Hybrid Electric Vehicles

Emilia Silvaş

2015

Integrated Optimal Design for Hybrid Electric Vehicles *by* Emilia Silvaş - Eindhoven University of Technology 2015 - PhD Thesis.

# Integrated Optimal Design for Hybrid Electric Vehicles

PROEFSCHRIFT

door

Emilia Silvaş

geboren te Novaci, Roemenië

Dit proefschrift is goedgekeurd door de promotoren en de samenstelling van de promotiecommissie is als volgt:

| voorzitter: | prof. dr. L.P.H. de Goey | |
| promotor: | prof. dr. ir. M. Steinbuch | |
| co-promotor: | dr. ir. T. Hofman | |
| leden: | prof. dr. H. Peng | University of Michigan, USA |
| | prof. dr. B. Egardt | Chalmers University of Technology, SE |
| | prof. dr. ir. J. Hellendoorn | Delft University of Technology, NL |
| | ir. H. Voets | DAF Trucks N.V., NL |
| | prof. dr. M.G.J. van den Brand | |

NOTATION

# Abbreviations

| Abbreviation | Description | Reference |
|---|---|---|
| $CO_2$ | Carbon Dioxide | p. 1 |
| HD | Heavy Duty | p. 1 |
| HEV | Hybrid Electric Vehicle | p. 3 |
| OEM | Original Equipament Manufacturer | p. 3 |
| HIT | Hybrid Innovation in Trucks | p. 2 |
| EM | Electric Machine | p. 3 |
| EMS | Energy Management System | p. 5 |
| $NO_x$ | Nitric Oxide and Nitrogen Dioxide | p. 4 |
| PM | Particulate Matter | p. 4 |
| EPA | US Environmental Protection Agency | p. 5 |
| NEDC | New European Driving Cycle | p. 5 |
| BEV | Battery Electric Vehicle | p. 18 |
| SLD | System Level Design | p. 23 |
| FD | Finite Domains | p. 25 |
| ECMS | Equivalent Consumption Minimization Strategy | p. 27 |
| (S)DP | (Stochastic) Dynamic Programming | p. 27 |
| RB | Rule Based | p. 27 |
| MPC | Model Predictive Control | p. 27 |
| GA | Genetic Algorithms | p. 32 |
| CSP | Constraint Satisfaction Problem | p. 44 |
| PBS | Platform Based Design | p. 45 |
| BB | Branch and Bound | p. 53 |
| CLP | Constraint Logic Programming | p. 53 |
| TPM | Transition Probability Matrix | p. 95 |
| MCMC | Markov Chain Monte Carlo technique | p. 99 |

# Symbols

| Symbols | Description | Reference |
|---|---|---|
| T | Topology | p. 25 |
| V | Vertex / node | p. 22 |
| E | Edge | p. 22 |
| **T** | A set of elements of type T | p. 22 |
| D | Domain of a variable | p. 22 |
| X | Variables | p. 6 |
| J | Optimization target/function | p. 6 |
| C | Battery capacity | p. 19 |
| $P_m$ | Electric motor power | p. 64 |
| $\Lambda$ | Driving cycle | p. 6 |
| $P_{ij}$ | The probability of going from current state $i$ to next state $j$ | p. 98 |
| F | Transition probability matrix | p. 98 |
| $\Phi$ | Optimization target | p. 22 |
| $M$ | Velocity classes | p. 99 |
| $N$ | Road slope classes | p. 99 |
| $O$ | Acceleration classes | p. 104 |
| $\tau$ | Node type | p. 22 |
| c | Constraint function | p. 22 |
| $\gamma$ | Gear number | p. 64 |
| *Superscripts* | | p. 22 |
| p | Possible | p. 25 |
| fe | Feasible | p. 25 |
| f | Functionality | p. 22 |
| c | Control | p. 19 |

# Special Symbols

| Symbols | Description | Reference |
|---|---|---|
| $\subseteq, \subset$ | Subset of | p. 25 |
| $\subsetneq, \not\subset$ | Not a subset of | p. 45 |
| $\leq, \geq$ | Inequality (smaller/greater or equal to) | p. 6 |
| $\mathbf{A}\bigcup\mathbf{B}$ | The union of two sets A and B: $\{x : x \in A \text{ or } x \in B\}$ | p. 25 |
| $\sum_{i=1}^{n} x_i$ | Sum over $i$; $i = 1, 2, ..., n$ $(= x_1 + x_2 + ...x_n)$ | p. 48 |
| $\prod_{i=1}^{n} x_i$ | Product over $i$; $i = 1, 2, ..., n$ $(= x_1 x_2 ...x_n)$ | p. 25 |
| $\mathbf{a} \mid\mid \mathbf{b}$ | The concatenation of vector a with vector b | p. 100 |

# SOCIETAL SUMMARY

**Integrated Optimal Design for Hybrid Electric Vehicles**

Increasing levels of air emissions, regardless of their source, harm the planet, both on the short, as well as on the long term. In the last decades significant increases in global emissions were measured that contributed to the growth of greenhouse gas emissions and global warming. For example, only between 1990 and 2007, $CO_2$ emissions from transport (land, water and air) increased by 45%. To constrain climate changes, these emission levels must be reduced. To this end, in the recent past, electric and hybrid cars have entered the market, especially, in the passenger vehicle category. With proven benefits, these new power trains will enter other markets as well, be it commercial trucks, buses, boats, ships and so forth.

In this thesis, the design of hybrid electric vehicles is studied, to provide efficient solutions (low energy and fuel consumption), with affordable and competitive prices. In particular, the research focuses on solutions suitable for long-haul heavy-duty trucks. To find the optimal design for a hybrid electric vehicle, its architecture, the components used (their sizes and technologies), the driving cycle and the optimal control algorithm are investigated. Starting from a set of components, a method for finding *all possible* architectures of hybrid electric vehicles is introduced. Then, the design problem is formulated as an optimization problem on several levels and with multiple objectives. The results presented in this thesis demonstrate significant potential for reducing the fuel consumption and emission by introducing new hybrid architectures and by integrated the optimal sizing and control of components. The design methods introduced here for hybrid electric trucks can be easily used in the design of other transport systems, optimizing the prototyping process and eliminating costly redesigns.

# SUMMARY

## Integrated Optimal Design for Hybrid Electric Vehicles

Current challenges for newly developed vehicles are addressed in various transportation sectors, with hybrid power trains, as viable solutions. These challanges include strict legislations on $CO_2$ or the foreseen future-lack of oil. Having more than one source of power, hybrid power trains give birth to a large design space for the physical system and increase the complexity of the controller. The strong coupling between the parameters of the physical system (e.g., topology) and the parameters of the controller transforms the problem into a multi-level problem that, if solved sequentially, is by definition suboptimal. To obtain an optimal system design, the physical system and its controller should be designed in an integrated manner.

The design of a hybrid electric vehicle (HEV) can be formulated as a multi-objective optimization problem that spreads over multiple levels (technology, topology, size and control). In the last decade, studies have shown that, by integrating these optimization levels fuel and energy benefits are obtained, which go beyond the results achieved with solely optimal control for a given topology. Due to the large number of variables for optimization, their diversity, the nonlinear and multi-objective nature of the problem, various design methodologies have been developed, yet none has proven to be widely accepted. Moreover, current design methods lack generality and a systematic analysis of the vehicle. In this thesis, defining such a design methodology is discussed, from the general problem definition to how to solve different design layers.

The first contribution of this work is a framework on how to automatically generate topologies for HEVs. The first HEVs design area, the topology, has the largest design space, yet, so far in literature, the topology design is limited investigated due to its high complexity. Having more than $10^{45}$ possible topologies, its design space may contain variations in the number, placement and type of components. In practice, using expert knowledge, a predefined small set of topologies is used to optimize their energy efficiency by varying the power specifications of the main components (sizing). By doing so, the complete design of the vehicle is, inherently and to a certain extent, sub-optimal.

Moreover, various complex topologies appear on the automotive market and no tool exists to optimally choose or evaluate them. Software packages, as ADVISOR or AVL Cruise could be used, yet they rely on rule based controllers and a very limited number of topologies. To overcome this design limitation, in this work, a novel framework is presented that deals with the automatic generation of possible topologies given a set of components (e.g., engine, electric machine, batteries or transmission elements). This framework uses a platform (library of components) and a hybrid knowledge base (functional and cost-based principles) to set-up a constraint logic programming problem and outputs a set of feasible topologies for HEVs. These are all possible topologies that could be built considering a fixed, yet large set of components. Then, by using these results, insights are given on what construction principles are mostly critical for simulations times and what topologies could be selected as candidate topologies for sizing and control studies. Such a framework can be used for any power-train application, it can offer the topologies to be investigated in the design phase and can provide insightful results for optimal design studies.

The second and third contributions deal with the integrated design of topology, sizing and supervisory control for HEVs. First, different existing bi-level optimization coordination strategies, with the outer loop using algorithms as Genetic Algorithms, Sequential Quadratic Programming, Particle Swarm Optimization or Pattern Search (DIRECT) and the inner loop using Dynamic Programming, are benchmarked to optimally size a parallel topology of a heavy duty vehicle. Secondly, nested design is applied to electrified auxiliary systems (such as the power steering pump, air brake and air conditioning compressors). At auxiliary sub-system level, the potential of reduced emissions/fuel comes mostly by eliminating the fixed-ratio dependency between the auxiliaries speed and engine speed that induces high energy losses. To study this potential, in this work novel topologies are introduced and then exhaustive search (combined with nested sizing and control) is used for each topology, to find its optimal design. The results show significant fuel reduction by hybridization, engine downsizing, electrification of auxiliary units and offer insights in the usability of nested optimization approaches in HEV design.

To enable and facilitate HEVs design and development, short, yet realistic, driving cycles need to be synthesized. The newly developed driving cycle should give a good representation of measured driving cycles in terms of velocity, slope, acceleration and so on. Current methods use only velocity and acceleration, and assume zero road slope. The heavier the vehicle is, the more important the road slope becomes in powertrain prototyping (as component sizing or control), hence neglecting it leads to unrealistic, sub-optimal or limited designs. To include slope, we extend existing methods and propose an approach based on multi-dimensional Markov chains. The validation of the synthesized driving cycle, is based on a statistical analysis (as average acceleration or maximum velocity) and a frequency analysis. This new method demonstrates the ability of capturing measured road slope information in the syntesized driving cycle. Furthermore, results show that the proposed method outperforms current methods in terms of accuracy and speed.

*CONTENTS*

CHAPTER

# ONE

# INTRODUCTION

**Abstract /** This chapter presents an introduction to hybrid electric vehicle design, including the powertrain and the auxiliary units. From the existing challenges, new directions for research are identified and the research objectives are defined.

## 1.1   Challenges in Vehicle Design

In our modern society, with a growing population size and that strives for an improved quality of life, we need a sustainable energy future. Increased levels of carbon dioxide ($CO_2$), the main greenhouse gas that originates for 90% from fossil-fuel combustion, contribute to the global warming effect in the atmosphere. Global $CO_2$ emissions are forecast to grow from the current 35.3 billion tonnes (Gt) per year to 46 Gt yr$^{-1}$ [1, 2], which largely reflects the increase in fossil energy consumption. The path that will be followed depends on how efficiently we use the current energy sources.

Despite the significant growth in the use of renewable energies, the transportation sector uses mainly petroleum-derived liquid fuels, accounting for 26% of the globally emitted $CO_2$. Road transport alone contributes to about one-fifth of the EU's total emissions of $CO_2$ in 2012, with particularity heavy-duty (HD) vehicles (trucks and buses) being responsible for about a quarter of these emissions. The negative impact on the environment will be even greater given the forecasts that support the transport of goods will grow significantly in the coming decades. In 1992, there were over half a billion cars and trucks worldwide and it is estimated that, by 2050, this number will exceed 2.5 billion.

To create a sustainable energy future, improving the efficiency of transport systems (i.e., the vehicles, the supply/demand/distribution infrastructures, etc.) is required. In particular, improving the energy efficiency of vehicles can greatly reduce the oil dependency. We focus here, on the heavy-duty vehicles sector, in which, as shown in Fig. 1.1 a substantial portion of the energy consumed is lost into heat (in average 50%) or other losses. To improve the energy efficiency of these vehicles, there are multiple research directions as lighter materials or more improved designs, but are limited. For instance, while reducing further the aerodynamic drag or the tire losses is possible, braking and idling losses will always be significant in conventional vehicles. Likewise, in engine-only vehicles, the sizing of the combustion engine will always be decided by the power it needs to provide.
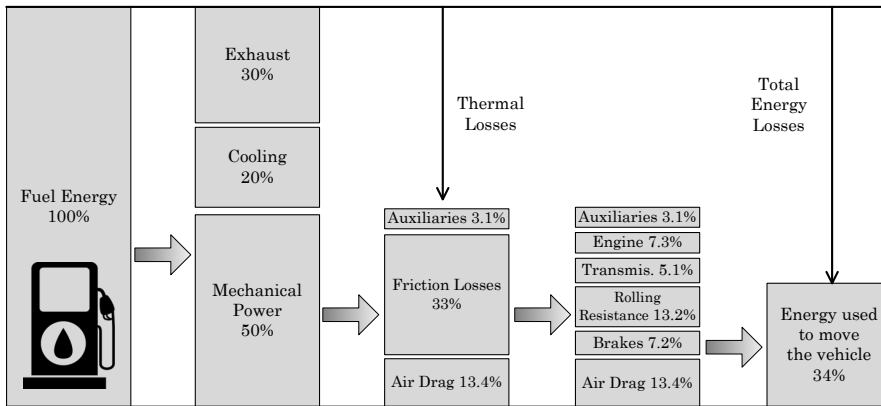


Figure 1.1: Breakdown of the average energy consumption in heavy duty vehicles (trucks and buses). Adapted with permission from ref. [3].

To reduce consumption, exhaust emissions and to increase vehicle performance, safety and engine efficiency, the automotive original equipment manufacturers (OEMs) are incorporating increased electronic content in vehicles. This includes stability controls, collision avoidance systems, electronic braking, thermoelectric technologies and navigation systems [4]. Studies have shown that improved low-cost wast-heat recovery can increase efficiency, especially, in HD vehicles, reducing both pollution and equipment sizes [5]. Further significant improvement of the energy efficiency of vehicles can be done by the electrification of the powertrain, which will be the focus of this work.

This thesis is part of the HIT (Hybrid Innovation in Trucks) project that ran from September 1, 2010 through June 30, 2014 in a collaboration between DAF Trucks N.V., Eindhoven University of Technology and different suppliers. In this project the aim was to improve the fuel consumption and $CO_2$ emissions of a long-haul heavy-duty truck. The prototype presented in Fig. 1.2, was built by DAF with a parallel hybrid configuration, and it was used, when necessary, as a benchmark for the results in this thesis. The methods presented in this thesis are applicable but not restricted to these types of applications.

Figure 1.2: DAF XF prototype heavy-duty hybrid electric truck with a parallel topology.

## 1.2 Hybrid Electric Vehicle System Level Design

Hybrid vehicles combine two, or more technology principles to produce, store and deliver power. Current market hybrid vehicles, typically, combine a combustion engine and an electric machine (EM), as power converters, and they are referred to as hybrid electric vehicles (HEVs). This hybridization allows a wide variety of possible topologies of the powertrain and configurations of the sub-systems. Depending on the powertrain arhitecture and the power control strategy selected, the powertrain may operate on battery only, engine only, or a combination of the battery and engine.

More than a decade ago, when hybrid cars were introduced first on the market, they emerged in a limited number of architectures, i.e., serial, parallel or mixed serial-parallel, as illustrated in Fig. 1.3. These topologies, and their applicability to various transportation sectors, have been researched intensively in recent years and are described in detail in survey articles such as [6–11] and books [12–15]. In a HEV, depending on its topology and component technologies, an electric machine can function as *motor* (delivering positive torque and speed to propel the vehicle) or as a *generator* (producing energy, from either the engine or from regenerative braking, to charge the battery). Conditional to the usage of the vehicle, energy savings can be obtained from brake energy recuperation, engine downsizing, reducing engine idling, etc. [12]. Since hybrid vehicles containing more than one source of power, there is a greater flexibility in the design and control of these systems. This flexibility is reflected also in the choice of the vehicle subsystems (such as the power steering or the air conditioning systems), that may be independent on the engine choice [16].

**Conventional Vehicle**

Combustion Engine — Transmission — Final Drive

···· Electrical power path
— Mechanical power path

**Series HEV**

Combustion Engine — Electric Machine ···· Battery ···· Electric Machine — Final Drive

Generator — Motor or Generator

**Parallel HEV**

Combustion Engine — Transmission — Final Drive

Battery ···· Electric Machine — a) or b) — Motor or Generator

**Series-Parallel HEV**

Combustion Engine — Electric Machine — Transmission — Final Drive

Battery ···· Electric Machine

Figure 1.3: Main topology classes in vehicles: conventional (solely fuel driven) and hybrid electric (series, parallel and series-parallel (with one or more planetary gear systems). Here dotted lines represent electrical links and solid lines represent mechanical links.

The complete design process of a HEV, together with its different (nested) design levels, is depicted in Fig. 1.4. The topology, technology and sizing of components are layers related to the physical system. The control layer is dependent on the physical system, yet it will not change its physical parameters (e.g., the battery size, electric machine type or gear ratios). These physical system parameters will act as bounds with which the control algorithm must cope. In addition, the HEV topology will define the variables of the control algorithm (i.e., their number and type). This inter-dependence (coupling) between the plant design layers and the control algorithm, supports the statement that the performance, which can be obtained from optimal per-layer design, is influenced by the design of other layers.

In general, a HEV is built such that operating costs and construction costs are minimized. Moreover, other performance criteria may be considered either as limits on the design or design targets. These can include $NO_x$ (Nitric Oxide and Nitrogen Dioxide), $CO_2$ or PM (Particulate Matter) emissions, vehicle weight, safety, comfort, handling and dynamic
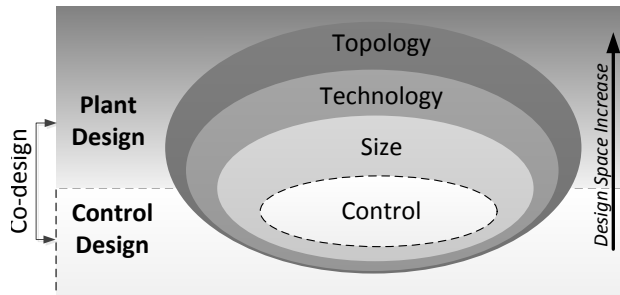
Figure 1.4: Hybrid electric vehicle system-level design (SLD) and its multi-layers

performance (such as acceleration or braking times). Based on these descriptions, the problem of designing a hybrid vehicle reduces to solving an optimization problem with multiple levels and multiple optimization targets. Moreover, the problem has discrete and continuous variables with the component models and the optimization functions generally being nonlinear and non-convex [12].

Understanding what is the best methodology to design a hybrid electric vehicle, requires knowing the characteristics of each level in detail. Often in literature the plant design layers are fixed, i.e., one particular vehicle is considered, and constructing the controller is investigated. How this control problem is defined and approached is discussed next, in Section 1.2.1. Moreover, this control design problem requires at least one driving cycle to evaluate the performance of the proposed algorithm. Since the choice of driving cycle will have a significant influence on the results, in Section 1.2.2 the possible options are summarized. In a similar manner, the controller can be fixed and different vehicle parameters can be varied. These sequential approaches are described briefly in Section 1.2.3 and highlights the need for more integrated design methods of HEVs, where plants and controller are designed together (Section 1.3).

## 1.2.1   Control Design

Building the control algorithm, i.e., the energy management system (EMS) of a HEV powertrain, consists of finding the power-converters setpoints that can deliver the driver's required power in an *optimal* way. This optimality, of the EMS, is analysed for a certain objective function, typically, fuel consumption, but can be extended to include pollutant emissions, drivability or aspects related to the battery (e.g., life degradation or charge).

For each HEV, the fuel consumption is evaluated in accordance with certain usability conditions. These are contained in the input driving cycle, $\Lambda$, as the NEDC (New European Driving Cycle) or the EPA Highway Fuel Economy Test Cycle [17]. This optimization problem is written in the following mathematical format: find the set $\mathbf{x}_c(t)$ of control

design variable values, within the design space that will minimize the objective function:

$$\mathbf{J_c}(\mathbf{x_c}(t), \Lambda)$$

subject to the inequality and equality constraints:

$$g_j(\mathbf{x_c}(t)) \leq 0, \quad j = 1, 2, ..., m,$$
$$h_l(\mathbf{x_c}(t)) = 0, \quad l = 1, 2, ..., e,$$

and to the system's dynamics:

$$\dot{\xi}(t) = f(\xi(t), \mathbf{x_p}, \mathbf{x_c}(t), t),$$
$$\xi(t_0) = \xi_0,$$
$$\xi(t_f) = \xi_f,$$

$$(1.1)$$

with $\mathbf{x_p} \in \mathbb{R}^n$ the set of plant design variables and $\xi$ the states of the dynamical system, e.g., the state of charge (SOC) of the electric buffer (continuous variable), gear number (discrete variable) or engine on/off (binary variable).

In cases where $\xi$ denotes the battery SOC, the final state conditions

$$\xi_f = \xi_0, \tag{1.2}$$
$$\xi_f = \xi_{min}, \tag{1.3}$$

constrain the charge sustaining, (1.2), or depleting, (1.3), behaviour of the energy storage pack at the end of the driving cycle. Thus, (1.2) is used for charge sustaining hybrids and (1.3) is used for plug-in HEVs. Constraints, $g_j$ and $h_l$ contain per-component operational boundaries, such as the engine torque, $T_e$, subject to the speed-dependent constraint, $T_{e,min}(\omega_e) \leq T_e(t) \leq T_{e,max}(\omega_e)$.

To solve the optimization problem in (1.1), there exist two large categories of methods. Introduced first, the *rule based algorithms* (including heuristic and fuzzy logic methods), use expert knowledge translated into boolean rules to decide the set-points for the power sources of the HEV [18–21]. These algorithms are sub-optimal, they require significant tuning effort and they usually change for each topology. Motivated by these, *optimization based algorithms* emerged and were used either for real-time control or for off-line design studies. Among often used algorithms for real-time control, we can find the Equivalent Consumption Minimization Strategy (ECMS) [22–28], Stochastic Dynamic Programming (SDP) Strategies [29–33], or Model Predictive Control (MPC) Strategies [34, 35]. Reviews of EMS can be found in review articles as [36–42]. Several of these algorithms are used and compared in [43] to control the Plug-In Chevrolet Volt. For off-line design studies Dynamic Programming (DP) is often used since it can find an optimal solution for the mixed-integer non-convex optimization problem. DP can also be used as a benchmark to compare and for development of rule-based algorithms. In this thesis, for various case studies in Chapters 4 and 5, this optimization algorithm will also be used.

## 1.2.2 Driving Cycle

The driving cycle, denoted as $\Lambda$, that is used for designing the HEV, significantly influences the design of the final system, its fuel consumption, its emissions and its performance [44]. Using a more realistic driving cycle implies that the HEV will be more efficient in real-life everyday driving. Very often, to restrict the time of synthesizing a controller (during simulations) these driving cycles are very short, which is the opposite of reality. In addition, most driving cycles contain only a velocity profile, considering zero altitude. This assumption is unrealistic and it will influence the performance of the HEV directly proportional to its weight (i.e., heavier vehicles consume more power to go up-hill and can regenerate more energy when driving down-hill).

Generally, there exist two types of driving cycles: *modal*, such as NEDC, and *transient*, such as VAIL2NREL or the FTP-75 ( US Federal Test Procedure) [45]. The *modal* cycles consist of acceleration, deceleration and constant speed segments, while the *transient* cycles contain multiple speed variations, resembling more measured driving cycles. When the cycle has a predictable pattern (such as the modal cycles), the engineers can design a vehicle that will perform well on that particular cycle, but will fail to perform well when driven normally. This effect, of designing a HEV with respect to only one cycle, is referred to as "cycle beating" and results in high emissions during normal driving of carbon monoxide (CO), hydrocarbons (HC) and ammonia ($NH_3$) [46]. In recent years, one option to avoid this effect was to use multiple cycles as input to the design, analyse the sensitivity of the design with respect to cycle variation and chose the most suitable design [47–50]. A second option, that can provide improved and faster results, is to use a synthesised cycle that resembles well (multiple) measured cycles [51–53]. Thus far, stochastic methods, based on Markov chains, that use solely velocity (and acceleration) and generate a purely synthetic driving cycle, from [54, 55], have shown better results then other existing methods. In [56] it is shown that one can reach improved vehicle designs at reduced computational costs with the use of such methods. These results motivate the incorporation of stochastic driving cycles in HEV optimization studies [56]. Moreover, these methods of driving cycle synthesizing leave room for improvement, where one could consider also the differences in road altitude making the cycle even more realistic. In this thesis, this challenge is analysed as described in the following sections.

## 1.2.3 Plant Design

In a conventional engine-driven vehicle, as depicted in Fig. 1.3, the sizes of the components (such as power specifications) are restricted and deducted from the performance and drivability conditions. These include *(i)* top speed; *(ii)* maximum grade at which the fully loaded vehicle reaches the legal top speed limit; *(iii)* acceleration time from standstill to a reference speed (100 km/h or 60 mph are often used); *(iv)* uphill driving capability; *(v)* braking distance form a reference speed and so on [12]. In hybrid electric

vehicles, although the same performance and drivability conditions apply, the flexibility in the sizing of the components, as-well as their placement (topology) is significantly higher.

To find the plant parameters, $\mathbf{x}_p$ (e.g., variables as battery sizing, topology type or gear ratios), that minimize certain design targets, the following optimization problem should be solved

$$\min_{\mathbf{x}_p} \; \mathbf{J}_p(\mathbf{x}_p)$$

subject to the inequality and equality constraints:                                    (1.4)

$$g_j(\mathbf{x}_p) \leq 0, \;\; j = 1, 2, ..., m,$$
$$h_l(\mathbf{x}_p) = 0, \;\; l = 1, 2, ..., e.$$

When the cost function $\mathbf{J}_p$ is dependent on solving the control problem (e.g., $\mathbf{J}_p$ contains the fuel consumption or emissions), (1.4) should be solved in a nested manner with the problem from (1.1). For instance, to size the power train components of a series-hybrid microbus, in [57] a *one-variable-at-a-time* exhaustive search is performed. In this approach, first the power generating group size is varied for a fixed battery pack and a value is selected. Accordingly, for the newly found power generating group size, the variation of the battery pack is investigated.

Another example can be found in [58], where three hybrid topologies (a start-stop, a full parallel and a mixed series-parallel) are compared to a conventional vehicle to find the most fuel efficient design. These sequential strategies using exhaustive search, where the plant is designed first (for instance looking for minimum cost), are simple and insightful which made them very popular among research and practice. However, they pose significant challenges in the computational burden, which grows quickly for increasing number of plant variables (that contain also the topology options).

Rules-based approaches and sequential coordination strategies resulted in sub-optimally designed systems, with high costs for the hybridization and an unattractive return on investment time for both the client and OEM [25]. If, when designing a HEV, one wants to evaluate the fuel consumption as-well, this requires simulating the vehicle over a given driving cycle. Implicitly, this requires a control algorithm and a structure for coordinating the design between various layers. All these motivated plant and control design in an integrated way, which is discussed in the next section.

## 1.3   Motivation for Integrated Plant and Control Design

The attainable performance by the control algorithm, limited by the physical system, encourages the integrated design of the plant and its controller. Since this new design problem is an extension of the optimization problem defined in (1.1), its solution is more

complex and more difficult to find. For instance, in a plant and control optimization problem there are more design variables, larger design spaces and various (conflicting) optimization targets at different levels. To approach this, in the various stages of the design process, specialists used their experience to make decisions and decrease the dimensions of the problem. The most common solutions in literature include the co-design of components sizing and controller by using a nested coordination structure. Examples include the design of parallel passenger cars in [59–64], a parallel hybrid electric heavy-duty truck [44, 65] a series hybrid commercial city bus [66] or a parallel HEV transit bus [67].

For each level of this design problem an optimization algorithm must be chosen to find the solution. For the control problem often Dynamic Programming is used, and for the component sizing problem often evolutionary optimization algorithms (such as Particle Swarm Optimization and Genetic Algorithms) or exhaustive search are used. The performance of these algorithms varies from the design of one vehicle to another since the optimization problem changes. Therefore, there is no universally accepted method that suits HEV design studies. All these options, together with a more detailed formalisation of the HEV design problem, are described in Chapter 2.

To reduce the consumption even more, in more recent studies also the topology of the vehicle is varied alongside with the components dimensions and the control algorithm. This further integration of the design layers is shown in [68] for a full-parallel and a torque assist HEV and in [69] for a hybrid and an electric submarine. The majority of these studies are restrictive in choosing different topologies, with parallel and mixed series-parallel being the most often studied. The authors of [70] have studied the topological variation of Toyota Prius and Chevrolet Volt using the generic state-space representation for the dynamics of HEVs with single planetary gears sets from [32]. It is shown in [70] that with small variations of the configurations, such as adding or eliminating a clutch, improvements can be attained in vehicle cost, topology complexity or fuel consumption. The generic state-space representation method goes beyond the intuitive selection of topologies for design and motivates the use more automated methods to select candidate topologies for optimization.

## 1.4   Research Objectives

This thesis aims to contribute in the techniques and methods used for hybrid electric vehicle design to enable fast simulations and the evaluation of hybrid vehicles. Such frameworks should optimize the prototyping process, should eliminate costly redesigns and should find HEVs with smaller operational and construction costs. As motivated in the previous sections, the multi-disciplinary nature of this design problem requires frameworks that facilitate the interaction between various layers/disciplines. To develop such an optimization methodology, the following key research objective should be investigated:

> *Develop a design methodology that yields an optimal hybrid vehicle with respect to imposed usability conditions and various design targets. Herein, one might use various topologies for the HEV powertrain components or other sub-systems, different component sizes and control algorithms.*

To address this research objective the following sub-objectives have been identified and addressed in this thesis:

**O$_1$** Identify what are the main challenges in designing hybrid electric vehicles and what interactions between the various design levels influence the optimality of the designed system.

**O$_2$** Develop a method of construction and automatic selection of hybrid topologies.

**O$_3$** Investigate the potential of reducing the operational and component costs by powertrain hybridization.

**O$_4$** Analyse the potential benefits of electrification of auxiliary systems present in a vehicle, such as the steering system, the air-conditioning system and so on.

**O$_5$** Build a method to synthesize a short driving cycle representative of real driving cycles, in which the characteristics of speed, acceleration and road altitude variations are accurately captured.

## 1.5   Thesis Contributions and Outline

This thesis contains another six chapters, of which five are research chapters and a final chapter that summarizes the research findings and presents recommendations for future research. In Table 1.1, the main topics studied in this thesis are summarized in connection with the chapters of which they are part.

Due to the significant variation in approaches and methods used to design a hybrid vehicle, in *Chapter 2* (publication 2 in Section 1.7) , we present a review of these. We define the optimal design problem of a hybrid vehicle, describing all its existing design levels shown in Fig. 1.4, and we highlight the most important assumptions that can be made in this process. Then, to identify future research lines and related challenges, we categorize more in detail the types of coordination architectures (e.g., sequential, nested, simultaneous) and the optimization algorithms used. A comparative study of various control algorithms applied to a Plug-in HEV, the Chevrolet Volt, is not included in this thesis but is a result of this doctoral study, and is presented in publication 4.

Table 1.1: Overview of the subjects included in this thesis, arranges by topic.

| Topic | | Chapter | | | | | |
|---|---|:---:|:---:|:---:|:---:|:---:|:---:|
| | | 2 | 3 | 4 | 5 | 6 | App. |
| **Theoretical Concepts** and **Methods** | $O_1$: Coordination Strategies | ✓ | | ✓ | ✓ | | ✓ |
| | $O_2$: HEV Topology Generation | | ✓ | | | | |
| | $O_3$: Optimization Algorithms | ✓ | | ✓ | ✓ | | |
| | $O_4$: Auxiliary Topologies Design | | | | ✓ | | ✓ |
| | $O_5$: Cycle Synthesis | | | | | ✓ | |
| **Design Study Cases** | $O_3$: Hybridization Potential | | | ✓ | | | |
| | $O_3$: Engine Downsizing Potential | | | ✓ | | | |
| | $O_4$: Auxiliary Units | | | | ✓ | | ✓ |
| | $O_5$: Cycle Compression | | | | | ✓ | |

The first level to be addressed in designing a hybrid vehicle, the topology generation, is discussed in *Chapter 3* and has been published in publication 3. Most often, scientists have neglected this layer and made assumptions or specific choices (such as selecting a parallel configuration). Here, to obtain the complete design space of topologies, the problem of generating hybrid topologies is introduced, described and solved. In the step of defining the problem, we use two types of topology construction constraints, some based on functionality and some based on cost. This is done to find hybrid electric vehicles with desired functionalities, that do not use components in a redundant or unnecessary way. This chapter proposes a methodology to find hybrid vehicle topologies that is easily modifiable and applicable to various power trains.

In *Chapter 4*, a comparison of the most used optimization algorithms in HEV studies is presented using as an example of a parallel architecture of a long-haul truck. In this comparison of various algorithms, we analyse the ability to find an optimal solution for the components sizing (battery, electric motor and combustion engine) and control problem, for minimum consumption and maximum profit. The trade-offs between these conflicting optimization targets is analysed in the form of a Pareto front and optimization algorithms are evaluated on various criteria (eg, tuning effort, suitability, etcetera). These results are summarized in publication 9, and were also used as a basis for publication 5.

The potential benefits obtained by using multi-level design are analysed in *Chapter 5* for the auxiliary systems present in a heavy-duty truck. Together with appendix A, this chapter summarizes the publication 7,8 and 10. In particular, various new topologies are proposed and optimized for the power steering system. Moreover, in Chapter 5, we investigate the effects of simultaneously designing various auxiliary systems.

*Chapter 6* introduces a new method of synthesizing driving cycles (publication 1). This method is an improvement to current methods, containing both information about the

change in elevation of the road and speed. For this multi-dimensional Markov chains are used to capture probabilistic properties of a driving cycle and different criteria in the time domain and frequency domain are used for validation. Based on previous chapters, in *Chapter 7*, conclusions and recommendations are formulated.

## 1.6    A Guideline for the Reader

The chapters of this thesis are generally self-contained and there is no need to read all chapters successively. Chapter 2 formulates the optimization problem and describes in more detail all the research directions addressed in this thesis, being a good introduction for all the remaining chapters. After Chapter 2, one might proceed to Chapters 4 and 5 for the optimal topology, sizing and control design studies or to Chapters 3 and 6 for novel theoretical concepts and methods for driving cycles and HEV topologies generation and synthesis.

## 1.7    List of Publications

The period of this doctoral study resulted in several publications, some of which are used in this manuscript.

## Refereed Journal Publications

[1] E. Silvas, K. Hereijgers, H. Peng, T. Hofman and M. Steinbuch. Synthesis of Realistic Driving Cycles with High Accuracy and Computational Speed, Including Slope Information. *Submitted for journal publication, under review.*

[2] E. Silvas, T. Hofman, N. Murgovski, P. Etman, M. Steinbuch. Review of Optimization Strategies for System-Level Design in Hybrid Electric Vehicles. *Submitted for journal publication, under review.*

[3] E. Silvas, T. Hofman, A. Serebrenik, M. Steinbuch. Functional and Cost-Based Automatic Generator for Hybrid Vehicles Topologies. *IEEE/ASME Transactions on Mechatronics*, 20(4):1561-1572, 2015.

[4] A. Sciarretta, L. Serrao, P.C. Dewangan, P. Tona, N.D. Bergshoeff, C. Bordons, L. Charmpa, P. Elbert, L. Eriksson, T. Hofman, M. Hubacher, P. Isenegger, F. Lacandia, A.

Laveau, H. Li, D. Marcos, T. Nüesch, S. Onori, P. Pisu, J. Rios, S. Silvas, M. Sivertsson, L. Tribioli, L., A.-J. van der Hoeven, and M. Wu. A control benchmark on the energy management of a plug-in hybrid electric vehicle. *Control Engineering Practice*, 29:287-298, 2014.

# Refereed Conference Publications

[5] M. Pourabdollah, E. Silvas, N. Murgovski, M. Steinbuch and B. Egardt. Optimal Sizing of a Series PHEV: Comparison between Convex Optimization and Particle Swarm Optimization. In *Proc IFAC Workshop on Engine and Powertrain Control, Simulation and Modeling*, Columbus, Ohio, pp. 1-7, 2015.

[6] Z. Pan, X. Zhang, E. Silvas, H. Peng and N. Ravi. Modelling and Optimization of All-Wheel-Drive Hybrid Powertrain for Pick-up Trucks. In *Proc ASME Dynamic Systems and Control Conference*, Columbus, Ohio, pp. 1-8, 2015.

[7] E. Silvas, E.A. Backx, T. Hofman, H. Voets and M. Steinbuch. Design of Power Steering Systems for Heavy-Duty Long-Haul Vehicles. In *Proc 19th IFAC World Congress*, Cape Town, South Africa, pp. 3930-3935, 2014.

[8] E. Silvas, E.A. Backx, H. Voets, T. Hofman and M. Steinbuch. Topology Design and Size Optimization of Auxiliary Units : A Case Study for Steering Systems. In *Proc FISITA World Automotive Congress*, Maastricht, The Netherlands, pp. 1-8, 2014.

[9] E. Silvas, N.D. Bergshoeff, T. Hofman and M. Steinbuch. Comparison of Bi-level Optimization Frameworks for Sizing and Control of a Hybrid Electric Vehicle In *Proc IEEE Vehicle Power and Propulsion Conference*, Coimbra, Portugal, pp. 1-6, 2014.

[10] E. Silvas, O. Turan, T. Hofman and M. Steinbuch. Modeling for control and optimal design of a power steering pump and an air conditioning compressor used in heavy duty trucks. In *Proc IEEE Vehicle Power and Propulsion Conference*, Beijing, China, pp. 1-6, 2013.

[11] E. Silvas, T. Hofman and Steinbuch. Review of optimal design strategies for hybrid electric vehicles. In *Proc IFAC Workshop on Engine and Powertrain Control, Simulation and Modeling*, Paris, France, pp. 57-64, 2012.

# TWO

# REVIEW OF OPTIMIZATION STRATEGIES FOR SYSTEM-LEVEL DESIGN IN HEVS

**Abstract /** The optimal design of a hybrid electric vehicle can be formulated as a multi-objective optimization problem that spreads over multiple levels (technology, topology, size and control). In the last decade, studies have shown that, by integrating these optimization levels fuel benefits are obtained, which go beyond the results achieved with solely optimal control for a given topology. Due to the large number of variables for optimization, their diversity, the nonlinear and multi-objective nature of the problem, various methodologies have been developed, yet none has proven to be widely accepted. This chapter presents a comprehensive analysis of the various methodologies developed and identifies challenges for future research. Starting from a general description of the problem, with examples found in the literature, we categorize the types of optimization problems and methods used. To offer a complete analysis, we broaden the scope of the search to several sectors of transport, such as naval or ground.

## 2.1   Introduction

Current challenges for newly developed vehicles, as strict legislations on $CO_2$ or the fore-seen future-lack of oil, are addressed in various transportation sectors, with hybrid power trains, as viable solutions. Having more than one source of power, hybrid power trains give birth to a large design space for the physical system and increase the complexity of the control algorithm. The coupling (dependency) between the parameters of the physical system (e.g., topology) and the parameters of the control algorithm transforms the problem into a multi-level problem (as depicted in Fig. 1.4) that, if solved sequentially, is by definition sub-optimal [71]. Therefore, the physical system and the control algorithm should be designed in an integrated manner to obtain an optimal system design.

Because of the large dimensions of the design space, computer simulations of dynamical systems, e.g., for different architectures and component sizes, have become more important as a preliminary step to building prototypes [72]. Sizing is defined for each component differently, typically being expressed in terms of power for engines and electric machines, capacity for energy storage devices, fixed rations for gears and so on. Computer simulations significantly speedup the control synthesis of a given design and topology. However, even with computer systems, the problem of finding the optimal vehicle design that provides the best control performance is typically intractable. Obviously it is not feasible (cost or time-wise), given a design space, to build all possible vehicles and evaluate which configuration and parameters provide the best performance for control. Moreover, even when designing the control algorithm, due to the nonlinear, mixed-integer and multi-dimensional (several states) characteristics of hybrid electric vehicles (HEV) control problem, the simulations require large computational times. Ergo, it is not time-wise feasible to simulate all combinations (i.e., brute force searches) of the design variables [44]. Instead, optimization-based frameworks for plant and control synthesis of HEVs are being developed. Starting from the optimal control and continuing to the optimal sizing, different optimization algorithms were used to obtain the maximum power train energy efficiency and/or the minimum total cost of vehicle ownership.

Based on examples from recent literature, in this chapter we introduce the general problem of optimally designing a HEV. Then we summarize the common challenges in this design problem and present the different methods and frameworks that have been developed to improve the design of HEVs. The focus of this overview is on frameworks that include the co-design of HEVs, i.e. concurrent plant (as topology or size) and control optimization.

The remaining sections of this chapter are organized as follows. After a description of HEV topologies is given in Section 2.2, the system-wide optimization problem is described in Section 2.3. Section 2.4 discusses existent methodologies used for integrating the plant and the control optimization, together with the used optimization algorithms. In Section 2.5, these algorithms are discussed and compared and in Section 2.6 conclusions are drawn.

## 2.2 Hybrid Electric Vehicles

As briefly described in Chapter 1 and through Fig. 1.3, three categories of topologies may be distinguished: *series*, *parallel* and *series-parallel*. Series HEVs, perform best in stop-and-go driving since there is no mechanical link between the combustion engine and the wheels. In this way the engine can be run at its most efficient point also in varying vehicle speeds. Moreover, because there is no mechanical connection between the combustion engine and the wheels, this configuration is rather flexible with regard to the physical location of the various components in the power train. This makes the series topology highly suitable for application with restricted (re)design space.

When a series HEV is not used in city driving high powers need to be transmitted to the wheels from the EM, hence large electrical machines are needed to achieve high vehicles speeds. In addition, this topology requires a double energy conversion for delivering the required power, which induces efficiency losses. In this configuration the size of the traction EM is deducted from the vehicle's required performance (such as the top speed requirement). Thus, the sizing of the power train reduces to finding the optimal sizing of the battery and the power generating group (combustion engine/generator).

In parallel HEVs the combustion engine and the electric machine are both connected to a mechanical transmission and they can generate power independently of each other. The electric machine can be connected before or after the transmission as shown in Fig. 1.3 with (a) and (b) on pg. 4. Moreover, the HEV can switch between the power sources given the driving conditions. In this configuration there is no separate generator. Whenever generating power is possible and needed (e.g., energy recuperated from braking) the electric machine functions as a generator.

Parallel HEVs have a direct mechanical connection between the engine and the wheels. This leads to smaller energy losses (as they don't require the dual energy conversion as the series topology) but also less flexibility in the mutual positioning of the power train components compared to the series HEV drivetrain.

Series-parallel HEVs have an extra direct mechanical connection between the generator and the traction motor via the transmission. These architectures combine the benefits from both series and parallel HEVs. They are usually constructed with one or more planetary gear sets (PGS), and require at least two electric machines. PGS are transmission elements with three connectivity points (ring, sun and carrier).These transmission elements, eliminate the need of a traditional stepped (manual or automatic) gearbox and other transmission components.

Due to their increased flexibility in operating the components (as in series HEVs) and the presence of mechanical links (as in parallel HEVs), series-parallel HEVs can lead to a reduced fuel consumption for a wide variety of applications [73]. Yet, at the same time, they come at a higher price and require more complex control strategies.

Except these three HEVs categories, others can also be found in literature or practice, e.g., the dual mode hybrid and the four quadrant transducer. These mostly vary in the construction of the transmission components and will not be addressed here. The interested reader could refer to [74–78] for more information.

The efficiency of hybrid topologies varies according to the conditions under which they are driven. The design choice for one or other architecture depends on the (intended) mission of the vehicle and the trade-off between cost and performance. Given the pros and cons of the serial, parallel and series-parallel topologies, these are each predominantly used in certain transportation sectors. Serial topologies are currently most often found in buses [67, 79–81], battery electric vehicles (BEV) [82] with range extenders, boats [83], heavy vehicles (military), locomotives [84–87] and other in-urban vehicles, such as taxis [88], while parallel topologies and series-parallel are very common in passenger vehicles [60, 89–91].

Due to the high-cost and complexity of series-parallel topologies, the parallel topologies are, at the moment, the most commonly produced type of HEVs. Consequently, the parallel hybrids dominate the literature on supervisory control strategies for HEVs [19, 24, 60].

For different applications, dedicated research has been conducted on technologies for hybrid components and storage devices (as batteries, fuel cells or others). Overviews of electric motor drives and storage devices are well presented in [7, 92–96]. The requirements of each application determine the suitability of a certain technology, as well as the required dimensions of the respective hybrid component. In fact, determining the technology and dimension of a particular power train component represents also a discrete choice. This makes the optimal design of the power train of a hybrid electrical vehicle a discrete programming problem in terms of topological connectivity, technologies, and dimensions of the HEV power train components.

In the first research efforts on HEV development, the various options (topology, type, size) were investigated for a restricted set of discrete design choices, (e.g., a battery versus fuel cells, or three dimensions for the same Li-ion battery). The limited search space already provided novel hybrid power train configurations with a lower fuel consumption than conventional vehicles. Recent research papers on HEV development increase the scale of the optimization problem, in an effort to further improve the HEV performance. Typically, one seeks to formulate and solve a system-wide optimization problem covering the various components and disciplinary aspects involved in the HEV power train design.

In the following section these approaches for design and control of HEVs will be presented and analysed, with their pros and cons. We address the design of hybrid electric vehicles alone, without considering their effect on infrastructures (charging, traffic/transport, communication). For details on co-optimization of both HEVs and infrastructure, interested readers are referred to [97–99].

## 2.3    Problem Statement for System Optimal Design

A hybrid vehicle contains multiple interconnected subsystems which, themselves, consist of several sub-systems. When a HEV is built, it is desired to minimize both operational and component/design cost.

### 2.3.1    Driving Cycle

To evaluate the fuel consumption of an HEV a drive cycle, $\Lambda$, is necessary. This is a series of data points,

$$\Lambda(t) = \begin{bmatrix} v(t) \\ \theta(t) \end{bmatrix}, \text{ with } t \in [t_0, t_f], \tag{2.1}$$

with $v(t)$ representing the speed of a vehicle over time, $\theta(t)$ representing the slope (gradient) of the road and $[t_0, t_f]$ representing the driving cycle length. The drive cycle represents the type of driving conditions in which the HEV is used. It is the main determinant for the fuel consumption and the design (such as dimensioning of components) of the vehicle.

Driving cycles, which can be either measured or artificially created, vary across applications, countries and organizations. Driving cycles are used to asses the performance of HEVs in different ways, as for example fuel consumption and pollution emissions [17,47,100]. In literature most driving cycles assume $s(t) = 0$. This is an important assumption for heavier vehicles, where the contribution in the total power demand, for $s(t) \neq 0$, becomes significant.

### 2.3.2    Plant and Control Optimization Problem

The HEV efficiency and cost is dependent on the components (their connections, technologies and sizes) but also on the control algorithm used. The varying parameters defining topology, sizing and control inputs constitute the design variables (denoted by $\mathbf{x}$) in the optimal design problem, for both the plant and the control of a HEV,

$$\min_{\mathbf{x}_{\mathrm{p}}, \mathbf{x}_{\mathrm{c}}(t)} \mathbf{J}(\mathbf{x}_{\mathrm{p}}, \mathbf{x}_{\mathrm{c}}(t), \Lambda)$$

subject to the inequality and equality constraints:

$$g_j(\mathbf{x}_{\mathrm{p}}, \mathbf{x}_{\mathrm{c}}(t)) \leq 0, \quad j = 1, 2, ..., m,$$
$$h_l(\mathbf{x}_{\mathrm{p}}, \mathbf{x}_{\mathrm{c}}(t)) = 0, \quad l = 1, 2, ..., e.$$

and to the system's dynamics:

$$\dot{\xi}(t) = f(\xi(t), \mathbf{x}_{\mathrm{p}}, \mathbf{x}_{\mathrm{c}}(t), t),$$
$$\xi(t_0) = \xi_0,$$
$$\xi(t_f) = \xi_f.$$

$$(2.2)$$

Here $\mathbf{x}_p \in \mathbb{R}^n$ and $\mathbf{x}_c(t) \in \mathbb{R}^z$ denote the design variable vectors with n independent plant variables and z independent control variables, $m$ the number of inequality constraints, $e$ the number of equality constraints, $\mathbf{J}$ is the cost function, and $\xi$ the states of the dynamical system, e.g., the state of charge (SOC) of the electric buffer. The additional state conditions from (1.2) and (1.3) apply here as-well. Furthermore, the constraints, $g_j$ and $h_l$ contain per-component operational boundaries, such as the engine torque, $T_e$, subject to the speed-dependent constraint, $T_{e,min}(\omega_e) \leq T_e(t) \leq T_{e,max}(\omega_e)$, component sizing boundaries, such as the engine power, $P_e$, $P_{e,min} \leq P_e \leq P_{e,max}$, or other boundaries related to the HEV topology (connectivity of components).

**Note**. For ease of understanding vectors are marked in bold, i.e., $\mathbf{x}$ is a vector of design variables, where each variable is denoted by $x$. Moreover, $(\cdot)_p$, represents a plant related variable (such as battery sizing) while $(\cdot)_c$, represents a control related variable (such as engine torque).

The inter-links between different levels of vehicle design are illustrated in Fig. 2.1. We distinguish three design levels: (a) determining the topology $T_k^f$, (b) determining component dimensions, and, (c) designing the control algorithm. Fig. 2.1 is a more detailed view of Fig. 1.4, in which the technology and sizing optimization are combined in one layer for ease of understanding and readability. Moreover, the topology design layer is split into a topology generation and topology optimization layers.
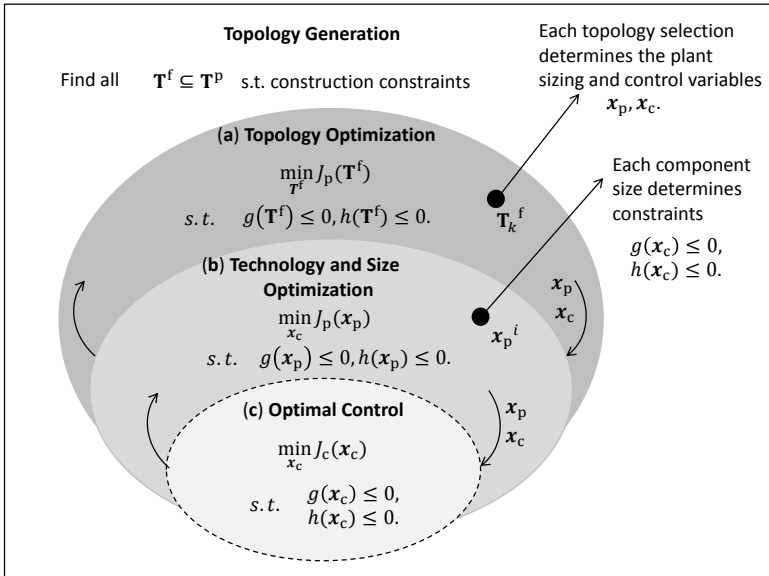


Figure 2.1: System-level design (SLD) layers and interlinks in HEVs

As already stated in Chapter 1, the coupling between the three design levels presents a multi-level optimization problem with discrete design variables (such as battery size, transmission gear, powertrain mode) as well as continuous design variables (such as engine torque, battery power). Furthermore, the component models and the optimization functions are generally nonlinear and non-convex [12].

## Design Space Selection

To illustrate the use of $\mathbf{x}_p$ and $\mathbf{x}_c$ in (2.2), consider the optimal sizing and control problem for a one-motor parallel HEV depicted in Fig. 2.2. For the powertrain topology and com-
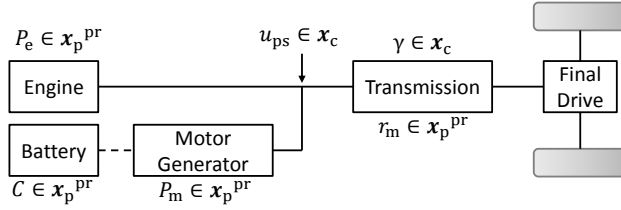


Figure 2.2: Design variables, for sizing ,$\mathbf{x}_p^{pr}$, and control, $\mathbf{x}_c^{pr}$, of a one motor pre-coupled parallel topology.

ponents in this figure [combustion engine, electric machines, battery and transmission], $\mathbf{x}_p$ and $\mathbf{x}_c$ become

$$
\begin{aligned}
\mathbf{x}_p^{pr} &= \begin{bmatrix} P_e & P_m & C & r_m \end{bmatrix}^T, \\
\mathbf{x}_c^{pr}(t) &= \begin{bmatrix} u_{ps}(t) & \gamma(t) \end{bmatrix}^T.
\end{aligned}
\tag{2.3}
$$

Herein $P_e$ is the maximum power of the engine, $P_m$ is the electric motor maximum peak power, $C$ is the battery capacity, $r_m$ is the maximum gear ratio, $u_{ps}$ is the power-split ratio that defines the portion of power delivered by the engine and electric machine, $\gamma$ is the gear number and the superscript $(\cdot)^{pr}$ indicates the parallel type of the topology. Next, $(\cdot)^s$ indicates a series topology and $(\cdot)^{ps}$ indicates a series-parallel topology.

For a series topology $\mathbf{x}_p$ and $\mathbf{x}_c$ become

$$
\begin{aligned}
\mathbf{x}_p^s &= \begin{bmatrix} P_e & P_{m1} & C \end{bmatrix}^T, \\
\mathbf{x}_c^s(t) &= \begin{bmatrix} T_e(t) & \omega_e(t) \end{bmatrix}^T,
\end{aligned}
\tag{2.4}
$$

with $T_e$ and $\omega_e$ the torque and speed of the combustion engine, for the input-split series-parallel topology $\mathbf{x}_p$ and $\mathbf{x}_c$ become

$$
\begin{aligned}
\mathbf{x}_p^{ps} &= \begin{bmatrix} P_e & P_{m1} & P_{m2} & C & Z \end{bmatrix}^T, \\
\mathbf{x}_c^{ps}(t) &= \begin{bmatrix} \omega_e(t) & T_{m2}(t) \end{bmatrix}^T,
\end{aligned}
\tag{2.5}
$$

with $T_{m2}$ the torque of the second electric machine and $Z$ the epicyclic gear ratio of the planetary gear set. For alternative topologies one may wish to include additional design variables related to clutches, more electric machines, more battery packs or alternative components.

When the topology or the technology are assumed variable too (besides the sizes of components), then more variables are included in the plant design variable vector, $\mathbf{x}_p$. Assume $\mathbf{x}_p$ consists of design variables from three plant design layers

$$\mathbf{x}_p = [\mathbf{x}_p^{top}, \mathbf{x}_p^{tech}, \mathbf{x}_p^{size}], \tag{2.6}$$

with $\mathbf{x}_p^{top}$, $\mathbf{x}_p^{tech}$ and $\mathbf{x}_p^{size}$ the plant design variable representing the topology, technology and size layers. Each instance of $\mathbf{x}_p^{top}$ will influence the size of $\mathbf{x}_p^{tech}$ and $\mathbf{x}_p^{size}$, as well as their corresponding control variables, exemplified in (2.3), (2.4) and (2.5). Furthermore, the selection of components sizing will, partially, determine the constraints for the control algorithm. Explicit derivations of the coupling between the sizing and the control layer, for different applications, and how they influence the overall design, are found in [71, 101].

Therefore, to find the vector $\mathbf{x}_p$ that minimizes the cost function $\mathbf{J}$, is a challenge for the chosen multi-level optimization methods, and for the optimization algorithms used for each individual level.

**Optimization Targets Selection**

$\mathbf{J} \in \mathbb{R}^k$ in (2.2) represents the vector of objective functions, that comprises the system-level design (SLD) objectives. As mentioned before, a HEV is generally built such that both operational and component/design cost are minimized. Nonetheless, other objectives, such as minimizing emissions or maximizing the payload of the vehicle, have been also used.

The most commonly employed objective functions, $J_i(\mathbf{x}) : \mathbb{R}^{n+z} \to \mathbb{R}^1$, are

$$J_1 = \int_{t_0}^{t_f} \dot{m}_f(t)dt, \qquad J_4 = \int_{t_0}^{t_f} NO_x(t)dt,$$

$$J_2 = \Psi_m + \Psi_i + \Psi_b, \qquad J_5 = \int_{t_0}^{t_f} HC(t)dt, \tag{2.7}$$

$$J_3 = -m_0 + m_b, \qquad J_6 = \int_{t_0}^{t_f} CO(t)dt.$$

Herein $J_1$ represents the $CO_2$ reduction, or the overall fuel consumption; $J_2$ is the hybridization costs, i.e., the summed cost of the motor, $\Psi_m$, the cost of the inverter, $\Psi_i$, and the cost of the battery, $\Psi_b$. $J_3$ is the payload weight of the vehicle (onboard passengers or

cargo), $m_0$, plus the weight of the battery, $m_b$. $J_4$, $J_5$ and $J_6$ are the nitrogen oxides (NO), hydrocarbons (HC) and carbon monoxides (CO) emissions.

The multi-objective character of the HEV system level design problem (SDL) (fuel, costs, etc..) requires dedicated multi-objective (MO) optimization algorithms/solvers, or reformulation of the problem into a single objective formulation. The latter, referred to as also as *scalarization* of the cost function, is often used and represents a choice of the designer.

There are multiple methods for objective function *scalarization* [102]. The weighted sum formulation equals

$$f(\mathbf{J}, \mathbf{w}) = w_1 J_1 + w_2 J_2 + ... + w_k J_k, \tag{2.8}$$

with $\mathbf{w}$ a vector of weight parameters, with

$$w_1 + w_2 + ... + w_k = 1. \tag{2.9}$$

The weights are adjusted such that a certain preference for the optimization targets is imposed. This scalarization, is used for example in [103, Ch.3],

$$f(\mathbf{J}, \mathbf{w}) = (w-1)\hat{J}_1 + w\hat{J}_2 \tag{2.10}$$

is proposed (with $\hat{J}$ representing the normalized[1] value of $J$) or in [104] where

$$f(\mathbf{J}, \mathbf{w}) = w_1 \hat{J}_1 + w_2 \hat{J}_5 + w_3 \hat{J}_6 + w_4 \hat{J}_4 \tag{2.11}$$

is used.

As mentioned before, when a HEV is built, it is desired to minimize both operational and component/design cost. The system-level design (SLD) problem is a challenge given that different optimization functions depend of different system levels. For example, minimizing the cost of electrification, $J_2$, is typically used for power-train component sizing while, $J_1$ is always used as objective for the control algorithm design. What are the possible optimization schemes and how the HEV design problem has been addressed so far it is discussed next.

## 2.4 Published HEV Design Frameworks

In the context of HEV prototyping, a design framework is a methodology that uses existing optimization algorithms combined on multi-levels, to find the best design for given targets and constraints. This describes how and in which order the coupled optimization problems at the various levels are solved in an effort to solve the overall system level design problem. Moreover, it relates to coordination methods in distributed multidisciplinary optimization, see for instance [105, 106], where the coordination method defines

---

[1]The authors define a normalized value $\hat{J} = \frac{J}{J^N} \in [0, 1]$, where $J^N$ is estimated as the largest possible value of $J$ within the search space.

how the coupled disciplinary subproblems are solved to arrive at the system optimal solution.

For the plant and control design problem, there are basically three coordination architectures, as shown in Fig. 2.3: *(i) alternating* plant and control design, i.e. first the plant is optimally designed. Using this outcome the controller is optimally designed. Subsequently, the plant is optimized again, etcetera. The coordinator alternates between optimizing the plant and optimizing the control until the coupled variables have converged. *(ii)* control design *nested* within plant design, i.e. every evaluation of a plant, requires the full optimization of the controller design; and *(iii) simultaneous* plant and controller design (i.e. solving (2.2) all-in-one). Often, *nested* coordination architectures are referred to as *bi-level*, implying a nested optimization between two design layers. These have been many times used in literature for components sizing and control studies.
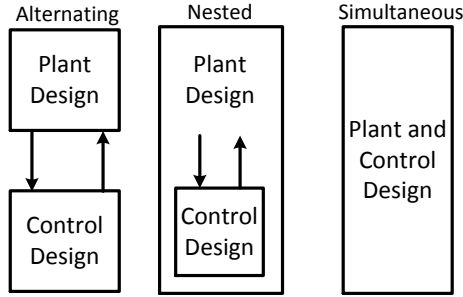


Figure 2.3: Coordination Architectures for System-Level Design (SLD) in HEVs.

In mid $'90$, when the hybrid vehicle market emerged, the plant design problem and the control design problem were treated completely independently. Nowadays, in most literature and practice, a clear distinction is made between the plant and the control design variables and objectives, where (2.2) becomes the following co-design problem

$$
\begin{aligned}
\min_{\mathbf{x}_{\mathrm{p}}, \mathbf{x}_{\mathrm{c}}(t)} \quad & \mathbf{J}(\mathbf{x}) = \{\mathbf{J}_{\mathrm{p}}(\mathbf{x}_{\mathrm{p}}, \mathbf{x}_{\mathrm{c}}(t)), \mathbf{J}_{\mathrm{c}}(\mathbf{x}_{\mathrm{p}}, \mathbf{x}_{c}(t))\} \\
s.t. \quad & g_j(\mathbf{x}_{\mathrm{p}}, \mathbf{x}_{\mathrm{c}}(t)) \leq 0, \quad j = 1, 2, ..., m, \\
& h_l(\mathbf{x}_{\mathrm{p}}, \mathbf{x}_{\mathrm{c}}(t)) = 0, \quad l = 1, 2, ..., e,
\end{aligned}
\tag{2.12}
$$

and to the system's dynamics as in (2.2).

The plant cost function, $\mathbf{J}_{\mathrm{p}}$, and the control cost function, $\mathbf{J}_{\mathrm{c}}$, may contain any combination of the objectives from (2.7).

For the plant design problem, in the literature also distinction is made between topology design and component sizing optimization. Usually, the component sizing problem is solved for a fixed topology. The choice of topologies to be analyzed has, so far, been

mainly dictated by practical experience rather than by a topology optimization procedure. A computational tractable method for combined topology and component sizing optimization of the plant design is an open research question.

In the next subsection we give an overview of the currently employed methods for topology optimization of the HEV plant. Most of these methods aim at finding feasible topologies, not necessarily optimal topologies. Subsequently, in the forthcoming subsections we survey methods for alternating, nested, and simultaneous plant and control design of HEV vehicles.

## 2.4.1   HEV Topology Generation or Selection

In practice, a HEV topology is often *selected* on the basis of criteria that derive from expert knowledge. In this approach the set of rules forming the criteria can be derived from expert knowledge, availability of components on the market, other HEVs and so on. The selected topology is very likely not optimal. Recent studies show that very small changes in known topologies, such as the Toyota Prius or Chevrolet Volt, can lead to more efficient HEVs (w.r.t. cost or fuel) [70].

Another approach for arriving at a suitable topology is to evaluate at all possible topologies that can be constructed from a predefined fixed set of components. This is sometimes referred to as *topology generation*.

Usually topology generation means the search for all feasible topologies, $\mathbf{T}^f$, within a (large) set of possible topologies, $\mathbf{T}^p$, given design constraints, $\mathbf{c}$,

$$
\begin{aligned}
Find\ all\ \ &\mathbf{T}^f \subseteq \mathbf{T}^p, \\
s.t.\ \ &\mathbf{c}(T^f) \leq 0.
\end{aligned}
\tag{2.13}
$$

A method to solve (2.13) was proposed in [107] where $\mathbf{c}$ consists of functionality (i.e., power delivery, hybrid functions, feasibility) and cost constraints. Each topology is modeled as an undirected connected finite graph, where each component is a node of the graph. Based on these nodes, a set of constraints are defined and (2.13) is solved as a constraint satisfaction problem over finite domains (FD) [108]. The authors of [107], apply this method on a set of 16 power-train components (including two PGS, two EMs, three clutches, etcetera) searching for feasible series, parallel, and series-parallel HEV topologies. They show that the initial search space of $5.7 \cdot 10^{45}$ possible topologies is reduced to 4779 feasible topologies.

Another recent method by [109] to solve (2.13) aims at developing series-parallel topologies with one or multiple PGS. This method models a topology as a bond graph and, similar to the previous method, uses constraints to arrive at feasible topologies. Using this method, in [110], the topology generation and optimization of a mid-size passenger

car is discussed. When series-parallel topologies with double planetary gears is used, in [111] and [112] a method to automatically model and exhaustively search for optimal topologies is proposed. The authors of [111] show, using Toyota Prius as a study case, that improved configurations (offering reduced fuel consumption) are found.

These studies show how the initial set of candidate topologies can be reduced in a systematic and complete way. At the same time, they highlight new challenges in defining and solving this kind of problems.

Once a topology has been decided on, the co-design problem (2.12) is to be solved. Next we distinguish sequential, alternating, nested, and simultaneous methods. *Sequential* is a special instance of the *alternating* coordination-strategy (plant and control subproblem are solved only once, sequentially) and is also referred to as a design-first-then-control methodology.

## 2.4.2   Design-First-Then-Control for HEV Design

The design-first-then-control is the simplest strategy one can envision; the coupling between the plant design and control design problem is neglected. Mainly due to its decentralized manner, this strategy has been a pioneer when approaching HEV design. The control problem is approached for a fixed plant, i.e., fixed (a), (b) and (c) layers in Fig. 2.1 on pg. 20.

The development of the control algorithm, i.e., the energy management system (EMS) of a HEV powertrain, consists of finding the set-points of the power converters that can deliver the driver's required power in an "optimal" way. Optimality is defined in terms of fuel consumption ($J_1$ from (2.7)), but may also include pollutant emissions ($J_4$ and $J_5$ from (2.7)), drivability, or performance criteria related to the battery (e.g., life degradation or charge). This optimal control problem, given by

$$
\begin{aligned}
\min_{\mathbf{x}_c(t)} \; & J_c(\mathbf{x}_p, \mathbf{x}_c(t), \Lambda) \\
s.t. \; & g_j(\mathbf{x}_c(t)) \leq 0, \quad j = 1, 2, ..., m, \\
& h_l(\mathbf{x}_c(t)) = 0, \quad l = 1, 2, ..., e, \\
& \text{and to the system's dynamics as in (2.2),}
\end{aligned}
\tag{2.14}
$$

has been approached by two main categories of methods as depicted in Fig. 2.4: (i) optimization based methods and, (ii) rule based methods.

The strategies based on rules, either heuristics [18] or fuzzy logic [19–21], are based on expert knowledge translated into boolean rules, to make the power sources work in their most efficient regions. These algorithms are easy to implement and they don't require high computation times. Yet they can not offer any proof of optimality of the solution found. They may require significant tuning effort and may change significantly

for each topology. This disadvantage has motivated the investigation and the applicability of rigorous optimization algorithms.
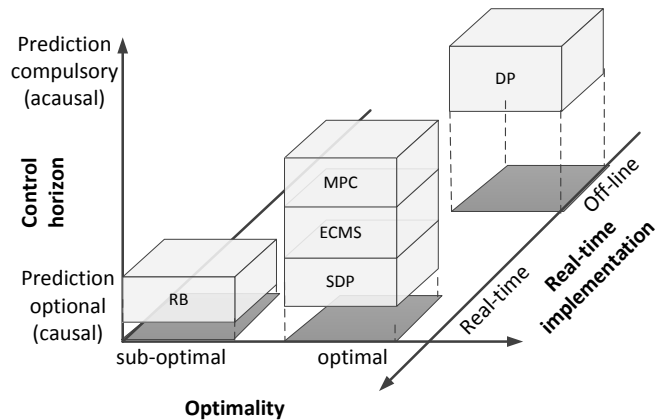


Figure 2.4: Classification of energy management strategy categories: optimality, control horizon and real-time implementation. RB = Rule based, MPC = Model Predictive Control, (S)DP= (Stochastic) Dynamic Programming, ECMS = Equivalent Consumption Minimization Strategy.

There exist a wide variety of optimization algorithms for controller design. Two categories may be distinguished: real-time implementable or off-line algorithms [113]. Dynamic Programming (DP) is widely used for off-line optimization and DP typically serves as a benchmark for evaluating other (real-time) algorithms [114]. There exist also optimization-based algorithms that can be online implementable. These are mostly based on Equivalent Consumption Minimization Strategy (ECMS) [22–28], Stochastic Dynamic Programming (SDP) Strategies [29–32], or Model Predictive Control (MPC) Strategies [34, 35]. Reviews of EMS can be found in review articles as [36–42]. Benchmark comparisons are given in [63] and [43], where several algorithms are implemented and compared for controlling the Plug-In Chevrolet Volt HEV.

Note, again, that all these energy/power control algorithms are derived for an a priory defined HEV. Therefore, the dependence between the system design and the control algorithm design is not taken into account. Yet, this coupling exists, e.g., the dimension of the battery will influence the optimal control problem. To overcome this limitation, attempts to design better systems have been developed using design-and-control methodologies (in either an *alternating, nested* or *simultaneous* fashion).

### 2.4.3    Alternating, Nested and Simultaneous Coordination Schemes

For each topology, to find the set of optimal $\mathbf{x}_p^*$ with a nested coordination scheme, various authors [57, 58, 62, 63, 115–117], have used exhaustive search in the plant design optimization problem, combined with a rule based or DP for control design. With exhaustive search, also referred to as brute force search, the design space is gridded and for each grid point the cost function is evaluated [118]. This is depicted in Fig. 2.5 for the parallel topology from Fig. 2.2 on pg. 21, where the hybridization potential is analysed in terms of fuel consumption for $\mathbf{x}_p^{pr} = \begin{bmatrix} P_m & C \end{bmatrix}^T$.
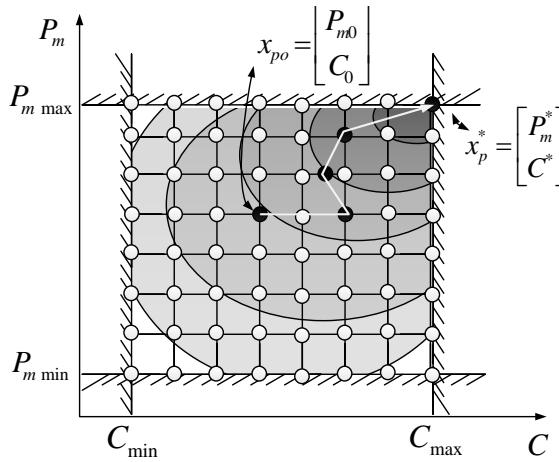


Figure 2.5: Design space exploration using exhaustive search (light grey dots), an optimization algorithm (dark grey points) and the interpolation contour lines of the cost function.

Using the values of the cost function at each point the shape of this function can be interpolated, and a design can be chosen. For the sake of clarity, we depict this for two plant design variables only. If more design variables are included the visualisation and interpretation of results will be difficult. Then, Latin Hypercube Sampling can be used to explore the cost function in all the feasible design spaces [119].

In [58], such a nested exhaustive search framework is used to compare four topologies (a conventional, a start-stop, a full parallel HEV and a power-split HEV), for a passenger car application given different driving cycles. Due to hybridization and engine downsizing, the authors present more than 33% $CO_2$ decrease for the full-parallel and power-split (similar to Toyota Prius) HEVs. In [62], focusing on the transmission selection, three full-parallel hybrid electric drivetrain topologies are investigated, In [57], *one-variable-at-a-time* exhaustive search is used for the component sizing optimization loop and DP is used for the control algorithm. Considering a series-hybrid microbus, the authors

define $\mathbf{x}_p^s = \begin{bmatrix} P_{e+m1} & C \end{bmatrix}^T$, with $P_{e+m1}$ representing the generating group power (i.e., the combined generator motor and engine) and $C$ representing the battery capacity. With a fixed battery pack the generating group of the series architecture ,$P_{e+m1}$, is varied in size and the possibility of downsizing or upsizing the engine is analysed. Once a value was found for $P_{e+m1}$, this is fixed, and the variation on the battery pack sizing is investigated. We refer to this as *one-variable-at-a-time* exhaustive search, since when mapping this problem to the previous example from Fig. 2.5, the authors vary one variable at a time, resulting in only one row/column, and repeat this process for all design variables.

The exhaustive search strategy is simple and insightful, but only works for a limited number of plant design variables. The computational burden quickly grows, for increasing number of plant variables. The computational time may be expressed as $T = T_a \cdot \prod_{i=1}^{N} g_i$, with $N$ the number of plant design variables, $T_a$ the time in which the optimal control problem is solved and $g_i$ the number of grid points for variable $i$. The grid needs to be sufficiently dense to guarantee a reasonable accurate interpolation between the grid points. Alternatively, for increasing number of plant variables, one may consider to use a Latin hyper cube design exploration with a radial basis of Kriging type of surrogate model for the interpolation [120].

In recent years, the usage of optimization-base multi-level design, (introduced already for different applications [121–123]), has seen an increased interest. By using an optimization algorithm for the plant design problem, one seeks to reduce the number of cost function evaluations, compared to exhaustive search (see for example Fig. 2.5), with a better exploration of the design space in the design region of interest.

The SLD problem is usually nonlinear and often also has mixed-integer characteristics. In the literature about multilevel optimization of HEV, a wide variety of algorithms has been selected for the plant optimum design. One may distinguish between derivative-free and gradient based algorithms. Examples of derivative free algorithms include: Dividing Rectangles (DIRECT) [130, 142], Particle Swarm Optimization (PSO) [103, 135, 136], Genetic Algorithms (GA) [17, 67, 143, 144] and Simulated Annealing (SA) [66, 145]. Articles that use a gradient based algorithm include Sequential Quadratic Programming (SQP) or Convex Optimization (CO) [137, 140, 141, 146]. In Table 2.1 a classification of several frameworks from existing literature is shown. This table tabulated the type of algorithm for the plant design problem, the type of algorithm for the control design problem, and the coordination strategy to arrive at the system optimal solution.

Vehicle simulation packages[1], containing rule based algorithms for HEV control, have facilitated the fast development and simulation of design frameworks. For instance, using a rule based (RB) control algorithm nested within multi-objective GA [17], in [67] the sizing of a parallel hybrid bus is discussed for multiple objectives, $J_1$, $J_4$, $J_5$ and $J_6$ from (2.7). Besides the benefits for design, the authors highlight that: (a) the increase

---

[1]Such as ADVISOR [http://www.nrel.gov/analysis/models_tools_archive.html] [Online; accessed 18-November-2014], or PSAT [http://www.transportation.anl.gov/modeling_simulation/PSAT/][Online; accessed 15-February-2012]

Table 2.1: Classification of several frameworks from existing literature, as a function of **coordination methods** and **algorithms** used for sizing and control design (ECMS = Equivalent Consumption Minimization Strategy, (S)DP = (Stochastic) Dynamic Programming, SQP = Sequential Quadratic Programming), SA = Simulated Annealing, PSO = Particle Swarm Optimization, RB = Rule Based, SADE = Self-Adaptive Differential Evolution, DS = Downhill Simplex Method).

| Algorithms | | Coordination Methods: |
|---|---|---|
| Component Sizing | Control | **Sequential** |
| Fixed | RB | Parallel HE Truck [124] |
| | ECMS | Parallel Small HEV [24], Through-the-road Parallel Midsize HEV [125] |
| | SDP | Mid-size Series-Parallel HEV [32] |
| | DP | Parallel HE Truck [124] |
| | | **Nested** |
| Exhaustive Search | RB | Large-size passenger parallel HEV [59], Medium-Duty Parallel HE Truck [115], Small passenger HEV with CVT [90], Torque-Assist Midsize HEV [126], Parallel HE Truck [44] |
| | ECMS | Fuel Cell HE Truck with two in-wheel EMs [116] |
| | DP | Passenger HEV (Parallel [60, 61], Torque-Assist [126], Large Parallel [62], Compact Parallel [63], Several vehicles [58]), Heavy-Duty HEV [119], HE microbus [57]. |
| SQP | RB | PNGV passenger HEV [127] |
| | DP | Parallel HE Class 8 Truck [65] |
| DIRECT | RB | Parallel passenger HEV [8, 64], Mid-size HE SUV [128] Mid-size parallel HE SUV [129], Parallel passenger HEV [130] |
| SA | RB | Parallel passenger HEV [8, 64, 130], Series HE Commercial City Bus [66] |
| DS | RB | Series passenger PHEV [131] |
| SADE | RB | PNGV parallel passenger HEV [132] |
| Single / Multi-Obj. GA | RB | Parallel passenger HEV [64, 130], Parallel HEV transit bus [67], Fuel-cell Parallel HEV [133], Parallel HEV [8], Hybrid and Electric Submarine [69] |
| | SQP | Hybrid and Electric Submarine [134] |
| | DP | Parallel Class 8 HE Truck [44] |
| PSO | RB | Parallel passenger HEV [8, 64, 104] |
| | DP | Midsize Parallel HEV [103, 135] Torque-assist and Parallel passenger HEV [68], Parallel Class 8 HE Truck [44], Series PHEV Bus [136]. |
| | | **Simultaneous** |
| Convex | Opt. | Series PHEV Bus [136–140] Parallel PHEV [141] |

of population size of the algorithm will result in improved accuracy of results; (b) no user-supplied weights of each objective must be provided; and, (c) more driving cycles must be used to improve this methodology and the design. This is addressed in [69] and [134], where the same strategy is applied to find the optimal design of a hybrid submarine, investigating three different topologies for four different driving cycles. This study shows that multi-objective GA can handle a very large design problem, with 16 objective functions and a 9 dimensional design space, with both discrete and continuous design variables.

One clear drawback in these studies is the usage of rule based algorithms for controller design, which is sub-optimal. An alternative is to use for example an evolutionary algorithm as Particle Swarm Optimization (PSO) in combination with DP for optimizing the control strategy, as used in [103, 135, 136]. In this novel framework, Dynamic Programming ensures finding the optimal control policy for every population point candidate selected by PSO in the outer-loop. The authors use this framework to optimally size and control a parallel passenger HEV, and compare its results with previously developed frameworks, that use SQP in the outer loop (plant design) and RB algorithms in the inner loop (controller design). It is shown that RB algorithms are less fuel efficient (by 11% for this case) and lead to a more expensive system (by 14%) than optimal solutions obtained by PSO.

The frameworks that solve the plant design problem using stochastic algorithms such as PSO, GA, or SA, or using deterministic search algorithms such as DIRECT, can handle nonlinear cost function and constraints, searching the design space globally. Yet, when the cost function behaves smooth and has only few local minimizers, a derivative based algorithm will offer a faster solution to the optimization problem. Also, a larger number of plant variables can be addressed in that case.

The typically used $J_1$ cost function from (2.7) is multi-modal (with many local minima), and sometimes noisy and discontinuous [130]. To ensure the receivability of the global optimum, in [137, 146, 147] and in [80] the HEV design problem is formulated as a convex optimization problem, with proposed convex component models and integer control signals obtained by heuristics. Comparative studies of the gradient-based and the derivative-free algorithms for HEVs optimal design are presented in [148]. Further, comparisons between only the derivative-free algorithms for HEVs optimal design can be found in [130] and [64].

## 2.5 Trends in Optimal System Level Design for HEVs

An important driver for optimization approaches in HEV vehicle design is the legislative restrictions which have become increasingly tight during the last two decades. Emission regulations have evolved from Euro 1 in 1993 to Euro 6 in 2014 (changing both permissiveness (e.g., $CO_2$ levels) and focus (e.g., from $CO_2$ to $NO_x$ or PM)). The number of

yearly publications on HEV optimization approaches has steadily grown (see Fig. 2.6).
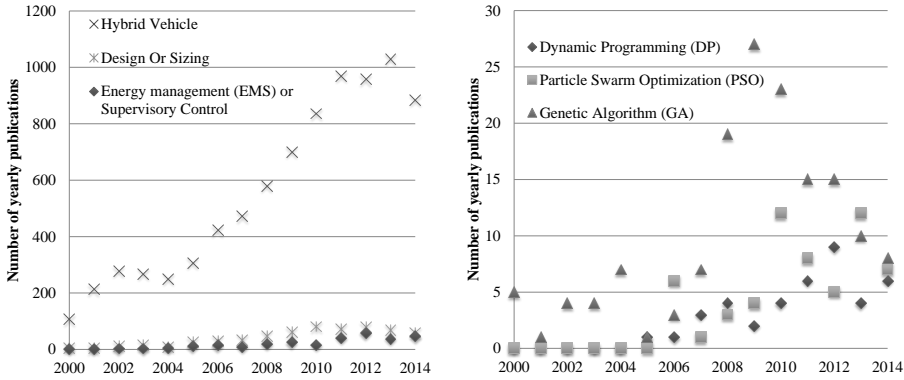


Figure 2.6: Research trends in hybrid vehicles design and optimization algorithms used. The curve shows the number of papers in the Google Scholar database containing the key words *hybrid vehicle* and the keywords in the legends as parts of their title.

When defining an optimization problem, its target is a formal transposition of vehicle manufacturer preferences on the constructed system. In turn, the manufacturer tries to meet all legislative restrictions and create a vehicle competitive on the market, appealing to customers and financially-beneficial. In this frame-up, the challenge to have a general problem definition is even bigger, since these dependencies are changing over time (e.g., emissions regulations). These challenges have led to constant development of control algorithms for HEVs (named either Supervisory Control or Energy Management Systems). In Fig. 2.6 one can see an ascending trend in the use of Dynamic Programming as a control algorithm. In fact, DP is used as a benchmark comparison for the development of other algorithms (real time implementable).

For solving the problem of optimal system design there is no universally accepted or widely used algorithm (as for example in control design DP). The trend in algorithms selection, for component sizing is to use evolutionary optimization algorithms. Among these, most commonly used optimization algorithms are GA and PSO, as shown in Fig. 2.6. Furthermore, multiple research articles report the computational inefficiency of exhaustive search, that leads to its inapplicability for large multi-dimensional design spaces.

Another trend is the increased focus on the driving cycles used in the HEV optimization problem formulation. Each manufacturer will design a car suitable for certain road types (road (e.g., highway, in-city, inter-urban), off-road, ship, rail or air) and applications (e.g., heavy duty vehicle, passages, bus), that will use a specific driving cycle. These range from high speed highway driving on flat road, to city driving with altitude variations, and all the variations in-between. The ideal HEV should be fuel efficient in all situations in

which it is used. In most cases, designers/researchers choose to vary the driving cycle in the design step of the hybrid vehicle to have a more efficient vehicle (in terms of energy) [48, 68, 116]. Also, synthetic cycles can be constructed to be shorter (enabling thus faster simulations or larger design space explorations) but more representative of the actual driving cycles. In this direction, the methods based on Markov Chain theory show promising results, as presented in [100, 149, 150].

Depending on the shape of the optimization function, and the types of constraints, an optimization algorithm may prove to be better than others. Typically, the road types and applications dictate a choice of topology, eliminating layers (a) and (b) in Fig. 2.1. In [130] and [44] different optimization algorithms, for the sizing loop (plant design), are compared to find the optimal design for one topology. For the control, one algorithm is used in all cases. At the expense of larger batteries, GA reaches a design with 7% reduced fuel consumption. Next, a design that doesn't require engine downsizing is reached with PSO algorithm, where the 5% fuel consumption is achieved with a smaller electric machine. Without continuing with this analysis, one must be aware that these results are sensitive to how the algorithms are tuned (such as maximum number of function evaluations and, to what supervisory control algorithm is used).

In the case of a strong nonlinear optimization function, the algorithms that use the gradient of the function, as SQP, often converge to a local minimum. To avoid premature convergence and local optima, one can start from different initial points, $x_{p0}$ or use a global optimization algorithm, as GA, PSO or another. Population-based evolutionary algorithms, as GA, PSO and SA, will have overall more function evaluations then gradient-based algorithms, since at each iteration (*generation*) they will evaluate $J$ for multiple starting points $x_{p0}$ (often named *population*).

Summarizing, different tricks must be applied when one desires to use a certain kind of optimization algorithm for sub-problem solving: (i) when convex optimization is used, the convexification of the optimization problem is required to guarantee finding the global optimum; (ii) when SQP is used, for the original problem (non-convex), the initial point $x_{po}$ can be varied to test the reach of local or global minimum; and (iii) when evolutionary algorithms are used various parameters have to be tuned (e.g., population size). Also, as stated earlier, it is important what coordination strategy is used, and which decomposition paradigm (overviews of such paradigms are found in [151] or [152]).

Designing a HEV with explicitly considering the coupling between the plant and its control has proved more promising than sequential design. These novel design approaches (nested or simultaneous) were investigated for the main components of the propulsion, i.e. electric motor, battery and combustion engine. Following this trend of combining the plant and control design, in the future more components can be considered as variables in the design process. Examples can include auxiliary units, e.g., air conditioning system or the power steering system, as considered in [44, 153, 154]. With the inclusion of more components as variables, the design problem becomes more difficult to define and handle.

## 2.6    Conclusions

This chapter reviewed the current state of design of hybrid vehicles, including architecture, sizing components, control algorithm and methods of finding the optimal system level design. Although, at first glance, there seem to be three major classes of HEV topologies to chose from (*serial*, *parallel* and *serial-parallel*), current market vehicles prove that minor design changes can lead to significant improvements in fuel consumption, costs of electrification, performance and generated emissions. These small changes, like the addition of a clutch or resizing the battery, cause many changes in different design levels (both at the subsystem level as-well as at the system level). Thus, the interaction between components is becoming increasingly important and, neglecting it in the design step leads to loss of potential after hybridization.

Starting with sequential designs, usually made in a top-down manner, a transition to coupled plant and control designs commenced in the last decade. The most popular variant being controller design nested within plant design. These approaches prove clear advantages but also introduce several challenges in solving this optimization problem. Sequential design is simple and intuitive, but neglects the influence from one design layer to another. The plant is designed without taking the controller into account. Subsequently, the controller is designed using the given design as is.

Bi-level optimization frameworks take the coupling between plant and controller design into account. One may distinguish a nested and an alternating formulation. Often used, nested optimization poses more challenges on finding a global optimal solution at the system level and creates a shift towards multi-disciplinary design. Even so, recent studies have shown that, HEV designs with significantly lower fuel consumption and emissions can be found. These are opportunities to be further investigated.

By analyzing existing publications, we can conclude that using optimization algorithms, to solve different optimization layers, have proven beneficial for design. These could be further used, in more extended coordination methods to include the selection of topologies and technologies. For instance, these extended coordination methods might include: (i) (simultaneous topology and sizing design) alternating with controller design; (ii) controller design nested with respect to simultaneous topology and sizing, (iii) topology alternating with sizing alternating with control; or (iv) simultaneous topology, sizing, and control design.

To substantially reduce the computational burden one can introduce approximations of the original problem (e.g., the convexification of the problem or metaheuristic models), can shorten the driving cycle used for design or can use parallel computing. Driving cycles used as input for the control algorithm (energy management strategy) should be build short, more realistic and more representative of realistic driving types.

How to address, in an (more) automatic way, multiple topologies with a large variety in the components types and numbers remains an open question. Further, the topology auto-

matic construction and optimization problems create challenges in the control algorithm development, that has to handle various topologies in an automatic way. To solve the system level design problem and find a HEV that can be market competitive, one may define the optimization targets to include besides fuel, also costs, emissions or performance aspects. Easy-to-use methodologies must be developed, to help developers, and industry in general, to reach better designs in early steps of HEV development process.

CHAPTER

# THREE

# FUNCTIONAL AND COST-BASED AUTOMATIC GENERATOR OF HEV TOPOLOGIES

**Abstract /** The energy efficiency of a hybrid electric vehicle is dictated by the topology (coupling option of power sources/sinks), choice (technology) and control of components. The first design area among these, the topology, has the biggest flexibility of them all, yet, so far in literature, the topology design is limited investigated due to its high complexity. In practice, a predefined small set of topologies is used to optimize their energy efficiency by varying the power specifications of the main components (sizing). By doing so, the complete design of the vehicle is, inherently and to a certain extend, suboptimal. Moreover, various complex topologies appear on the automotive market and no tool exists to optimally choose or evaluate them. To overcome this design limitation, in this work, a novel framework is presented that deals with the automatic generation of possible topologies given a set of components (e.g., engine, electric machine, batteries or transmission elements). This framework uses a platform (library of components) and a hybrid knowledge base (functional and cost-based principles) to set-up a constraint logic programming problem and outputs a set of feasible topologies for hybrid electric vehicles. These are all possible topologies that could be built considering a fixed, yet large, set of components. Then, by using these results, insights are given on what construction principles are mostly critical for simulations times and what topologies could be selected as candidate topologies for sizing and control studies. Such a framework can be used for any power-train application, it can offer the topologies to be investigated in the design phase and can provide insightful results for optimal design analyses.

# 3.1   Introduction

Optimal design studies are required for the upcoming hybrid powertrains introduced on the market, where various targets are to be considered. Besides fuel, which has been the biggest drive in developing hybrid vehicles, original equipment manufactures (OEMs) need to optimize their designs for emissions (e.g., $CO_2$, NOx), performance, costs or comfort [155, 156]. Driven by the OEMs engineering experience and the non-triviality characteristic of the choosing a topology question, design studies, for sizing and control, of hybrid powertrains assume the topology to be known [21, 64, 157]. This traditional, heuristic, design approach is hard to re-use, decreases the hybrid electric vehicle (HEV) chance to comply with future exhaust emission legislation and, usually, leads to costly re-design steps. These disadvantages arise mostly because the dependencies between various levels of design are neglected. Ergo, there is a need of integrating the topology design with control or sizing design, such that the explicit coupling between these design areas is addressed.

Prior studies [115, 126, 130, 141, 147] have shown that by integrating the sizing and control design of HEV, one can improve the energy efficiency significantly. More recent studies have also tried to show the influence of topology change of one or more components [6, 62, 68, 70, 96, 158–161] or to integrate the topology selection, as a discrete choice, with the sizing and control of components [44, 162, 163]. Yet, no methodology exists to build or determine suitable topologies candidates for these sizing or control studies and, as substitute, a discrete and limited set of topologies is used. Endeavors of developing topological synthesizing frameworks can be found in the works of [164] and [165], which are constructed for one particular *sub-system* of a bigger system (e.g., gearbox, electric machine).

In this chapter, to attain a hybrid electric powertrain optimal design, a constraint-search-based topology generation tool is introduced. This design framework requires a structured system-based approach to find the set of feasible topologies. Once this set is found, the design of individual topologies can be further reduced to match a particular application (e.g., an in-city bus), or, can be further optimized in terms of sizing and control. Automatically generating topologies is a heavy-computational problem [166], solvable within a finite time and design space only if the number of components is limited [108]. To solve this design challenge, the proposed framework is based on a limited set of components, from which it can find all *feasible* topologies. This limited set of elements can be seen also as a library of mechanical or electrical components from which one wants to construct topologies. By *feasible* domain we refer to a set of topologies that: (i) can ensure energy is delivered to the wheels; (ii) represent a hybrid electric configuration; (iii) avoid the redundant usage of components; and, (iv) can ensure certain hybrid modes/functionalities, if desired (e.g., Brake energy recuperation).

The proposed automatic topology generation methodology starts with defining in a more abstract manner the functionality that a hybrid vehicle should provide. This definition is

then completed by adding constraints on component connectivity and made robust again variations of the design dimensionality (e.g., more components can be added without breaching the problem setup). The benefit of such a tool lies also in the fact that, simple principles can restrict more then $5.7 \cdot 10^{45}$ design space (i.e., all possible solutions that can be constructed form a limited set of components) to a 4779 feasible set of hybrid topologies with at most 16 components each. The strength of this method is the flexibility and modularity of its construction and the high level of detail it provides for the construction of new hybrid vehicles.

The remaining sections of this chapter are organized as follows. After a brief description of HEV topologies and their design challenges is given in Section 3.2; the library of mechanical components is described in Section 3.3. Section 3.4 describes the constraint satisfaction problem, and how can this be implemented for automatically generating HEV topologies; and, Section 3.5 presents the search algorithm. Next, Section 3.6 reports results of the application of this design framework, and it is followed by concluding remarks in Section 3.7.

## 3.2 Topologies of Hybrid Electric Vehicles

Among the vast area of hybrid vehicles, three main categories of topologies can be distinguished: *series*, *parallel* and *(mixed) series-parallel*. The characteristics of these topologies are not going to be addressed in details here, seeing that in-depth details descriptions of them are given in comprehensive articles as [6,7,10,11,156]. The focus in view of this chapter is on the variety that these topologies have, and how, proven by current hybrids, they influence the fuel consumption, OEMs system costs and the return on investment of the customer. Each of these topology families (series,parallel) contains various descents that enable extra functionality modes (e.g., electric or engine-only driving) with the usage of extra components, as for example, clutches, brakes, etc. This is easily seen in current market examples, as the parallel Honda Civic, or the series-parallel General Motors (GM) Voltec, depicted in Fig. 3.1. Although, variants of hybrid cars, already, exist on the market, the topology (and its number of components) is not straightforward nor easy to choose. Several comparisons between topologies exist, and among recent ones, in [70] the configurations of power-split hybrids of Prius and Chevrolet Volt are compared. Using a dynamic modeling both configurations are compared and modified into Prius+ and Volt-, with no loss of performance. This demonstrates that small design variations can bring significant benefits in terms of costs, fuel or another design target. It is, therefore, important to investigate what are the trade-offs between these design targets, and how optimally global sets of parameters can be identified on a wide variety of topologies.

On today's market, there exist, increasingly, complex topologies, including power split devices, multiple clutches or brakes, more complex gearboxes, more motors and more battery packs. All these are design choices and the chosen ones will result in a certain
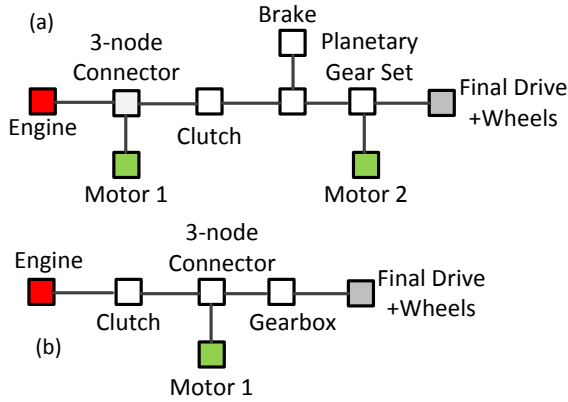
Figure 3.1: Two topologies examples found in current market vehicles, (a) GM Voltec and (b) Honda Civic.

system cost, energy efficiency, vehicle performance, emissions, and so on. This shows the difficulty of choosing a topology and motivates the need for automatic methods to synthesize these architectures for hybrid vehicles.

### 3.2.1   Hybrid Vehicle Functionality

In contrast to other vehicles, i.e., combustion-only or full-electric driven, hybrids are characterized by at least two prime movers, usually, referred to as *combustion engine* and an *electric machine*. With hybrids configurations, the fuel consumption and the emissions of a vehicle can be reduced, while achieving the same performance. This is attained by smartly combining the benefits of pure combustion engine driving with full-electric driving [12].

If one regards the prime movers as *power sources* and the wheels as *power consumers*, then any other choice of components connecting these two constitutes the topology. Depending on this topology choice, certain *functionalities*, or *modes*, of the hybrid power-train are (or not) enabled. In both, academia and industry, one can find different names for these *operation modes*. In principle, six categories are distinguished, and described below.

**Engine-only mode (Conventional vehicle)** represents conventional driving, i.e., similar to as the vehicle would not be a hybrid. In this case, the combustion engine is the only power source, which provides the requested traction power. This mode is possible if all

other power sources in the hybrid driveline can be decoupled from it (using clutches or bakes).

**Electric-only mode (Battery drive, Stop Go, Zero Emission)** refers to pure-electric driving with one or multiple electric machines. This mode requires the possibility of decoupling the engine from the driveline and its usability depends on the size of the battery.

**Motor-Assist, Motor power assist, or Boosting** refers to any combination of at least two different power sources in delivering the required power. These modes emphasise the ability of an electric motor to help share the load with an engine towards an optimal fuel driving and, furthermore, enable engine downsizing without loss of performance.

**Regenerative braking mode (Brake Energy Recovery)** refers to the process of recovering the kinetic energy of a slowing down vehicle into another form of energy, which can be used, directly, or stored until needed. This mode is both different and an improvement when compared with conventional braking systems, where the excess kinetic energy is converted to heat by friction, ergo wasted.

**Start-Stop mode** enables the vehicle to switch off its engine when stopped and turn it back on when needed. This functionality is achieved with an electric machine used either as a starter motor or as a full functioning electric machine, operating at higher voltages.

**Charging mode (Battery recharge)** is a mode where the engine is used both for propulsion as-well as charging the battery.

**Re-charge (Plug-in)** refers to the ability of the vehicle to be recharged from an energy grid, and it is not by itself a driving mode, but more of a technological feature.

To illustrate, several functionalities (i.e., regenerative braking, engine only, hybrid modes, pure electric) typically present in a hybrid car are depicted in Fig. 3.2, together with their power flow directionality. Here dots can represent component choices and lines their connectivity. By following a certain reasoning about the closing and openings of the clutches and brakes, these modes can be easily identified, for any topologies, (e.g., Fig. 3.1).

Note that, by having all modes in one topology does not directly imply the maximum driveline efficiency nor an optimal fuel consumption of a vehicle. The more complex one topology is, the more modes this vehicle can drive in yet also higher costs. Essentially, as mentioned before, the choice of topology (and its optimal parameters) will dictate system costs, fuel consumption, emission levels, functionality, complexity and weight. Therefore, an optimal selection of topology is required and must be integrated with an optimal sizing and control design of the vehicle. This leads back to the question introduced in the beginning, *how* to build all possible topologies (given a finite components set). To achieve this family of solutions, in the following sections, we map the functionalities that the system is supposed to have to a set of possible components, and
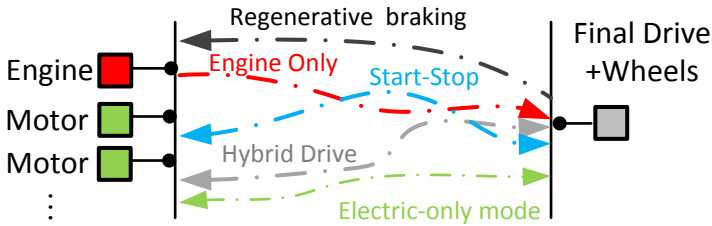
Figure 3.2: Operational modes and their power flows in hybrid topologies

overall build a framework to generate these topologies.

## 3.3   Mechanical and Electrical Components Library

A finite set of components constitutes a library from which any existing (i.e., known market HEV topologies, as the Toyota Prius) or future topology can be build. Besides the power sources (*internal combustion engine*, *electric machine*) and consumers (*wheels*) mentioned before, for further functionalities other transmission components are used (e.g., *clutches*, *brakes* or *power split* devices). This limited set of components, referred to as the *design platform* in design studies by [166, 167], is defined in Table 3.1, denoted by $\tau_i$, and is used here as a pre-defined input to the topology generator.

Table 3.1: Library of components used to generate topologies

| Component Number, $\tau$ | Component Name | Maximum Number of Instances | Number of Edges |
|---|---|---|---|
| 1 | Engine | 1 | 1 |
| 2 | Electric Machine | 2 | 2 |
| 3 | Gearbox | 1 | 2 |
| 4 | Planetary Gear Set | 2 | 3 |
| 5 | Differential+Wheels | 1 | 1 |
| 6 | Clutch | 3 | 2 |
| 7 | Brake | 3 | 1 |
| 8 | 3-node connector | 3 | 3 |

In Table 3.1, a 3-node connector represents a component that can connect 3-edges of other components, e.g., a torque coupler or power electronics. One example of a torque coupler is depicted in Fig. 3.1, where the electric machine connects, with fix or no gears, to the main shaft of the engine. This 3-node connector element is defined to confine

the design space, the computational time, and to maintain a certain level of abstraction as regards to other works in this research area. Furthermore, in the virtue of the same reasons, in this study only the principal propulsion components are considered and extra auxiliary units (e.g., power steering system, air compressors, power take offs, etc) are not considered. We are interested to attain all possible *series*, *parallel* and *(mixed) series parallel* topologies that can have at most two electric machines, a gearbox and two planetary gear sets. Moreover, several clutches and brakes can be used, which gives rise to a enormous design space of $5.7 \cdot 10^{45}$. We neglect here very particular cases, as topologies with in-wheel motors and we do not analyse the connectivity of the energy buffers (i.e., fuel tank and batteries). Without loss of generality, given this framework, this can be easily extended, later on, to include these or other particular design principles.

### 3.3.1 Modular Graph Representation of Topologies

Each component instance, denoted as $V$, that can appear in a topology, can be seen as an abstract representation of a real system, or collection of sub-systems that has certain functional principles. The automatic generation of topologies requires these components to have a modular and fixed formalized structure. This, to enable the computer-added synthesis of all possible topologies. For each component of this library several attributes are defined as follows: *(i) component type*, denoted as $\tau$ and, *(ii)* a *maximum number of instances*, i.e., how many times this component can be presented in a topology. The maximum number of appearances has been chosen such that, roughly, all possible topologies are covered.

**Definition 1** *A hybrid vehicle topology is an undirected connected finite graph, denoted as $T = (\mathbf{V}, \mathbf{E})$, characterized by a set of nodes (components), $\mathbf{V}$, and edges (connections between components), $\mathbf{E}$, with the set $\mathbf{E}$ containing two-element sub-sets of $\mathbf{V}$. Furthermore, each node $V \in \mathbf{V}$, representing a particular component, is characterized by the component type ($\tau_i$) and instance, which define the degree of the node.*

For ease of readability, the subscript of each V will combine these characteristics (*component type* and *instance*) as

$V_{61}$ represents a node of component type $\tau = 6$, first instance (i.e., the first clutch),

$V_{62}$ represents a node of component type $\tau = 6$, second instance (i.e., the second clutch).

**Note**. For ease of understanding sets are marked in bold, i.e., $\mathbf{T}$ is a set of topologies, where each instance is denoted by $T$.
When the element V is a conventional, 5 or 6-speed manual transmission, it will have

an input and an output, which will be modeled as two edges. Using Definition 1, the conventional topology shown in Fig. 3.3 is written as

$$
\begin{aligned}
T &= (\mathbf{V}, \mathbf{E}), \\
with\ \mathbf{V} &= \{V_{11}, V_{61}, V_{31}, V_{51}\}, \\
\mathbf{E} &= \{\{V_{11}, V_{61}\}, \{V_{61}, V_{31}\}, \{V_{31}, V_{51}\}\}.
\end{aligned}
\tag{3.1}
$$
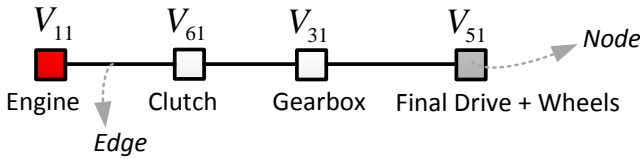


Figure 3.3: Undirected connected finite graph representation of a conventional powertrain topology.

We denote the set of all possible topologies $\mathbf{T}^p$. Furthermore, we distinguish between *feasible* topologies $\mathbf{T}^{fe}$ and *infeasible* topologies $\mathbf{T}^i$. We say that a topology T is *feasible* if and only if $T$ satisfies the following criteria: (i) can ensure energy is delivered to the wheels; (ii) represents a hybrid electric configuration; (iii) avoids the redundant usage of components; and, (iv) can ensure certain hybrid modes (functionalities). Otherwise, we say that the topology is *infeasible*. In the following sections, these criteria are transformed into constraints and the whole problem of generating such feasible topologies, $\mathbf{T}^{fe}$, is formulated as a constraint satisfaction problem (CSP). For this topology graph representation, we chose a level of detail that results in easy reconfigurable systems which mimics real vehicles. The components defined in the library (Table 3.1) define real life components, but can also be seen as a cluster. For example, a gearbox can be any transmission element (as for example a Continuous Variable Transmission) that has two edges.

## 3.4   Automatic Topology Generation Problem

Considering a predefined set of mechanical and electrical components, the problem of automatic generation of topologies reduces to finding all $\mathbf{T}^{fe} \subsetneq \mathbf{T}^p$ fulfilling all functional constraints of a hybrid vehicle. This is a feasibility search problem (NP-complete) [168, Ch.

8] that can be formulated as

$$\text{Find all } \mathbf{T}^{fe} \subseteq \mathbf{T}^p,$$
$$s.t.$$
$$\mathbf{c}^f_{1,\dots,l} \subseteq \mathbf{C}$$
$$\mathbf{c}^c_{l+1,\dots,z} \subseteq \mathbf{C} \tag{3.2}$$
$$\mathbf{C} = \mathbf{c}^f_{1,\dots,l} \bigcup \mathbf{c}^c_{l+1,\dots,z},$$

where $\mathbf{c}^f_{1,\dots,l}$ represents the $l$ functionality related constraints, $\mathbf{c}^c_{1,\dots,z}$ represents the $z$ cost related constraints and $\mathbf{C}$ the complete set of constraints for the problem. If, for example, also a minimal cost has to be considered, then the feasibility search problem becomes an optimization problem [169], and (3.2) becomes

$$\min_{\mathbf{T}^{fe} \subsetneq \mathbf{T}^p} \Phi(\mathbf{T}^{fe}),$$
$$s.t.$$
$$\mathbf{c}^f_{1,\dots,l} \subset \mathbf{C}$$
$$\mathbf{c}^c_{1,\dots,z} \subset \mathbf{C} \tag{3.3}$$
$$\mathbf{C} = \mathbf{c}^f_{1,\dots,l} \bigcup \mathbf{c}^c_{1,\dots,z},$$

where $\Phi(\mathbf{T}^{fe})$ is the optimization target, e.g., costs or number of components. In this chapter, we would like to obtain the complete family of solutions that satisfy functionality and cost-related constraints, hence to solve (3.2) rather then (3.3).

## 3.4.1 Hybrid Topology Synthesis Framework

The automatic generator of topologies proposed in this work and depicted in Fig. 3.4, is a combination of a

**i** *top-down approach*, e.g., mapping of each desired functionality of the system design level to constraints on the generated topologies, with a

**ii** *bottom-up approach*, e.g., building a topology by choosing particular components of the library, defined in Table 3.1, by reflecting on which are the functional principles of these components and what transmission components they need when forming a topology.

Such an approach, refereed to, as *platform-based design (PBS)* in [167, 170], was successfully used in [166] to synthesize topologies for an aircraft electric power system, and in [171] for designing wireless systems. Thorough this work, we use PBS to determine how to build constraints for the problem described in (3.2), thereby providing a structured way of definition, modification, or extension of constraints for a given platform.
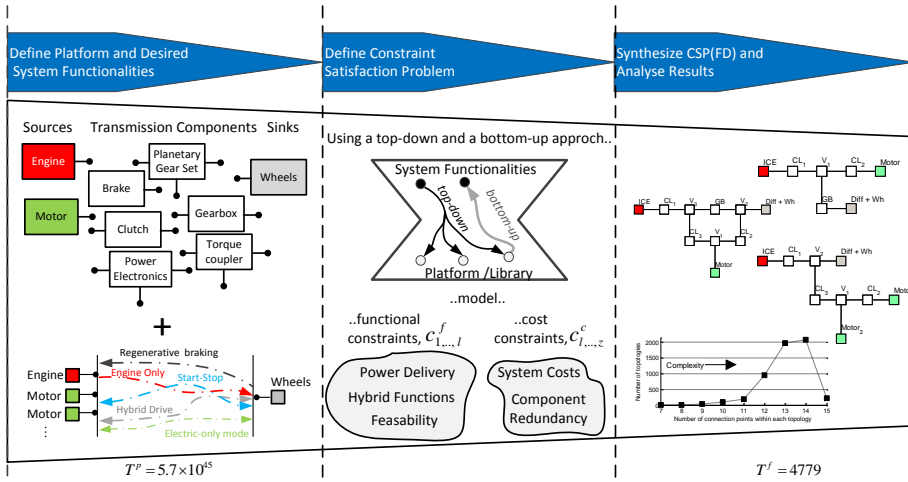
Figure 3.4: Illustrated description of the framework for generating hybrid powertrain topologies using functional and cost based principles

## 3.4.2   Formalizing the Constraint Satisfaction Problem

A CSP is, formally, defined by a set $< \mathbf{X}, \mathbf{D}, \mathbf{C} >$, where $\mathbf{X}$ is a finite set of variables, $\mathbf{D}$ is a set of corresponding domains and $\mathbf{C}$ is a finite set of constraints [108, 169]. The domain of a variable is the set of possible values that this variable can take. For these variables, $\mathbf{X}$, and their domains, $\mathbf{D}$, a set of constraints are build, restricting the values that the variables can simultaneously take. Formally, a constraint $C_{ijk...}$ between the variables $X_i, X_j, ..., X_k$ is any subset of the possible combinations of values of $X_i, X_j, ..., X_k$, i.e.,

$$C_{ijk...} \subseteq D_i \times D_j \times D_k \times .... \tag{3.4}$$

A constraint is said to be satisfiable if by assigning appropriate logical values (i.e., *true*, *false*) to its variables, this constraint holds. Summarizing, the CSP is a feasibility search problem for properly defined $< \mathbf{X,D,C} >$.

For instance, consider the classic crypt-arithmetic puzzle example: *Replace each letter by a different digit such that*

$$SEND + MORE = MONEY$$

*is a correct equation*, presented in [108, Ch.8]. Given this CSP, its set of elements are $\mathbf{X} = \{S, E, N, D, M, O, R, Y\}$, with their domain, the set of digits, $D = \{0..9\}$ and the constraints..

$C_1$  The sum must work out $1000 \cdot S + 100 \cdot E + 10 \cdot N + D + 1000 \cdot M + 100 \cdot O + 10 \cdot R + E = 10000 \cdot M + 1000 \cdot O + 100 \cdot N + 10 \cdot E + Y$;

$C_2$  the eight variables must all be assigned a different value.

$C_3$  $S$ and $M$ cannot be 0.

Solving this constraint satisfaction problem can find, among others, the solution $S = 9$, $E = 5$, $N = 6$, $D = 7$, $M = 1$, $O = 0$, $R = 8$, $Y = 2$. A solver can be used to explore all possibilities and yield the complete set of solutions to the CSP.

In a similar manner, to position the question of automatic generation of powertrain topologies as a CSP problem, the variables and their domains are identified as

$$\mathbf{X} = \mathbf{V} \cup \mathbf{E}, \tag{3.5}$$
$$\mathbf{D} = \{0,1\}^{|\mathbf{V} \cup \mathbf{E}|}, \tag{3.6}$$

with $\mathbf{V}$ the variables representing nodes and $\mathbf{E}$ the variables representing edges, both defined in (3.1). The values of 0 and 1 that components, $\mathbf{V}$, and edges, $\mathbf{E}$, can take represent their absence and presence, respectively. For instance, $V_{41} = 1$ would mean that the first PGS is present in the topology and $(V_{41}, V_{11}) = 0$ would mean that the first PGS is not directly connected to the engine.

### 3.4.3   Functional and Cost Based Principles for HEV Design

To construct a feasible HEV topology, defined in Sec. 3.3.1, generally, there are two categories of constraints that can be used. The first category, referred to as functionality constraints, has to ensure the proper functioning of the vehicle (i.e., criteria points (*i*), (*ii*) and (*iv*) in Sec. 3.3.1) and all its subsystems, whereas the second category, referred to as cost constraints, restricts the redundant usage of components (i.e., criteria point (*iii*)). The problem of mapping functional descriptions, explained in Section 3.2.1, to a possible topology is the core of platform-based design-by refinement paradigm [167]. This requires a prior description of the functionality that the system must employ and other restrictions on the design (cf. Sec. 3.2 and 3.3). Moreover, this top-down mapping of functional descriptions is combined with the bottom-up mapping of component functional constraints in order to create a generic, structured approach, that is easily reusable.

**Functionality Constraints**

For a functional solution to be found, three categories of constraints are explain sequentially through examples: (a) graph consistency; (b) powertrain hybridization and modes; and, (c) components and sub-systems correct functionality.

(a) Each candidate topology, $T^p$, is functional if the power sources are directly or indirectly related to the wheels via connecting elements, i.e., the graph is connected. Consider the following constraint: *"Each planetary gear set (PGS) should be connected to*

*3 other nodes"* as defined in Table 3.1. Taking the node representing the first planetary gear set, $V_{41}$, for a consistent solution, this implies the following constraints:
(1) if the PGS is present then there are exactly three other nodes connected to it;

$$V_{41} = 1 \rightarrow (V_{41}, V_{11}) + (V_{41}, V_{21}) + .. + (V_{41}, V_{83}) = 3, \tag{3.7}$$

(2) If the PGS is absent then there are no nodes connected to it;

$$V_{41} = 0 \rightarrow (V_{41}, V_{11}) + (V_{41}, V_{21}) + .. + (V_{41}, V_{83}) = 0, \tag{3.8}$$

(3) If a PGS connection is present then the PGS is present.

$$\begin{aligned} (V_{41}, V_{11}) + (V_{41}, V_{21}) + .. + (V_{41}, V_{83}) = 3 \rightarrow V_{41} = 1, \\ (V_{41}, V_{11}) + (V_{41}, V_{21}) + .. + (V_{41}, V_{83}) = 0 \rightarrow V_{41} = 0. \end{aligned} \tag{3.9}$$

Recall that $(V_{41}, V_{11})$ denotes a variable, as defined in (3.5). Furthermore, (3.7), (3.8) and (3.9) can be written as

$$(V_{41}, V_{11}) + (V_{41}, V_{21}) + .. + (V_{41}, V_{83}) = 3 \cdot V_{41}, \tag{3.10}$$

When both planetary gears sets are considered, $V_{41}$ and $V_{42}$, (3.10) yields $c_1^f$ as

$$\sum_{\tau,i} (V_{4n}, V_{\tau i}) = 3 \cdot V_{4n},$$
$$\forall\, i \in \{1, 2, 3\}, \tau \in \{1, .., 8\}, n \in \{1, 2\}. \tag{3.11}$$

Sequentially, to have consistency in the solutions found, similar constraints are built for all components defined in Table 3.1. To ensure no self-loops (i.e., the connection of one node to itself) exist the connection of one element to itself is constraint by $c_2^f$ in Table 3.2. More, the complete set of constraints used to generate topologies is presented in Table 3.2 and next, various types of constraints are explained and supported by examples. This search problem, defined in Table 3.2, can be then implemented using any solver suitable to CSP as it will be shown in Section 3.6.

(b) For powertrain hybridization, i.e., to have a hybrid electric vehicle, each topology should contain at least one node of type $\tau = 1$ (engine), one of type $\tau = 2$ (motor), one of type $\tau = 5$ (wheels) and one of type $\tau = 6$ (clutch). This will be constraint by $c_3^f$, which imposes the first instance of these elements to be present in all $\mathbf{T}^{fe}$. Next, each candidate topology is functional if the power sources, $\tau = 1$ (engine) and $\tau = 2$ (motor), are directly or indirectly related to the loads $\tau = 5$ (diff+wheels) via connecting elements, $(c_4^f)$, i.e., each solution is a connected graph.

Since, we are searching for all feasible HEV topologies within the design space, we do not build constraints for each functioning mode defined in Sec. 3.2.1. Enabling engine ON/OFF and full-electric driving are assumed to be desired in all topologies, i.e., there should be always one node of type $\tau_6$ (clutch) on one path between a node of type $\tau_1$

(engine) and a node of type $\tau_5$ (wheels). The placement of this $\tau_6$ is enforced through $c_5^f$ to be in direct connection with $\tau_1$, by constraining the edge between them, $(V_{11}, V_{61})$, to be always present, while positioning the clutch prior to the gearbox is another option. Although, usually, this clutch is part of the gearbox, or neglected from topology descriptions, we choose to place it next to engine for completeness and because not all topologies contain a gearbox. The remaining of the functioning modes, e.g., ICE only, are not enforced and will be used to post-process the results.

(c) Clutches and brakes are components used to couple or decouple parts of the driveline and their connectivity is constraint to ensure this functionality. For instance, no brakes or clutches are used to decouple the wheels from the remaining power train, and will be constraint here as well by $c_6^f$, $c_7^f$ and $c_8^f$. For brakes, we consider usual operation cases (a and b in Fig. 3.5), where the brakes are used to prevent freewheeling of the PGS (see also the GM Volt topology in Fig. 3.1.a). This implies that if a $\tau_6$ (clutch) is connected to a $\tau_4$ (PGS), this is done with an additional $\tau_8$ (virtual node), which enables another power path, or the usage of a brake ($c_6^f$, $c_7^f$ and $c_9^f$). As the defined platform contains
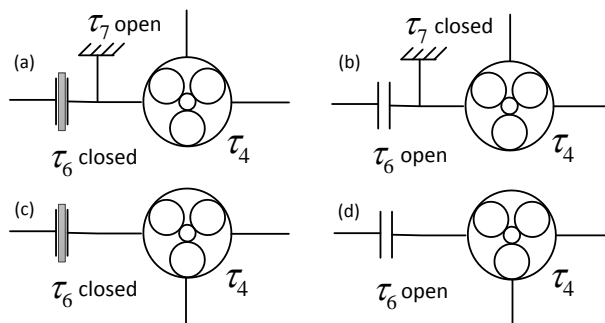


Figure 3.5: Different ways to connect a PGS using clutches and brakes

many two- or three-edges nodes (e.g., $\tau_6$ (clutches), $\tau_4$ (PGS)), a significant number of undesired loops can be obtained, if not restricted. By loop we refer to any part of the graph in which the search can be more than unidirectional (there are multiple options for transmitting power). These loops can result in an functional (yet redundant) HEV or in an nonfunctional vehicle. Examples of loops related to the expected functionality of the vehicle and its sub-components are depicted in Fig. 3.6. The depicted loops are counter examples for their corresponding constraints and all $c_{10}^f$ throughout $c_{22}^f$ restrict similar constructions.

Table 3.2: Definition of the automatic generation of HEV topologies problem

Find all $\mathbf{T}^{fe}(\mathbf{V},\mathbf{E}) \subsetneq \mathbf{T}^p(\mathbf{V},\mathbf{E})$,
Subject to

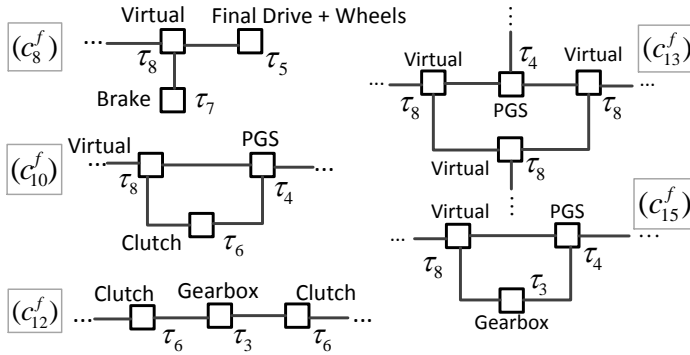| No. | Functional constraints | No. | Cost Constraints |
|---|---|---|---|
| $\mathbf{c}_1^{f*}$ | $\sum_{\tau,j}(V_{4n},V_{\tau j}) = 3 \cdot V_{4n}$<br>*similar constraints are implemented for all components. | $c_1^c$ | $(V_{8i},V_{8j}) + (V_{8i},V_{8k}) + (V_{8j},V_{8k}) < 3$ |
| $c_2^f$ | $\sum_{\tau,j}(V_{\tau j},V_{\tau j}) = 0$ | $c_2^c$ | $(V_{6i},V_{6j}) = 0$ |
| $c_3^f$ | $V_{11} + V_{21} + V_{51} + V_{61} = 4$ | $c_3^c$ | $(V_{6p},V_{8i}) + (V_{6p},V_{8j}) + (V_{6k},V_{8i}) + (V_{6k},V_{8j}) < 4$ |
| $c_4^f$ | $V_{41} + V_{81} > 0 \rightarrow V_{11} + V_{21} = 2$ | $c_4^c$ | $\sum_{i=1}^{3}(V_{7i},V_{8j}) < 2$ |
| $c_5^f$ | $(V_{11},V_{61}) = 1$ | $c_5^c$ | $(V_{31},V_{8i}) + (V_{6p},V_{8i}) + (V_{31},V_{6p}) < 3$ |
| $c_6^f$ | $(V_{6p},V_{41}) + (V_{6p},V_{42}) + (V_{6p},V_{51}) = 0$ | $c_6^c$ | $(V_{21},V_{8i}) + (V_{22},V_{8i}) \leq 2$ |
| $c_7^f$ | $\sum_{k,s,j}(V_{7k},V_{sj}) = 0$ | $c_7^c$ | $(V_{21},V_{6p}) + (V_{6p},V_{8i}) + (V_{6j},V_{8i}) + (V_{22},V_{6j}) \neq 4$ |
| $c_8^f$ | $(V_{11},V_{8i}) + (V_{51},V_{8i}) > 0 \rightarrow (V_{7j},V_{8i}) = 0$ | $c_8^c$ | $(V_{7n},V_{8i}) + (V_{6p},V_{8i}) + (V_{6k},V_{8i}) < 3$ |
| $c_9^f$ | $(V_{7i},V_{8j}) = 1 \rightarrow (V_{41},V_{8j}) + (V_{42},V_{8j}) = 1$ | $c_9^c$ | $(V_{8i},V_{8j}) + (V_{6p},V_{8i}) + (V_{6p},V_{8j}) < 3$ |
| $c_{10}^f$ | $(V_{4i},V_{8j}) + (V_{4i},V_{6p}) + (V_{6p},V_{8j}) < 3$ | $c_{10}^c$ | $(V_{6p},V_{8i}) + (V_{6p},V_{8j}) + (V_{8j},V_{8k}) + (V_{8i},V_{8k}) < 4$ |
| $c_{11}^f$ | $\sum_{p=1}^{3}(V_{31},V_{6p}) \leq 1$ | $c_{11}^c$ | $(V_{6p},V_{8i}) + (V_{6p},V_{4k}) + (V_{31},V_{4k}) + (V_{31},V_{8j}) + (V_{8i},V_{8j}) < 5$ |
| $c_{12}^f$ | $(V_{4n},V_{8i}) + (V_{4n},V_{8j}) = 2 \rightarrow (V_{8i},V_{8k}) + (V_{8j},V_{8k}) \neq 2$ | $c_{12}^c$ | $(V_{6p},V_{8i}) + (V_{6p},V_{8j}) + (V_{31},V_{8i}) + (V_{31},V_{8j}) < 4$ |
| $c_{13}^f$ | $(V_{4n},V_{8i}) + (V_{4n},V_{8j}) + (V_{6p},V_{8i}) = 3 \rightarrow (V_{6p},V_{8j}) \neq 1$ | $c_{13}^c$ | $(V_{31},V_{8i}) + (V_{31},V_{8j}) + (V_{8i},V_{8j})) < 3$ |
| $c_{14}^f$ | $(V_{4n},V_{8i}) = 1 \rightarrow (V_{31},V_{4n}) + (V_{31},V_{8i}) < 2$ | $c_{14}^c$ | $(V_{31},V_{8i}) + (V_{31},V_{8j}) + (V_{8i},V_{8k}) + (V_{8j},V_{8k})) < 4$ |
| $c_{15}^f$ | $(V_{8i},V_{8j}) + (V_{4n},V_{8i}) + (V_{4n},V_{8j}) < 3$ | $c_{15}^c$ | $(V_{8i},V_{8j}) + (V_{31},V_{8i}) + (V_{31},V_{8j}) < 3$ |
| $c_{16}^f$ | $(V_{4n},V_{8i}) + (V_{31},V_{4n}) + (V_{31},V_{6p}) + (V_{6p},V_{8i}) < 4$ | $c_{16}^c$ | $V_{31} + V_{42} < 2$ |
| $c_{17}^f$ | $(V_{4n},V_{8i}) + (V_{4n},V_{8j}) + (V_{31},V_{8i}) + (V_{31},V_{8j}) < 4$ | $c_{17}^c$ | $(V_{21},V_{4n}) + (V_{22},V_{4n}) < 2$ |
| $c_{18}^f$ | $(V_{4n},V_{8i}) + (V_{8i},V_{8j}) + (V_{31},V_{8j}) + (V_{31},V_{4n}) < 4$ | $c_{18}^c$ | $(V_{31},V_{8i}) + (V_{31},V_{6p}) + (V_{6p},V_{8j}) + (V_{6k},V_{8j}) + (V_{6k},V_{8i}) < 5$ |
| $c_{19}^f$ | $(V_{31},V_{4n}) + (V_{4n},V_{8i}) + (V_{8i},V_{8j}) + (V_{8j},V_{8k}) + (V_{31},V_{8k}) < 5$ | $c_{19}^c$ | $(V_{6p},V_{8i}) + (V_{6p},V_{8j}) + (V_{8j},V_{8k}) + (V_{31},V_{8k}) + (V_{31},V_{8i}) < 5$ |
| $c_{20}^f$ | $(V_{8i},V_{8j}) + (V_{8j},V_{4n}) + (V_{4n},V_{8k}) = 3 \rightarrow (V_{31},V_{8i}) + (V_{31},V_{8k}) < 2$ | $c_{20}^c$ | $(V_{6p},V_{8i}) + (V_{6p},V_{31}) + (V_{31},V_{8j}) + (V_{8j},V_{8k}) + (V_{8i},V_{8k}) < 5$ |
| $c_{21}^f$ | $(V_{41},V_{42}) + (V_{41},V_{8i}) + (V_{42},V_{8i}) < 3$ | $c_{21}^c$ | $(V_{6p},V_{8i}) + (V_{6p},V_{8j}) + (V_{6k},V_{8j}) + (V_{6k},V_{8k}) + (V_{8i},V_{8k}) < 5$ |
| $c_{22}^f$ | $((V_{41},V_{42}) + (V_{41},V_{8i}) + (V_{42},V_{8j}) + (V_{8i},V_{8j}) < 4$ | $c_{22}^c$ | $(V_{6p},V_{8i}) + (V_{31},V_{6p}) + (V_{31},V_{8j}) + (V_{6k},V_{8j}) + (V_{6k},V_{8k}) + (V_{8i},V_{8k}) < 6$ |
| $c_{23}^f$ | $(V_{2k},V_{6n}) + (V_{31},V_{6n}) < 2$ | | $\forall\, n \in \{1,2\},\ i,j,k,p \in \{1,2,3\},\ s \in \{1,..,7\}$ |
| $c_{24}^f$ | $(V_{2k},V_{31}) = 0$ | | |
| $c_{25}^f$ | $V_{22} = 0 \rightarrow V_{4n} = 0$ | | |
| | $\forall\, \tau \in \{1,..,8\},\ n \in \{1,2\},\ i,j,k,p \in \{1,2,3\},\ s \in \{1,..,7\}$ | | |

Figure 3.6: Counter-examples for functionality constraints

To compel a more real representation of existing topologies in the current hybrids market, we assume that the gearbox will not be used by the motor, constraining their direct connection with $c_{25}^f$ or their connection via a clutch $c_{24}^f$. Given these 25 functionality constraints, assuming that cost of components is not yet considered, all the topologies obtained, $\mathbf{T}^{fe}$, are able to transfer power from sources to consumers.

**Cost Constraints**

Once a feasible candidate topology has been found, which satisfies the constraints $c_{1,..,22}^f$, it is important to analyse it further for redundant usability of components. Such constructions are restricted using the *cost* constraints, $\mathbf{c}^c \in \mathbf{C}$ in (2.13), fully described in Table 3.2.

For instance, connecting three $\tau_6$ (clutches) in a row brings no extra functionality, increases the system cost and complexity, and is eliminated by $c_2^c$. More, connecting three $\tau_8$ (virtual nodes) to each other creates another virtual node and can be restricted by $c_1^c$. Based on the same judgement, loops as depicted in Fig. 3.7 are also eliminated. Aside of these unnecessary loops, a $\tau_8$ (virtual node) is not allowed to be connected to two $\tau_7$ (brakes) ($c_4^c$) nor two $\tau_2$ (motors) ($c_6^c$), the latter one being considered a sizing investigation.

Due to the typically high gearbox ($\tau = 3$) efficiencies, constraints are built to restrict its decoupling via clutches. Examples of these types of loops are graphically depicted in Fig. 3.8 and constrained by $c_9^c$ throughout $c_{22}^c$. By using $c_{16}^c \triangleq V_{31} + V_{42} < 2$, the appearance of the second $\tau_4$ (PGS) is not allowed if $\tau_3$ (gearbox) is present. This is enforced for decreasing the amount of solutions and for reaching cost-wise realistic solutions.
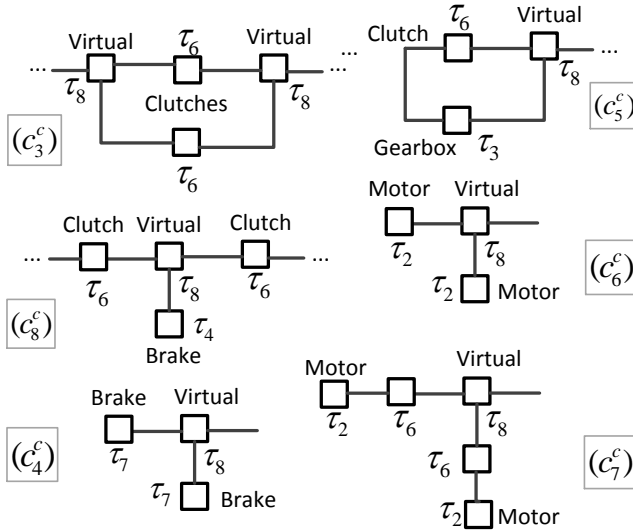
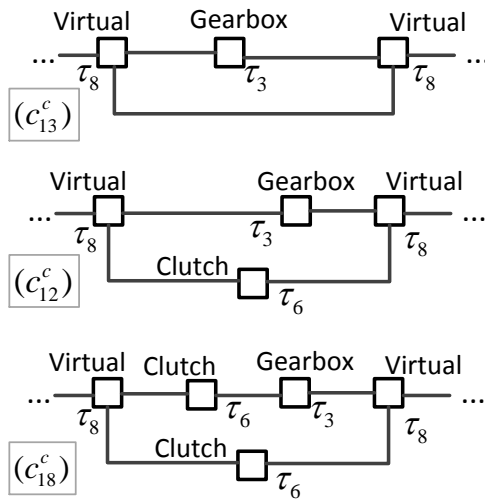Figure 3.7: Counter-examples for cost constraints



Figure 3.8: Examples of loops that decouple the gearbox and their corresponding constraints

## 3.5 Search Algorithm and Implementation

Since the value of the variables in this synthesis problem is represented by integer numbers and there is a finite number of components, this CSP problem becomes a constraint logic programming problem over finite domains (CLP(FD)) [108]. CLP(FD) are typically solved using a form of search and, among other used techniques, the most used are variants of backtracking, constraint propagation, and local search. In [169] an evaluation is done for constraint programming (CP) as a technique for solving CSP problems, and compared with operational research (OR) methodologies as simulated annealing (SA), genetic algorithms (GA), branch and bound (BB), tabu search (TS) and integer programming (IP). These comparisons are used here to motivate the selection of CP for implementing the topology generation problem.

According to [169], although computationally more expensive CP gives better quality solutions than methods as genetic algorithms, simulated annealing or tabu search. Moreover, the computational burden of CP performance improves greatly if additional constraints are introduced (e.g., symmetry) as-well as additional problem-specific information which is not always straight-forward in, for example, IP (Integer Programming). When compared with local search heuristic algorithms as simulated annealing, CP is more suitable for tightly constraints problems.

Comparing the method proposed in this chapter with previous methods (heuristic) choice of topologies [6, 62, 68, 70, 96, 158–161], we can highlight that this method offers a simple and complete solution in a very short time, whereas previous methods do not. As long as the constraints set, **C**, is well-defined, the search algorithm will converge to the set of solutions. The calculation time greatly depends on the number of mechanical components (elements) considered, the restrictiveness of the constraints and number, and the search algorithm. The problem defined in this chapter, in Table 3.2, is solved in less than 5 minutes[1].

## 3.6 Design Results

The proposed topology generation framework was implemented as a Constraint Logic Programming over Finite Domains (CLP(FD)) [108] program in SWI$^©$ (Prolog) [172] and the results were graphically depicted using Matlab$^®$. Examples of simple generated topologies are depicted in Fig. 3.9, were current passenger HEV (Honda Civic IMA, Opel Ampera) or heavier commercial vehicles (Mercedes Atego BlueTec Hybrid, DAF LF Hybrid) can be identified, and examples of more complex topologies are depicted in Fig. 3.10.

Comparing topologies can be done at different abstractization levels, as for example con-

---

[1]The computation was performed on a 64-bit Intel(R) Core(TM) i7 Computer @ 2.2 GHz and 8 GB RAM.
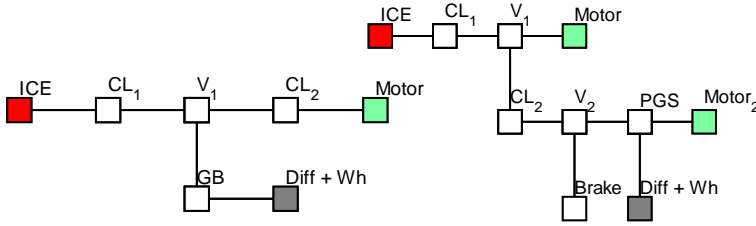
Figure 3.9: Examples of simple generated topologies: (left) Mercedes Atego BlueTec Hybrid, DAF LF Hybrid or Honda Civic IMA and (right) Chevrolet Volt / Opel Ampera
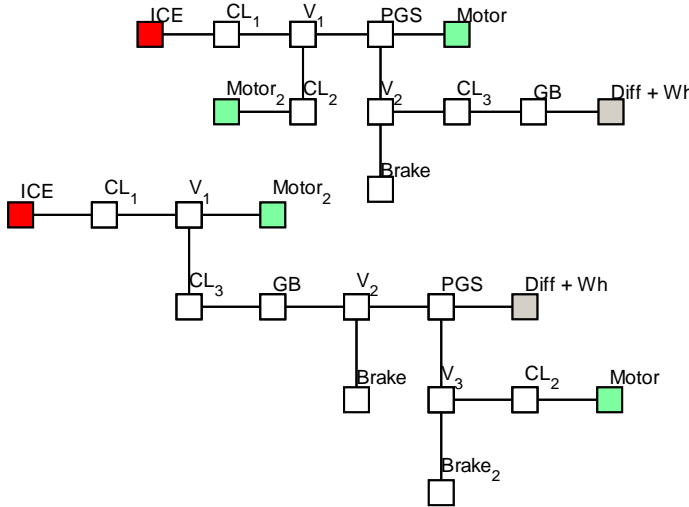


Figure 3.10: Examples of more complex generated topologies

sidering their number of nodes, construction complexity, costs, efficiency or control flexibility. In this chapter, the complexity of topologies is analysed as a function of their number of nodes, which requires no vehicle application knowledge and maintains a more general level of the methodology. Obviously, the larger the number of nodes and connections, the greater complexity of the physical construction of these power trains. This analysis can also indicate a directly proportional dependency to the control algorithms complexity and system cost. The analysis of each topology efficiency, functionality and cost will not be addressed as this stage, but it will be considered in the future.

Topologies or component variations will change the library of components defined in

Table 3.1 on pg. 42. The methodology to generate topologies is robust against these variations. For instance, with the addition of more electric machines or more batteries (i.e., maximum number of instances of the existing components), the search problem will be the same, and, most likely, the number of results will be bigger. At the addition of extra components to the library, new constraints must be defined to reflect the functionality and restrictions of these new components.

### 3.6.1 Design Space Complexity Analysis

By using the set of 47 constraints (conform Table 3.2) to solve (2.13) and by varying the *maximum number of appearances* of each component (i.e., third column in Table 3.1) the design space can be further analysed. This study does not give any indication of which topology is better for a vehicle (e.g., commercial or passenger vehicle), but provides a clear picture of all the possibilities that a manufacturer has when constructing a new hybrid car. In Fig. 3.11, several categories of topologies are identified based on their main construction characteristics and in Fig. 3.12 the dependency of the number of topologies on the number of connection points within a topology is shown.
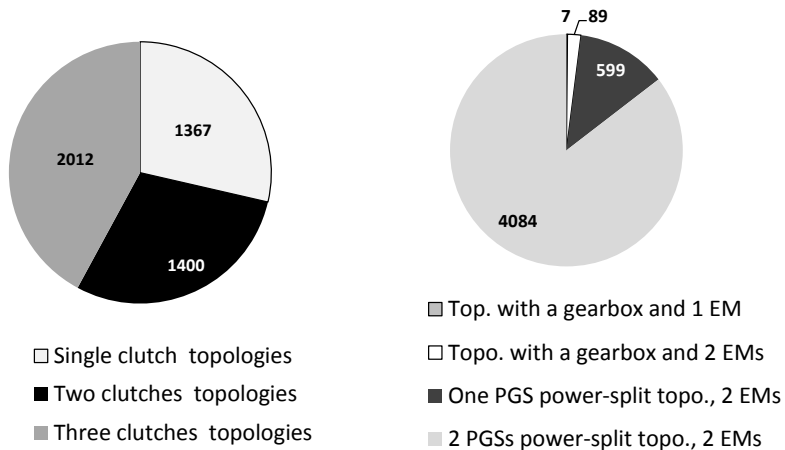


Figure 3.11: Clustering of the total 4779 HEV generated topologies

Although some found solutions can be symmetric (i.e., equal in functionality), this aspect was not considered in this research and will implemented in future work as preprocessing. Moreover, we observed from preliminary work that symmetry elimination does not change the trends presented in this section.

From the analysis of the results presented in Fig. 3.11, one can observe that topologies
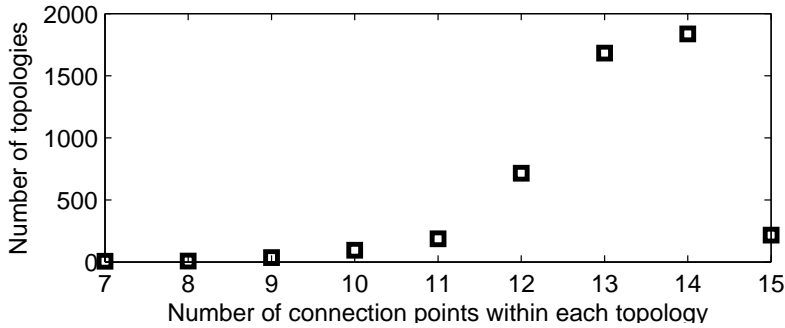
Figure 3.12: The number of generated HEV topologies as a function of their number of nodes.

which are very complex, including more than two planetary gear sets and two electric machines, represent the majority of solutions. Recent hybrid topologies, used in passenger vehicles, contain a transmission composed of a planetary gear set which combines two electric motors for driving. This is not yet used in heavy vehicles, where direct drive and manual or semi-automatic transmissions are widely used and effective. There exist 7 topologies with one gearbox and one electric machine (as for example one-motor parallel hybrid electric vehicle exemplified in Fig. 3.9-left, cf. Fig. 3.12) and 81 topologies with a gearbox and two electric motors. If no planetary gear set is allowed when having a gearbox, then there exist a limited set of 88 topologies suitable for heavy duty vehicles.

### 3.6.2    Discussion on Further Selection or Optimization of Topologies

The group of solutions when planetary gear sets and multiple virtual elements are added increases significantly. More than 4000 solutions contain more than 10 connection points, making them quite complex topologies to construct, control and, potentially, too costly. Complex topologies, as shown in Fig. 3.10, might not bring sufficient fuel efficiency to overcome the relative large cost of hybridization, therefore resulting in a long return on the investment for both the customer and the manufacturer. Thus, one option in reducing further the set of solutions is to restrict their complexity in terms of the number of nodes.

When solving the search problem defined in this chapter, no preference is given to nodes (all nodes are equally important). Yet, their importance, i.e., influence on the design results, can be analysed when looking at the complete set of generated power-train topologies, $T^{fe}$. A node is more important in the complete solutions set if this node appears predominately in the generated topologies. This can be seen in Fig. 3.13, where the complete set $T^{fe}$ is depicted. Easily seen from Fig. 3.13, through the removal of a single PGS or a Virtual component, $T^{fe}$ is significantly reduced (see also Fig. 3.11 and 3.12). Hence, the dimensions of the solution set, $T^{fe}$, increases with the increase of the maxi-
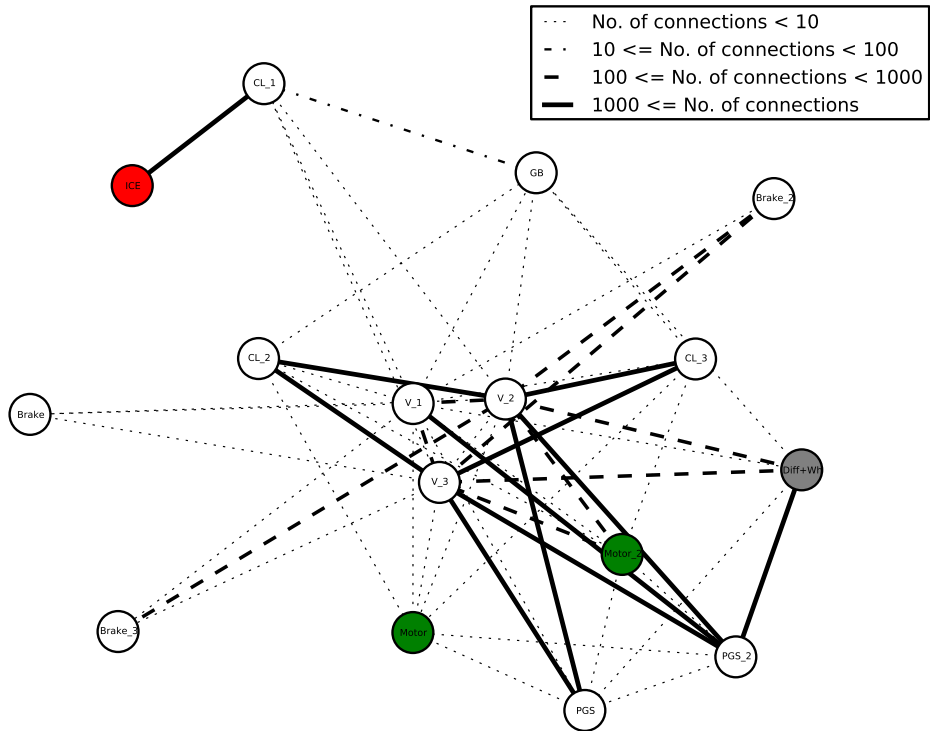
Figure 3.13: Graphical representation of the importance of each node/component in the topology graph for the whole family of generated topologies

mum number of element-instances in Table 3.1, but it depends also on the importance of the node. In this reasoning, a node with a large number of edges will expand more the set of results.

The analysis of topologies costs necessitates component cost models. Since these models are application driven (the price for one kWh of an EM used in heavy duty HEV is different than the price for one kWh of an electric motor used in hybrid passenger vehicle), the cost is not considered in this chapter. Although our aim was to provide a method generally applicable, analysing the synthesised topologies also form a cost perspective can be an improvement to the methodology.

Another way to further reduce the number of solutions (feasible topologies) may include, besides cost analysis, the analysis of efficiency [173], complexity of construction, the comparison of system's functionalities, verifying the ability to follow a driving cycle and so on. The analysis of the powertrain efficiency can be done, for instance, in a static manner (similar to a cost analysis). Next, the complexity of construction can be related to the importance of nodes. Using expert knowledge rule-base filters can be defined to

eliminate topologies that are hard-to-build or control. Analysing system's functionalities can be done for eliminating architectures that have the same functioning modes, by using a search algorithm (such as a combination of forward propagation and backtracking). The latter solution, of analysing the ability of a topology to follow a driving cycle and compare the results based on the fuel consumption, requires dynamic models that can, in a more automatic way, model this large set of solutions. Additionally, a control algorithm that can be applied to these topologies should be developed.

## 3.7  Conclusions

The contribution of this chapter is two-fold. First, we present a methodology to automatically generate, easily and in a structured way, hybrid vehicle topologies and second, we evaluate this method by investigating the results, classifying them and determining important trends in HEV topologies development. To begin with, a platform (library of components) was defined together with functionality and cost based principles. Using such principles, we set-up and implement a constraint logic programming problem, reducing the enormous original design space to a limited set of feasible topologies. The strength of this method is the flexibility and modularity of its construction and the high level of detail it provides for the construction of new hybrid vehicles.

It has been shown that, as a result of introducing new components the set of solutions increases significantly, yet no conclusion can be drawn on their fuel or cost efficiencies. Future work should address specific applications and how this generator can automatically filter out unsuitable topologies. Furthermore, to obtain an optimal system, studies to optimally size and control the components should be made.

# FOUR

# BI-LEVEL OPTIMIZATION FRAMEWORKS FOR SIZING AND CONTROL OF A HEV

**Abstract /**  This chapter discusses the integrated design problem related to determining the power specifications of the main subsystems (sizing) and the supervisory control (energy management) of a given hybrid electric vehicle. Different bi-level coordination schemes, with the outer loop using optimization algorithms as Sequential Quadratic Programming, Particle Swarm Optimization, Genetic Algorithms, or Pattern Search (DIRECT) and the inner loop using Dynamic Programming, are benchmarked to optimally size a parallel topology of a heavy duty vehicle. Herein, the main components of the powertrain are investigated for the plant design, e.g., the engine, the electric machine and the battery pack. The aim of this study is to find the optimal system design for the lowest fuel consumption, for the lowest hybridization costs and for the combination of both. Since the sizing and control of a hybrid vehicle is inherently a mixed-integer multi-objective optimization problem, the Pareto analyses are also addressed. The results shows significant fuel reduction by hybridization and engine downsizing and offer insights in the usability of these nested coordination schemes for system optimal design.

---

# 4.1   Introduction

More stringent emission legislations and oil-supply forecasts have motivated the development of hybrid and electric vehicles. This partial or complete electrification of vehicles has expanded the complexity of design, requiring nested optimization methods for improved fuel consumption. Using these approaches in addition to a (sub-)optimal control algorithm, the vehicle parameters are also (sub-)optimally chosen, together resulting in reduced fuel consumption or lower emissions levels [8, 155]. Moreover, these new designs, with the combustion engine possible downsized, should meet the same performance criteria (e.g., profile acceleration, top speed) and should be sufficiently inexpensive to infiltrate the market. Consequently, this multi-objective optimization problem, with both time dependent (e.g., power-split signal) and discrete variables (e.g., battery size), puts challenges on which methods to be used in the outer loop (sizing design) and inner loop (control design).

The first studies in this direction have used rule-based algorithms to control the hybrid electric vehicle (HEV) and brute force approaches to investigate the effect of size variation on fuel consumption. Although the results have improved, this nested approach was not resulting in an optimal vehicle-level solution neither an optimal control solution. As described in more detail in Chapter 2, this led to the introduction and widely usability of Dynamic Programming (DP) and Equivalent Consumption Minimization Strategy (ECMS) for the (sub-)optimal HEV control [63, 174]. Moreover, because brute force (BF) searches are very computationally time-consuming, the necessity of an optimization algorithm in the outer loop appeared. For that reason various algorithms have been proposed in literature, e.g., Sequential Quadratic Programming (SQP), Genetic Algorithms (GA) [130, 175], Particle Swarm Optimization (PSO) [8, 68, 130, 176, 177], DIviding RECTangles (DIRECT) [8, 148]. [8, 61, 62] or others [67, 178]. These approaches have shown the benefit of explicitly addressing the coupling between different optimization areas but they have not proven the global optimality of the solution. Thus, to chose one or another approach requires a comparison of them against a benchmark case.

To perform this comparison, in this chapter we have selected four widely used global optimization algorithms (SQP, PSO, GA and DIRECT) for sizing investigation and compared them for a parallel HEV design, as similar in [8, 64]. In addition to these existing studies, we compare the results with a brute force search and analyse the Pareto front for multiple objectives (fuel and cost).

This chapter is organized as follows: Section 4.2 presents the parallel HEV to be used and preliminary necessary information. Then, Section 4.3 introduces the nested optimization problem and the bi-level framework used. Section 4.4 shows the results of using these different algorithms and Section 4.5 summarizes conclusions based on the presented results.

## 4.2 System Description and Preliminaries

The topology considered here is a parallel hybrid electric truck, fully loaded (40 ton), depicted in Fig. 4.1, used in a heavy duty long haul application. As the aim is to investigate the hybridization potential of a conventional vehicle, the main powertrain components (i.e., engine, motor and battery) are preconditioned to be scalable.
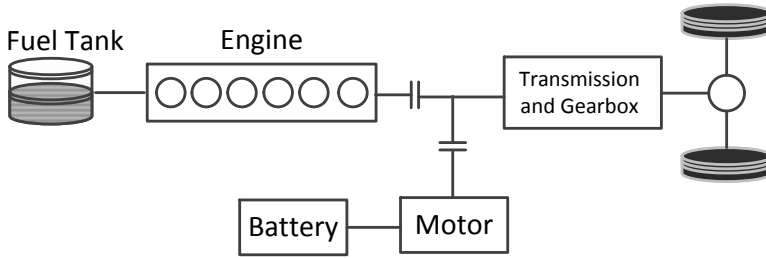


Figure 4.1: Parallel hybrid topology

The power demanded to propel the vehicle, $P_v$, is approximated by the sum of the required power to achieve the desired velocity and all other power losses by

$$
\begin{aligned}
P_v(a_v, v_v) &= P_r + P_a + P_p + P_k, \\
&= v_v(c_r \cdot m \cdot g + \frac{\rho_a \cdot A_f \cdot c_d \cdot v_v^2}{2} + m \cdot g \cdot sin(\alpha) + m \cdot a_v).
\end{aligned}
\tag{4.1}
$$

Here $P_r$ represents the rolling resistance losses, $P_a$ represents the aerodynamic friction losses, $P_p$ represents the power loss caused by gravity in non-horizontal driving and $P_k$ represents the kinetic power need to achieve a desired acceleration $a_v$. Next, a 12-speed automated manual gearbox is modeled by gear-dependent ratios, $\gamma_i$, and efficiencies, $\eta_{\gamma_i}$, for $i \in [1, ..., 12]$.

Both the 340 kW diesel engine and the 60 kW permanent magnet electric machine are characterized by static efficiency maps, which are scaled, for sizing investigations, linearly in torque. The battery is modeled using an equivalent circuit model [12] and it's capacity is scaled by increasing or decreasing the number of parallel-connected battery modules at a fixed voltage. The drive cycle used here is a typical long haul driving cycle, where highway driving is more dominant (approx. 85%).

From literature, [61, 141] and current market trends analysis, the cost models (expressed

in euros ($\mathord{\in}$)) used in this problem are defined by

$$
\begin{aligned}
\Psi_m &= 1000 + 20 \cdot P_m, \\
\Psi_i &= 500 + 10 \cdot P_m, \\
\Psi_b &= 1000 + 250 \cdot C, \\
\Psi_e &= 250 + 25 \cdot P_e,
\end{aligned}
\tag{4.2}
$$

where $\Psi_m$ is the cost of the electric motor, $\Psi_i$ is the cost of the inverter, $\Psi_b$ is the cost of the battery, $P_m$ is the maximum power of the motor, $C$ is the battery capacity, $\Psi_e$ is the cost of the engine and $P_e$ is the power of the engine. Weight and price of the electric motor and battery are induced by the materials used to produce them, which can be scaled linearly from a certain base value. The engine weight will be the same because the volume will not change, but the price will also scale linearly because the prices do differ per maximum power.

## 4.3  Problem Definition

In the most general statement, the design of a HEV, for optimal sizing and control, is an multi-objective optimization problem as defined in (2.2), that can be written as,

$$
\begin{aligned}
\min_{\mathbf{x}} \ \mathbf{J}(\mathbf{x}) &= [J_1(\mathbf{x}), J_2(\mathbf{x}), ..., J_k(\mathbf{x})]^T \\
s.t. \ g_j(\mathbf{x}) &\le 0, \ \ j = 1, 2, ..., m, \\
h_l(\mathbf{x}) &= 0, \ \ l = 1, 2, ..., e.
\end{aligned}
\tag{4.3}
$$

where $\mathbf{x} \in \mathbb{R}^{n+z}$ represents the design variable vector with $n+z$ the total number of independent $n$ sizing variables and $z$ control variables, $\mathbf{J}(\mathbf{x}) \in \mathbb{R}^k$ the vector of objective functions, $j$ the number of inequality constraints and $l$ the number of equality constraints on the complete vector of design variables $\mathbf{x}$. Each $J_i(\mathbf{x}) : \mathbb{R}^{n+z} \to \mathbb{R}^1$ represents one cost function, as exemplified in (2.7). Among the examples in (2.7) the most used optimization targets, that we will also used in this case study, are given by

$$
\begin{aligned}
\text{Fuel consumption/CO}_2 : J_1 &= \sum_{i=0}^{t_f} P_f(i), \\
\text{Hybridization costs} : J_2 &= \Psi_m + \Psi_i + \Psi_b + \Psi_e,
\end{aligned}
\tag{4.4}
$$

where $[0, t_f]$ is driving cycle length and $P_f$ is the fuel consumption. Other cost functions exemplified in (2.7) may include the minimization of the total energy of the vehicle, other emissions, or performance targets, but they will not be addressed in this case study.

The HEV control problem requires fixed sizing of components which makes this, inherently, a bi-level optimization problem [71] as depicted in Fig. 4.2. Here the outer loop searches for plant variables and the inner loop searches for control variables.
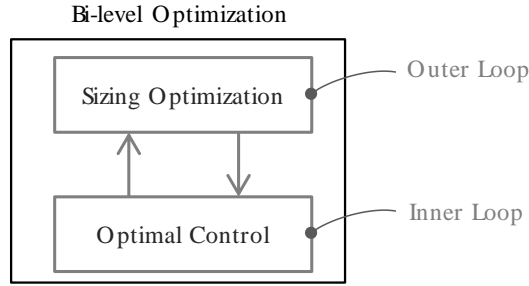
Figure 4.2: Bilevel sizing and control optimization problem

Then, the problem of optimal sizing is defined as

$$\min_{P_{\mathrm{e}},P_{\mathrm{m}},C\in\mathscr{D}} \mathbf{J}_{\mathrm{p}}(P_{\mathrm{e}},P_{\mathrm{m}},C)$$
$$s.t. \quad g_j(P_{\mathrm{e}},P_{\mathrm{m}},C) \leq 0, \quad j=1,2,...,m, \quad (4.5)$$
$$h_l(P_{\mathrm{e}},P_{\mathrm{m}},C) = 0, \quad l=1,2,...,e,$$

and the problem of optimal control is defined as

$$\min_{u_{\mathrm{ps}}(t),\gamma(t)\in\mathscr{U}} \mathbf{J}_{\mathrm{c}}(u_{\mathrm{ps}}(t),\gamma(t),\Lambda)$$
$$s.t. \quad \dot{\xi}(t) = f(\xi(t),u_{\mathrm{ps}}(t),\gamma(t),t),$$
$$g_j(u_{\mathrm{ps}}(t),\gamma(t)) \leq 0, \quad j=1,2,...,m, \quad (4.6)$$
$$h_l(u_{\mathrm{ps}}(t),\gamma(t)) = 0, \quad l=1,2,...,e,$$
$$\gamma \in \{1,2,...,12\}, \ u_{\mathrm{ps}} \in [-1,1].$$

Here $P_{\mathrm{e}}$ is the maximum power of the engine, $u_{\mathrm{ps}}$ is the power-split signal, $\gamma$ is the gear number, $\Lambda$ is the input driving cycle characterized by slope, velocity and time and $\xi(t)$ is the state-of-charge of the battery over time. More, the cost function for the control problem (4.6) is fuel consumption, i.e., $\mathbf{J}_{\mathrm{c}} = J_1$, and the cost function for the sizing problem (4.5) is the maximization of profit, i.e. $\mathbf{J}_{\mathrm{p}} = \Sigma(w_1 J_1 - w_2 J_2)$ with $w_1 = w_2 = 1$. This type of scalarization of the multi-objective optimization problem is widely used in this classes of problems and formulates a single-objective optimization problem such that the optimal solutions to the single-objective optimization problem are Pareto optimal solutions to the original multi-objective optimization problem.

## 4.3.1 Bi-level Optimization Frameworks

Due to the non-convex and sometimes noisy or discontinuous nature of the cost function $J_1$, various derivative-free global optimization algorithms have been proposed in existing

literature to solve the bi-level sizing and control problem of a HEV. A larger overview of these algorithms was introduced in Chapter 2. As a result of their wide usability and good results, in this chapter PSO, GA and DIRECT have been selected and will be compared for the outer loop of the design problem. Their advantage are that they search the complete design space and they can find the global minima. More, a gradient based method, namely SQP, and a brute force search will also be used to benchmark the above mentioned algorithms. For this, pre-implemented Matlab algorithms and the PSO from [103] have been used. The optimal control problem is solved using deterministic dynamic programming (DP), [174], which ensure finding the global optimum for the problem, i.e., it finds the control inputs $u_{ps}(t)$ and $\gamma(t)$ that globally minimize $J_c$ for a given driving cycle, $\Lambda(t)$. Dynamic programming (DP) is a numerical method in which the larger problem is solved by breaking it down into simpler sub-problems. Furthermore, for every sub-problem all possible ways to solve it are examined, working backwards in time from the final step of the control problem, $t_f$, to the initial one $t_0$ (given from the driving cycle, $\Lambda$). Then, in the forward simulation direction the best solution will be selected. As explained in Chapter 2, for off-line design studies this algorithm has been widely used due to its ability of finding the global optimum solution of the given problem.

## 4.4   Optimization Results

To analyse the potential of both hybridization and engine downsizing, two case studies have been build. The first is used to compare the bi-level optimization frameworks for optimally choosing the electric motor and battery size and the second case shows the benefits of downsizing the engine together with the hybridization step using BF search.

### 4.4.1   Case1: Hybridization Potential

The optimization problem constraints and the initial design variables values are given in Table 4.1. A first optimization problem evaluation was done using BF search as shown in Fig. 4.3, from which one can already observe the difference in the sizing design, when two different cost functions are used. When considering only fuel consumption as an

Table 4.1: Initial design variables and boundary constraints

|  | $\mathbf{x}_0$ | $\mathbf{x}_{min}$ | $\mathbf{x}_{min}$ |
|---|---|---|---|
| Max. motor power, $P_m$, [kW] | 65 | 10 | 120 |
| Battery capacity, $C$ [kWh] | 6.5 | 1 | 12 |
| Normalized power-split signal, $u_{ps}$ [-] | n/a | -1 | 1 |
| Gear number, $\gamma$ [-] | n/a | 1 | 12 |

optimization target, the biggest battery and the biggest motor are chosen, however, this is not the case when component costs are also considered. More, variation in the cost models $\Psi_m$, $\Psi_i$, $\Psi_b$ and $\Psi_e$, will shift the optimum point found for the multi-objective optimization problem.
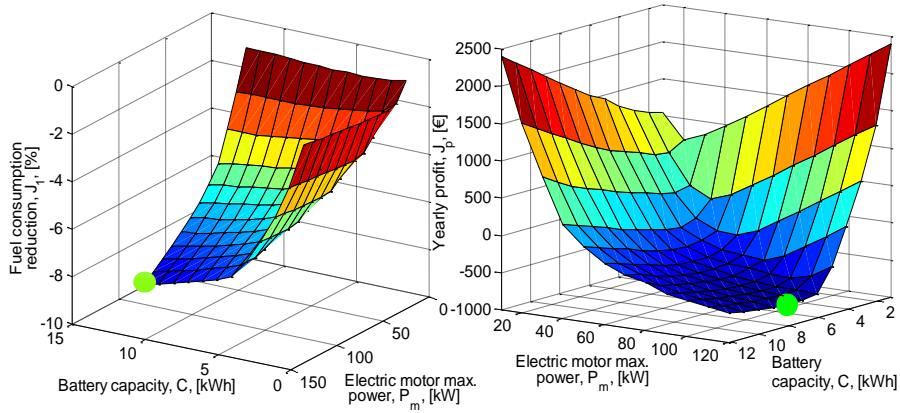


Figure 4.3: Brute force design results for minimum fuel consumption (left), i.e., $J_p = J_1$ and maximum profit (right), $\mathbf{J}_p = \Sigma(w_1 J_1 - w_2 J_2)$ with $w_1 = w_2 = 1$.

To reach the results in Fig. 4.3, 144 function evaluations were computed on one PC[1] in 8 hours. Because this search is computational exhaustive and not applicable to higher dimensionality problems, the search direction through the design space of the four mentioned optimization algorithms above, are compared in Fig. 4.4 and 4.5 and their results are compared in Fig. 4.6 and Table 4.2.

Table 4.2: Main characteristics of the considered algorithms

|  | BF | SQP | PSO | GA | DIRECT |
|---|---|---|---|---|---|
| Computational burden | - - | ++ | - | - | ++ |
| Search complete design space | ++ | - - | ++ | ++ | ++ |
| Global optimum | - - | - | ++ | ++ | ++ |
| Reusability / Tuning effort | n/a | + | - - | - - | ++ |
| Derivative free | n/a | no | yes | yes | yes |
| Suitable for high dimensions prob. | no | yes | yes | yes | yes |

---

[1] For all simulations a PC with Intel i7 processor at 3.2 GHz and 4 GB of memory has been used.
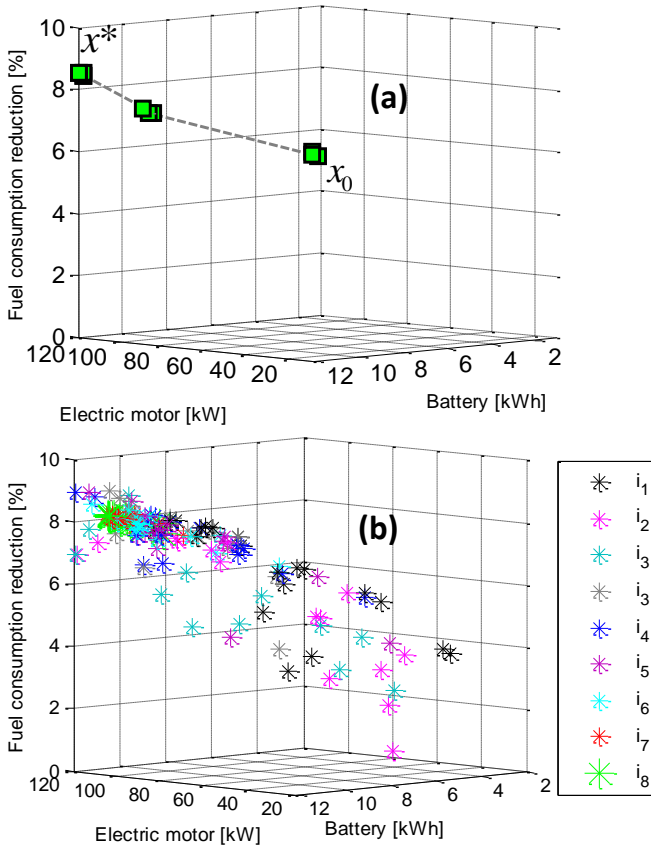
Figure 4.4: (a) SQP and (b) PSO applied to HEV battery and motor optimal sizing: function evaluation, convergence and fuel reduction percentage.

Given the driving cycle, the results indicate that up to approximately $P_m = 60$ kW, a big part of the kinetic energy of the moving vehicle can be regenerated and used for later usage. For even higher electric machine power, there are still fuel benefits from even more regenerated braking energy and more freedom of the combustion engine operating points. Yet, for very large motors the overall magnitude of these benefits is decreasing. The fuel benefits of changing the battery capacity is explained by the maximum power the battery can deliver: *(i)* at low battery capacity, up till approximately $C = 5$ kWh the potential of the electric motor is limited due to the operating limits of the battery; *(ii)* at higher battery capacity the potential of the electric motor is fully used and there is more freedom in the state of charge trajectory.
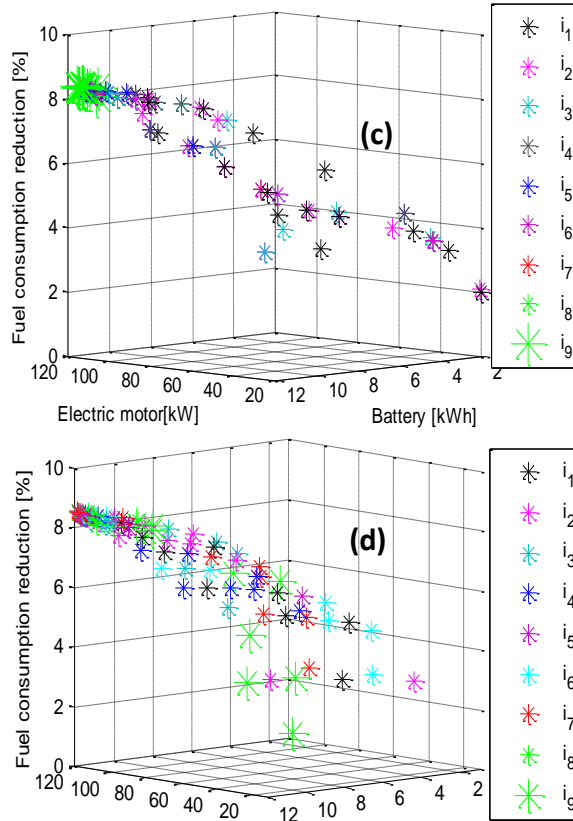
Figure 4.5: (c) GA and (d) DIRECT applied to HEV battery and motor optimal sizing: function evaluation, convergence and fuel reduction percentage.

Although for only two variables the cost function has no visible or evident local minima these results can be used to conclude on the usability of these algorithms in future similar studies where more variables are introduced for more topologies. PSO, GA and DIRECT use more function evaluations than SQP but they also benefit from the fact that they search the complete design space. GA and PSO are more computationally expensive (10 hours simulation time) when compared with DIRECT (2 hours) and SQP (0.7 hours). For $J_p = J_1$ all algorithms converge to the vicinity of the same local optimum, which in this case is also the global optimum, see Fig. 4.3, 4.4 and 4.5. Resulting from these type of simulations, the advantages and disadvantages of using these algorithms for vehicle sizing optimization, in nested frameworks, are presented in Table 4.2 and Fig. 4.6.
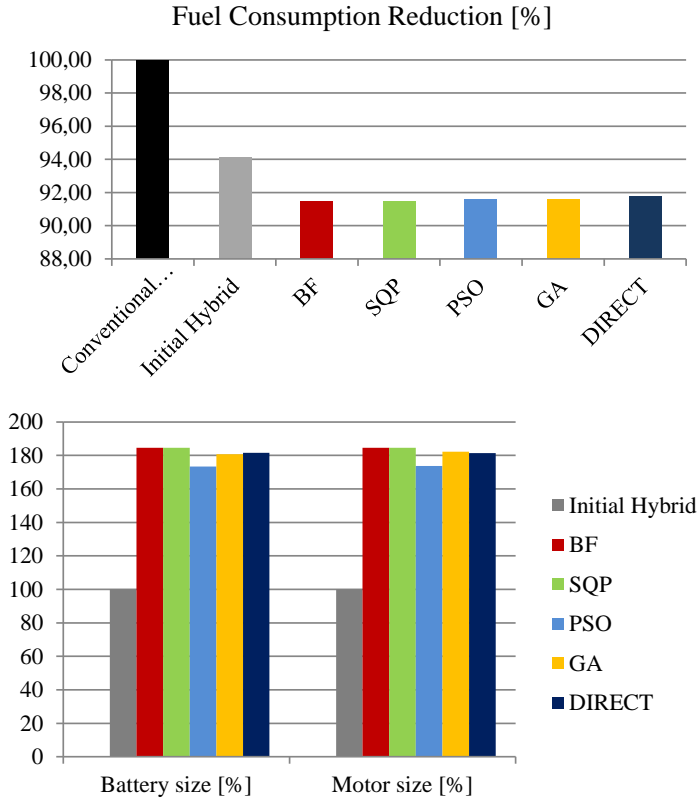
Figure 4.6: Optimal values found and fuel consumption for each algorithm

The tuning effort and the high number of function evaluations make PSO and GA less favourable than DIRECT or even SQP. Nonetheless, for highly nonlinear problems SQP is likely to get stuck in local minima, which requires extra effort to avoid that. BF type searches provide insights in the cost function shape but grant no optimality guarantee or indication of possible minima. This kind of searches are mostly used in industry to derive trends in the system design for discrete component choices.

## 4.4.2  Case 2: Hybridization and Engine Downsizing

When also downsizing of the engine is considered the fuel consumption of the driveline can be decreased even more. Moreover, varying the maximum engine power, combined with power from the electric part of the drivetrain, could give extra benefits in component cost. Fig. 4.7 and 4.8 show the results for both minimum fuel consumption, $J_p = J_1$ and maximum profit, $\mathbf{J}_p = \Sigma(w_1 J_1 - w_2 J_2)$. In Fig. 4.7, the white area at the bottom repre-
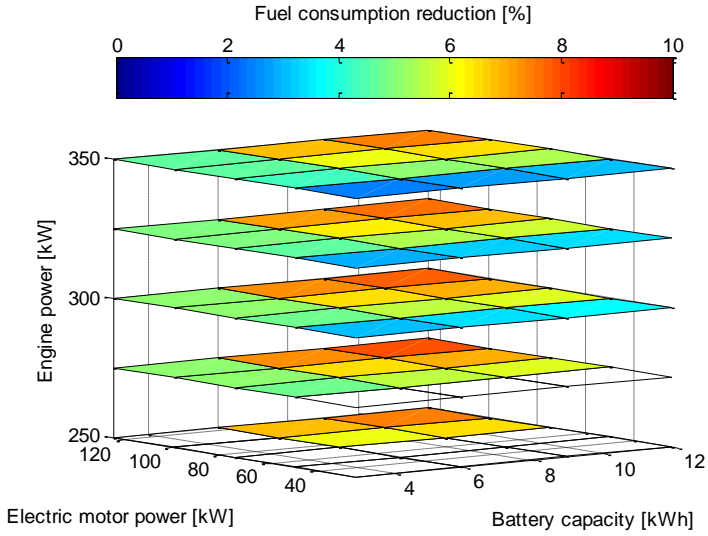
Figure 4.7: Brute Force search results for sizing optimization of engine, electric motor and battery - fuel consumption.
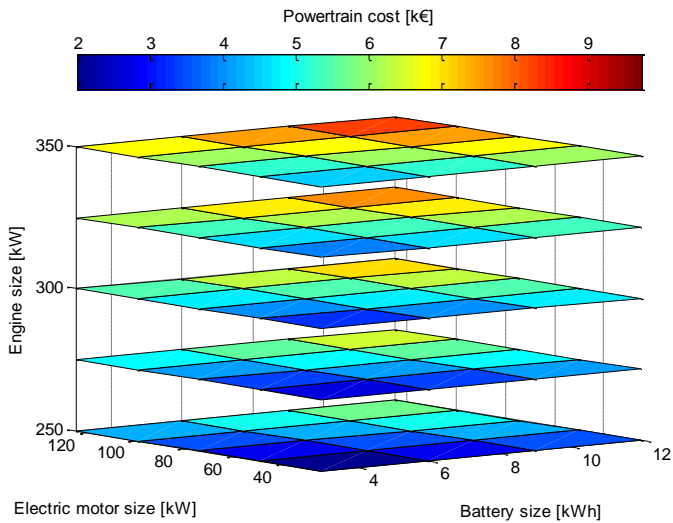


Figure 4.8: Brute Force search results for sizing optimization of engine, electric motor and battery - hybridization cost.

sents the infeasible design area, since certain constraints are violated (e.g., the maximum required power in the cycle cannot be ensured). For maximum profit over the vehicle lifetime, both hybridization and engine downsizing are recommended.

From such a brute force search design trends can be identified. For instance, as depicted in Fig. 4.7, for large fuel consumption reduction one might choose a downsized engine of $P_e \in [280, 320]$ kW, combined with a large electric machine and battery pack, such as $P_m \in [80, 120]$ kW and $C_b \in [8, 12]$ kWh. On the contrary, as depicted in Fig. 4.8, to restrict the powertrain costs one might choose a downsized engine of $P_e \in [280, 320]$ kW, combined with a medium electric machine and battery pack, such as $P_m \in [20, 60]$ kW and $C_b \in [2, 8]$ kWh.

Based on these studies we can conclude that the current widely-used approaches, in which components sizing are based on solely powertrain fuel consumption, are limited. Such approaches will lead to the selection of large components (see Fig. 4.3), which in turn will lead to expensive and uncompetitive vehicle. The introduction of a cost model, for each component, can improve results and may also make it more realistic. This can be used as part of the cost function or as a constraint. This study did not consider auxiliary systems present in a vehicle, such as the steering system, the air conditioning compressors, the air compressors, the water pump, and so on. We have restricted this case study since increasing the search space (i.e.,the dimensionality of the problem) becomes too time consuming. These auxiliary systems, and their potential in terms of electrified power trains, are addressed in the next chapter. For improved designs, these design studies could be combined.

**Pareto Set Analysis**

In a multi-objective optimization problems there exist, typically, an infinite number of *optimal* solutions as a function of the prior-defined preferences of the designer, $w_1$ and $w_2$. In order to analyse this compromise, in Fig. 4.9 the Pareto Set is shown for this problem, where each point is a (sub-) optimal solution, i.e., a certain component sizing combination, to the bi-level optimization problem in (4.5) and (4.6). More, each point indicates a certain articulation of preferences (choice of weights $w_1, w_2$), for the optimization problem. This shows the trade-off of choosing between $J_1(\mathbf{x})$ (i.e., fuel consumption / operational costs) and $J_2(\mathbf{x})$ (hybridization costs) for the outer sizing loop.

Four cases are highlighted in Fig. 4.9, where the two cost functions are either minimum or maximum, e.g. the cheapest system is denoted by (d) while the most fuel efficient system is denoted by (c). Furthermore, (a) denotes the design for which $J_2(\mathbf{x})$ is maximized (e.g., the most expensive vehicle), while (b) denotes the design for which $J_1(\mathbf{x})$ is maximized (e.g., the least fuel efficient vehicle). The design vector $\mathbf{x}^*$ is a Pareto optimum if and only if, for any $\mathbf{x}$ and

$$J_1(\mathbf{x}) \leq J_1(\mathbf{x}^*) \Rightarrow J_2(\mathbf{x}) \geq J_2(\mathbf{x}^*). \tag{4.7}$$
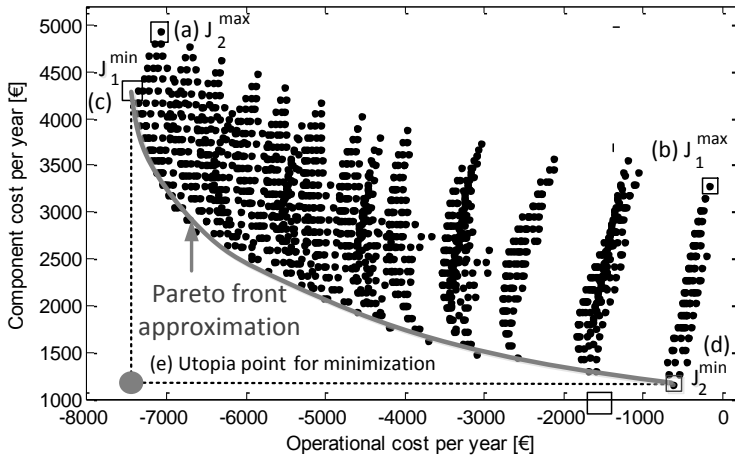
Figure 4.9: Pareto Front approximation for $J_1$ and $J_2$

The distance between the non-reachable utopia point for minimization, (e), and the Pareto set points gives an indication of which point should be chosen for design, as the Pareto optimum. One simple method, used by [179], is to choose an **x** based on the values of the design objectives and how well they match the preferred values. The curved gray line represents the Pareto front approximation, that indicates the optimal trade-off between operational and hybridization costs.

## 4.5 Conclusions

In this chapter several bi-level optimization frameworks (brute-force, SQP, DIRECT, GA, PSO in the outer loop and DP in the inner loop) were used and compared to optimally size and control a parallel hybrid heavy-duty vehicle. Although insightful, using brute force search, to find the optimal sizing values becomes too computationally expensive and insufficiently accurate. To this end, four other less exhaustive algorithms are compared here to find the optimal design of a HEV. By hybridization up to 8% of fuel reduction can be achieved at the expense of large, expensive components. More, when the engine is downsized the fuel can be decreased more while the component costs are reduced.

Considering the multi-objective fashion of the problem a trade-off Pareto analysis is presented, where fuel and component cost are discussed. All algorithms performed well, however from a computational perspective DIRECT is preferred for non-convex problems and SQP for convex problems. Further work involves increasing the design vari-

ables number (e.g., gearbox sizing optimization), the number of topologies used and the application of more driving cycles and/or usage conditions.

For the case study defined in this chapter, we used linear cost models that do not vary with time. Considering the varying markets and the significant developments done to improve technologies, one could forecast the changes of these models and include them in the optimization problem. Moreover, since these cost models can vary with the application studied (such as passenger cars, ships, buses, long-haul trucks and so on) their level of detail could be improved to capture this information.

# FIVE

# NESTED OPTIMAL DESIGN OF ELECTRIFIED AUXILIARY UNITS

**Abstract /** The electrification of auxiliary systems represents a large potential to reduce the emissions and fuel consumption in heavy hybrid vehicles, such as buses and trucks. This potential comes mostly by eliminating the fixed-ratio dependency between the auxiliaries speed and engine speed, that induces high energy losses. For the electrification of auxiliary systems there are many design options, such as the architecture, dimensioning of components or the ability for control on demand. In this work, the nested design of multiple auxiliaries is addressed, by looking at topologies, sizing and control in an integrated manner. This nested design approach, where the plant and control parameters are found together, has proven beneficial in other research fields and can be applied to auxiliaries as-well. First, by analyzing the potential of reducing fuel consumption of auxiliary components in a heavy-duty truck two auxiliaries are chosen to be studied. Then, novel topologies are introduced for these two auxiliary units, namely the power steering pump and the air compressor. The optimal design is found, for each topology, using a nested optimization coordination strategy. Then, for both auxiliaries a topology is chosen and

more extensive simulation are shown to analyse the tradeoffs between different controls, plant design and different driving conditions. The results of this study show that significant energy gains can be obtained if auxiliary systems are electrified and optimally designed. Moreover, the nested structure proposed in this chapter facilitates such studies, reducing computation time and aiming at the system-level optimality.

# 5.1   Introduction

Auxiliary systems present in heavy vehicles, such as buses, trucks or construction machineries, consume significant amounts of fuel. In engine-only powered vehicles auxiliary systems are generally connected by a belt or a gear to the internal combustion engine (ICE) as shown in Fig. 5.1. This connection induces energy losses and restricts the independent control of these components. In fact, these components work all the time when the ICE is on, not just when needed. The introduction of hybrid electric vehicles
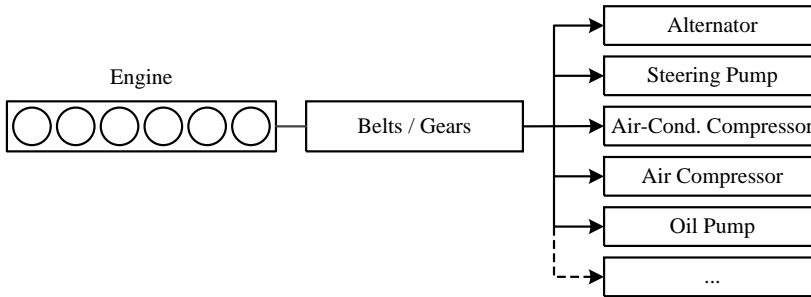


Figure 5.1: Topologies of auxiliary units in engine-driven conventional vehicles.

offers flexibility for auxiliary systems positioning and operation. New architectures can be built, to eliminate the fixed-ratio dependency, increasing the control flexibility and allowing independent use of components when needed. Moreover, by combining the plant and the control algorithm design, the energy efficiency of using these components can be increased.

## 5.1.1   Auxiliary Units in Heavy-Duty Vehicles

Motivated by emission legislation and to decrease ownership costs, the *reduction of fuel* consumption is one of the major targets of the truck industry for the coming decades. From earlier studies it is known that the fuel consumption caused by auxiliary units adds up to a significant amount of the total consumption. The exact numbers depend especially on the vehicle usage, i.e., driving cycle and operating conditions, and cannot be generalized.

For example, for heavy-duty trucks (US vehicle classes 7 and 8), in [180] it is shown that auxiliary units can consume between 3% and 11%. This variation is found by looking at five standard different driving cycles, with mostly urban character and no slopes. When using predominant highway driving, typical for long-haulage traffic in Europe, the auxiliaries are found to consume between 4.7% and 7.3% [181] and up to 4% in [153] (see Fig. 5.2). For buses, where the air is used a lot to provide cooled air for passages, in [182] the authors report that the consumption can be up to 25% of the total power.
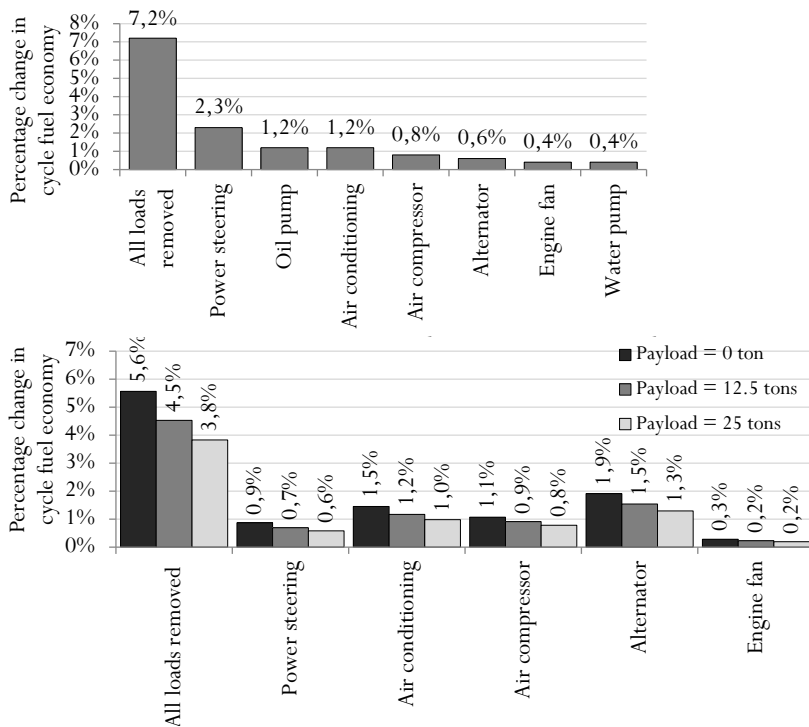
Figure 5.2: Fuel economy improvement when auxiliary components are removed, estimated in [181] (top) and, in the case of the parallel HD Truck under study in this Chapter (results presented in [153]) (bottom).

This high consumption exists because auxiliary units are very inefficient at nominal operating conditions. This is caused by the combination of the plant and control design, chosen to meet worst-case requirements. To deal with these worst-case scenarios, highly oversized components are used, dramatically reducing the overall efficiency. Hence, the electrification of auxiliary units, would eliminate the fixed engine-auxiliary dependency, being a potential for fuel reduction.

A second benefit of electrifying auxiliary units is reducing ICE *idling*. During their rest periods at truck stops, the ICE is *idled* to power the climate control (i.e., heater and air conditioning) and the cabin accessories (e.g., refrigerator, microwave oven, television), which requires, on average, 4-6 kW [183]. Moreover, the engine is also *idled* to avoid start-up problems at cold weather. An idling engine has an efficiency of about 3%, compared to 40% when driving on the highway [183] and involves disadvantages as air pollution, excessive engine wear, discomfort and noise. The amount of engine idling is not well known and it depends on various conditions, for instance geographic location and season. Based on rough estimations made by industry, [184] reports an average of 6 hours/day in the US. For certain conditions (e.g. during winter) this may even be higher, up to 40% of the time. Therefore, reducing the need for engine *idling* could decrease energy consumption.

The entrance into future *$CO_2$ free zones* of cities, requires also the electrification of certain auxiliary, as the steering system or the air brake compressor. As figure 5.2 shows, the air compressor and the power steering system are some of the major energy consuming auxiliaries. Therefore, these components are discussed in more detail in this chapter.

In the last decade, for various auxiliary units, isolated solutions with variations occurring either in their topology, technology or control have been proposed. For example, in [153] and [185] an electro-hydraulic steering system is compared with a conventional steering system for a truck and a passenger car, respectively. But to design a hybrid vehicle, the whole set of auxiliary systems must be designed optimally, not just a component. This design problem becomes an optimization problem on multiple levels (plant and control) which, when solved sequentially leads to sub-optimal designs.

## 5.1.2   Contribution and Outline of This Chapter

To find a system-optimal design for the auxiliary units, a multi-level optimization structure has to be implemented, where the dependency between different design layers is explicitly considered (as previously discussed in Chapter 2). In this chapter the complete plant (i.e., its topology, technology and component sizes) and the control algorithm are optimized for the power steering system and the air compressor, taking into account practical constraints of a conventional truck (Class 8). The choice of these two auxiliary systems is based on a prior feasibility study made for a typical long-haulage truck with different payloads, presented in [153]. Moreover, for defining a novel topology, we uses the results presented in Appendix A [16], where six alternative power steering configurations are investigated. The study in Appendix A considers also secondary aspects such as added complexity and costs.

From these prior studies, i.e., [16] and [153], a more ideal topology is proposed for the steering system. Then, the possible topologies for the air compressor are introduced together with their models. Using a nested coordination strategy, the combined optimization of the conventional power steering system and air compressor, in an alternative

topology, is defined. In this nested optimization problem, Dynamic Programming is used to find the continuous and discrete control inputs and Sequential Quadratic Programming is used to find the discrete plant parameters, as gear ratios. The results shows that a system-optimal design of these auxiliaries could potentially reduce the total fuel consumption by approximately 0.3 L/100 km on long-haulage routes.

The remaining sections of this chapter are organized as follows. Section 5.2 introduce steering system topologies and highlights their fuel benefits. Section 5.3 introduce the air compressor system topologies and highlights their fuel benefits. Next, in Section 5.4 the problem of optimally design two auxiliary units is introduced, considering both the plant and the control algorithm and optimization results are presented. In Section 5.5 conclusions are drawn.

## 5.2   Power Steering System Topologies

The power steering system is one of the major energy consuming auxiliaries in a long-haul truck [153, 181]. The supporting steering force of a conventional hydraulic power steering (HPS) system is delivered by an engine driven fixed displacement pump (FDP) as depicted in Fig. 5.3. This has been designed to deliver sufficient oil flow and pressure for
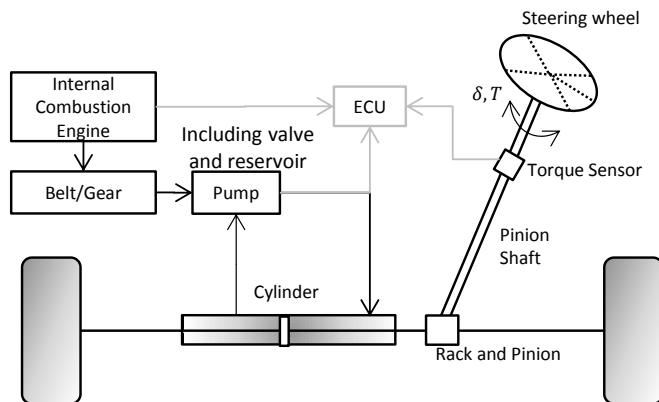


Figure 5.3: Simplified schematic representation of a conventional steering system

low speed manoeuvring, i.e., at engine *idling*. When the pressure level at the output side becomes higher than the set value of the pressure relief valve, the pressure relief valve opens and redirects the excess of flow back to the (low pressure) inlet. This overflow is proportional to engine speed and introduces high parasitic losses, as graphically depicted in Fig. 5.4. On the other hand, the actual required steering pressure decreases as vehicle speed increases. Therefore, the parasitic loss, induced by the power steering system, is

relatively higher for long-haul trucks, that drive most of the time on the highway. In such conditions the assistance from the power steering pump remains unused for 76% of the time [185].
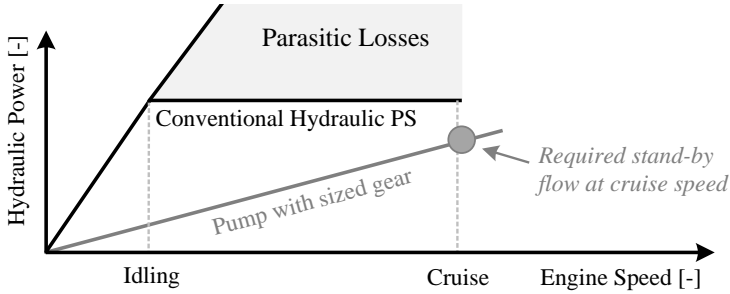


Figure 5.4: Output power of the sized pump as a function of engine speed

To eliminate this fixed speed dependency, between the engine and the steering system, a new topology has to be introduced. In Appendix A we introduced, modeled and investigated six topologies to find the design and control policy offering the minimum fuel consumption. To design new architectures multiple components were used, as gears (planetary, spur or ball-screw) and an electric machine. These six topologies depicted in Fig. 5.5, where square boxes mark the component sizing parameters analysed in Appendix A. Here $P_e$ is the electric machine rated power, $i_1$ and $i_2$ are fixed gear ratios
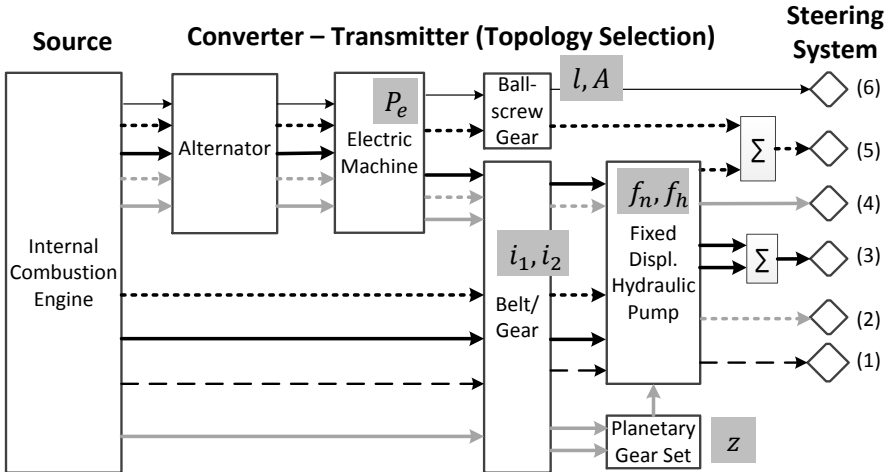


Figure 5.5: Overview of the six possible topologies (one per line type) for the Power Steering System. Red boxes mark the component sizing parameters analysed in [44].

between the ICE and the pump and between electric machine (EM) and the pump, $l, A$ are the ball-screw lead and the steering house piston area, $z$ is the fixed ratio of the planetary gear set (PGS) and $f_n, f_h$ are the minimum constant flow on highway and on national roads used to develop the control strategy.

The purpose of the alternative power steering (PS) topologies is to increase the controllability, in order to reduce the parasitic losses indicated in Figure 5.4. In Fig. 5.5, the first topology (*topology no. 1*) is the conventional hydraulic power steering. To introduce the PS topology used in this work, the remaining topologies from Fig. 5.5 are briefly described next.

## 5.2.1 Electro-Hydraulic Power Steering

In an electro-hydraulic power steering system (*topology no. 2*) the pump is not mechanically coupled to the engine but instead it is driven by an EM. In this way, the angular velocity of the pump (and volume flow within the hydraulic system with that) can be controlled independent from the engine speed. This not only increases the efficiency at part load, but also makes it easier to implement (efficient) speed dependent power steering. To ensure that the power steering system responds adequately, the pump should not be switched off completely when no steering power is required. Instead it has to be operated at a certain stand-by speed to be able to build up pressure quickly. Hence, there are still parasitic pumping losses involved and, steering force "on demand" is not possible. To further increase the efficiency, combining several small electro-hydraulic pumps may be favorable.

## 5.2.2 Electric Power Steering

In an electric power steering system *(topology 6)*, the hydraulic system is completely omitted. Instead, the steering force is delivered by an electric motor, which can be located at different locations in between the steering wheel and the wheels. The required motor torque, in an electric PS system can be independently controlled. This is based on the torque sensor output, vehicle speed and the angular position of the steering wheel. In this way the characteristics of the steering system can be adjusted to the driving conditions to provide the desired level of comfort and feedback to the driver. An additional benefit of an electric PS system is that the power steering system can be used actively for stability control, lane keeping assistant, side wind compensation and collision avoidance.

The electric PS system enables true steering "on demand" and seems to be the most efficient way of power steering. Moreover, the system implementation is simpler when compared with hydraulic PS, due to the absence of the hydraulic circuit.The overall system weight and size may be advantageous as-well over a conventional hydraulic PS system.

Unfortunately, there are additional issues, which especially hold for trucks. For instance, the required power to drive the electric motor has to be delivered by the battery. This is a major limitation for an engine-only driven truck, where the relatively low battery voltage, results in a maximum electrical power draw of $2,4$ kW. Moreover, the EM has to be powerful enough to steer the wheels at vehicle standstill which requires a very high torque output. Since it has a significantly lower power density than its hydraulic counterpart, it may also be heavier than the conventional pump.

### 5.2.3   Hybrid Topologies

As proposed in [186], the combination of an electro-hydraulic system and a downsized conventional engine-driven pump is also a topology candidate (*topology no. 3* in Fig. 5.5). As mentioned before, in case of a hydraulically actuated PS system, a stand-by flow is required to achieve the desired response. Because an electro-hydraulic system involves a dual energy conversion (from mechanical to electrical and vice-versa), the efficiency of a gear driven hydraulic pump itself is usually higher. By combining both systems, the parasitic loss caused by the overflow can be minimized, while hydraulic pressure is delivered by the mechanically driven pump as much as possible. Since the output flow of the pump increases linearly with pump shaft speed, the flow at engine speeds below cruise speed will be insufficient (see Fig. 5.4). The electro-hydraulic system can be controlled such that it delivers the remainder of the required flow. The pump size can be optimized for specific duty cycles, e.g. highway driving.

A second implementation of such a "hybrid" topology, using an electro-hydraulic system and a downsized conventional engine-driven pump, can be constructed using a Planetary Gear Set (PGS) *(topology 4)*. Here, a single pump can be driven both by the ICE and the EM simultaneously, which reduces leakage and bearing losses. The combination of gear ratios should be optimally chosen, such that the overall power consumption is minimized. In this manner the efficient FDP configuration is utilized at highway speeds without introducing the parasitic losses of overflow. At lower speeds, the EHPS configuration is used to deliver the remainder of the flow (see Fig. 5.4). Due to the capability to split the required input power of a single pump, it is called power split EH-HPS.

A third hybrid topology *(topology 5)*, can be represented by a combined hydraulic PS with an electric power-steering. Again, the fixed displacement pump is scaled such that the delivered flow meets the request at high speeds. An EM delivers the remainder of the requested power at lower speeds. Due to the presence of hydraulic PS, the torque demand on the electric machine is reduced. This may make *(topology 5)* a more viable solution for heavy duty trucks compared to pure electric PS. As a result of the dual force delivery, the force induced on the ball nut rack by the hydraulic PS system can be reduced. This allows a reduction of the frontal area of the hydraulic cylinder, which inherently reduces the required oil flow and thus energy consumption of the hydraulic PS system.

Without going further in detail, one can conclude that, to reduce the fuel consumption of

the PS system a more flexible topology is essential [16, 154]. Yet, since solely electric PS can require very large EM and it's limited by the battery size, the hydraulic power delivery could be maintained. The hydraulic power delivery, in itself, is very efficient. However, due to the gear ratio that has been selected to meet the worst case requirements, the parasitic losses introduced in the system (at nominal operating conditions) are high. The optimal design studies presented in Appendix A show that up to 80% of fuel consumption can be reduced if variable flow is applied intensively. In this chapter we propose an architecture for the PS system that can overcome the disadvantages of the conventional system. This novel topology depicted in Fig. 5.6, consists of a two speed-gearbox which drives the conventional fixed displacement pump. This two-speed gearbox is chosen since a stand-by flow is always required from the power steering pump (as it can never be completely switched off). Moreover, using such a gearbox the high
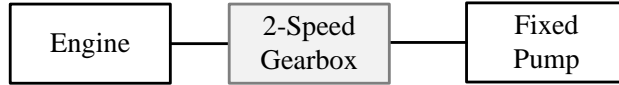
Figure 5.6: Novel power steering system topology.

efficient mechanical connection between the auxiliary and the engine is maintained. The optimal design of the gear ratio will be discussed in Section 5.4. The technical implementation of the variable gears is not considered at this point.

To develop the optimum design for the power steering system, modular and scalable models of components are required. The analytical model used here is proposed in Appendix A, [16]. This model include both leakage losses and torque losses, and it is characterized by a volumetric, $\eta_v$, and a hydro-mechanical efficiency, $\eta_{hm}$,

$$\eta_{tot} = \eta_{hm} \cdot \eta_v. \tag{5.1}$$

We assume the 2-speed gearbox as fixed gear ratios, $i$, between the input and the output shaft, for which $i = \frac{\omega_o}{\omega_i}$ holds (where $\omega_o$ and $\omega_i$ are the angular speeds of the output and input shaft respectively). Similar to Chapter 4, the ICE is modelled with an engine map, containing the fuel consumption as a function of output torque and angular speed.

The duty cycle used here is drive cycle dependent and therefore the optimal solution for inner city driving will not always equal the optimal solution for highway driving. For the results presented here, focused on long-haul usage, a mixed cycle measured on a fully loaded tractor-trailer is used, that combines various road segments, with a predominant (85%) highway driving.

## 5.3   Air Compressor Topologies Design

This section introduces the air compressor system, analyzes its conventional topology and introduces two new possible topology. The aim is to select a possible topology that can decrease fuel consumption for this auxiliary. Similar to the power steering pump, the air compressor is permanently driven by the internal combustion engine and at a fixed ratio to it. In this pneumatic system, compressed air is stored in vessels that serve as buffers and supply pressurized air to the air consumers. The main air consumers on board are the service brakes, the clutch and the gearbox. Other air consumers are the Emission Aftertreatment System (EAS), which uses air pressure to supply AdBlue to the engine, and the turbo waste gate.

The air compressor is modelled through 2D look-up tables that contain the required input torque and the resulting intake flow as a function of the outlet pressure and angular speed from [187]. Then on/off switching of the air compressor is controlled based on the pressure level at the inlet of the air buffers. Reaching the upper pressure limit switches the compressor off while reaching the lower pressure limit switches the compressor on. The compressor is said to be in *idle mode* when it does not deliver pressurized air to the vessels but still introduces drag losses as a function of its angular speed. The pressure in
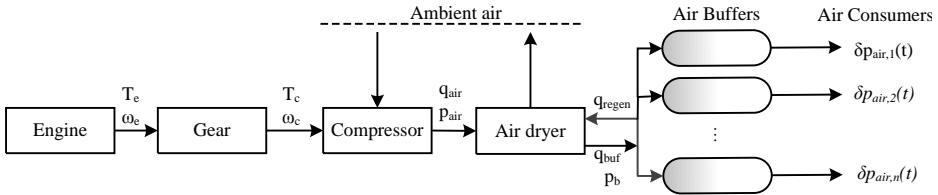


Figure 5.7: Schematic overview of the pneumatic system.

the vessel, $p_a$, is determined from the ideal gas law as

$$p_a = \frac{m_a \cdot R \cdot \Theta_a}{V}, \tag{5.2}$$

where $m_a$ is the air mass, $R$ is the gas constant, $\Theta_a$ is the air temperature and $V$ is the volume of the vessel. For solving the optimal sizing and control problem, we further assume the temperature in the vessels to be constant and equal the ambient temperature, and we lump all air buffers into one. These are not restrictive assumptions since, for the optimization study, one should know only the total air consumption (given that all the air has to be delivered by a single compressor).

Since the air compressor can be switched off completely, a maximum flexibility would be achieved with the implementation of a variable gear and a clutch. To gain insight in the

efficiency improvements caused by these components, in Fig. 5.8, three different topologies are defined. Since this is a more idealistic design, based on these three categories, five cases are build. The first topology (cases 1 and 2) is the conventional topology that is
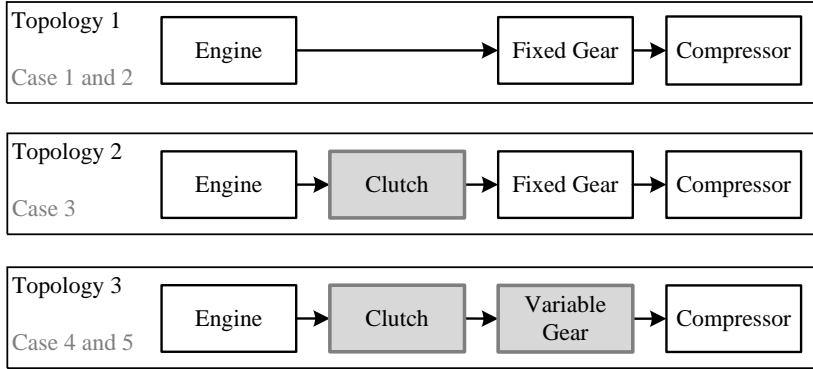


Figure 5.8: The three air compressor topologies analysed, with an increasing level of flexibility.

typically used in trucks. Case 1 is the reference situation, where the on/off switching of the compressor is determined by the minimum and maximum pressure of the air buffer. In case 2, the air compressor is also used as an extra engine brake when the vehicle slows down or drives downhill. Hence, the idle mode of the compressor can be activated when the pressure in the air buffer has not reached the lower limit yet, resulting in more flexibility (i.e., idle control). To increase the controllability of the air compressor, in topology two a clutch is added (case 3). In topology 3 (case 4 and 5), the controllability is further increased by means of a variable gear. In case 4, a gear efficiency of 99% is assumed, whereas in case 5 the gear efficiency is assumed to be 80%.

For these 5 cases the control variables $\mathbf{x}_c$ are

$$\mathbf{x}_c = \{c_1, i(t)\}, \tag{5.3}$$

with $c_1$ the closing and opening of the clutch and $i(t)$ the variable gear ratio. For topology 3, where both the clutch and the variable gear are present, the optimal control problem becomes,

$$
\begin{aligned}
\min_{u(t) \in \mathscr{U}} \Phi(u(t)) = &\min_{u(t)=\{c_1(t),i_1(t)\} \in \mathscr{U}} \int_0^{t_f} \dot{m}_f(c_1(t), i_1(t)) dt, \\
\text{s.t. } & i_1(t) \in [0.5, 1.5], \\
& p_b \in [p_{b,min}, p_{b,max}], \\
& p_b(0) = p_{b,max}, \\
& \dot{p}_b(t) = F(p_b(t), c_1(t), t), \\
& c_1(t) \in \{0, 1\}.
\end{aligned}
\tag{5.4}
$$

Table 5.1 shows the fuel consumptions that resulted from simulations of the 5 cases. The optimal control inputs, such as the clutch opening and closing, is guaranteed by the DP algorithm. In the reference case, the air compressor consumes 0.1496 L/100km, i.e., average power consumption of 617 W. The second case (topology 1 with idle control)

| Case | Clutch [Y/N] | Gear | Gear eff. [%] | Idle Control [Y/N] | Fuel Cons. [L/100km] | Improvement [%] |
|------|--------------|-------|---------------|--------------------|----------------------|-----------------|
| 1 | N | 1.412 | 99 | N | 0.1496 | Ref. |
| 2 | N | 1.412 | 99 | Y | 0.1355 | 9 |
| 3 | Y | 1.412 | 99 | Y | 0.0151 | 90 |
| 4 | Y | Var. | 99 | Y | 0.0133 | 91 |
| 5 | Y | Var. | 80 | Y | 0.0159 | 89 |

Table 5.1: Fuel consumption of an optimally controlled, engine driven air compressor for different cases

results in a fuel economy improvement of 9% compared to the reference case. Although the speed of the air compressor is still completely dictated by engine speed in case 3, the compressor can be switched off completely, which removes the drag losses in idle mode. The fuel economy improvement that has been achieved with this topology is 90%. The additional improvement of the fourth case, providing full flexibility due to a variable gear ($\eta$= 99%), is only 1%. When the variable gear efficiency is lowered to a more realistic 80% (case 5), the resulting improvement is worse than that of case 3, where only a clutch was added. Therefore, it will not be beneficial to implement such a variable gear for the air compressor, especially since it also increases system complexity.

We investigate the improvement of adding a clutch to the air compressor topology also for the SAE J1343 duty cycles [188]. These cycles are often used in literature for studies on auxiliary units and are presented in Table 5.2. Although these standards have been

| Type of Operation | Duty Cycle [%] | Pumping Power [kW] | Unloaded Power [kW] | Average Power [kW] |
|-------------------|----------------|--------------------|---------------------|--------------------| 
| Long-Haulage | 5 | 6 | 2.4 | 2.6 |
| Short-Haulage | 10 | 6 | 2.4 | 2.8 |
| Local-Haulage | 30 | 6 | 2.4 | 3.5 |

Table 5.2: Overview of the SAE J1343 duty cycles as in [188].

defined in the year 2000, the duty cycle of 5% that was defined for long-haul cycles is in good correspondence with the 4% that resulted from our simulations. In particular,

the defined average power consumption of the air compressor is much higher than the average 617 W that resulted from our simulations. Therefore, the focus should be on the relative improvement that one can achieve with a novel topology. Fig. 5.9 shows the duty cycles as they are defined in the SAE standards [188] and the improvement that could be achieved when a clutch is added between the engine and the air compressor. The 88% improvement on the long-haul cycle is in good correspondence with the 90%
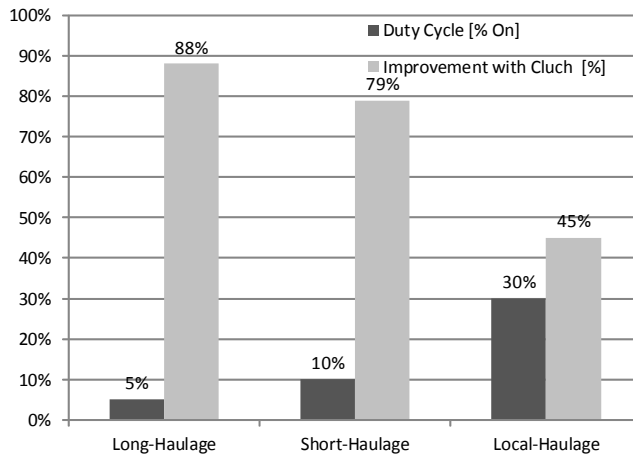


Figure 5.9: Improvement of the air compressor power consumption when a clutch is used, for the SAE J1343 standard cycles

that resulted from previous simulations listed in Table 5.1. Based on these results, for the integrated optimization study in Section 5.4, topology 2 will be used.

## 5.4   Integrated Sizing and Control

To come to a system-optimal design, the optimization of individual auxiliary topologies should be combined into a single, integrated optimization, to take dependencies among various auxiliaries into account. Based on Sections 5.2 and 5.3, in this section the power steering pump and the air compressor are considered in the topology depicted in Fig. 5.10. This approach could be in a similar fashion applied for more or other auxiliaries. The goal of this section is to find the system-optimal design and controller for the engine driven power steering pump and air compressor of a conventional truck. We aim at optimizing the design and control of both auxiliaries in a combined nested coordination structure.

This topology has 2 discrete gears to drive the power steering pump and a clutch between
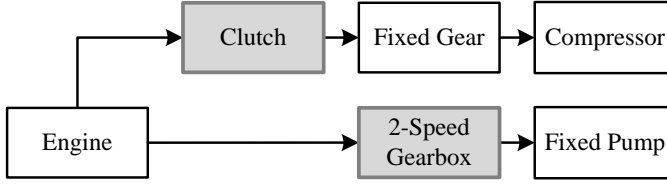
Figure 5.10: Topology used for the combined optimization of the clutch (actuation) and the gearbox (design and actuation)

the engine and the air compressor. The idea behind the 2 discrete gears, detailed in Section 5.2, is that the hydraulic power steering system has a cruising state and a steering state, which is very much as any variable flow principle. In this way, the flow of the fixed displacement pump can be efficiently reduced at highway driving.

To ensure the required steering assistance can be delivered in all situations, the first gear of the gearbox, $i_{g1}$, is constraint to be equal to the gear ratio used in he conventional system, i.e. 1.412 (see Appendix A). The second gear, $i_{g2}$, must be optimally found. For this, we define three different minimum flows cases, namely $q_{min} = 6$, $q_{min} = 8$ and $q_{min} = 10$ L/min. A minimum flow constraint is necessary for safety reasons, as it takes some time before the pump delivers the required flow and pressure when it is accelerated from a stand-by mode [16].

The nested optimization problem of this combined optimization is formulated as shown in Fig. 5.11, where the continuous control variable $\gamma(t)$ (i.e., the gear number) is determined from the discrete design parameter $i_{g2}$ (i.e., second gear ratio). In this figure $q_s$ is the system flow and $q_{min}$ is the minimum flow as introduced before.

We use Sequential Quadratic Programming (SQP) to solve the plant optimization problem and Dynamic Programming to solve the clutch control problem. The selection of gears $\gamma(t) \subset \{i_{g1}, i_{g2}\}$ is solved by

$$\gamma(t) = \begin{cases} i_{g1} \text{ if } q_s(i_{g2}, t) < q_{ref}(t), \\ i_{g2} \text{ if } q_s(i_{g2}, t) \geq q_{ref}(t). \end{cases} \tag{5.5}$$

When the second gear is sufficient to deliver the required minimum flow, this gear is selected. Otherwise the first gear is selected. This first gear is typically oversized to comply to worst case scenarios. For instance, for the long-haulage route used here the required gear range is $i_g \in [0.13, 0.56]$, which is much lower then the fixed ratio used in the conventional system $i_g = 1.412$.

The results of the gear design optimization problem is depicted in Fig. 5.12 where the Brute Force (BF) search results are included as well. Fig. 5.12 shows that the plant optimization cost function is convex, which ensures SQP is able to find the global optimum

**Plant Design**: Gear Ratio 2

$\Lambda$ (driving cycle)

$q_{\min}$ (Minimum flow constraint)

$i_{g20}$ (initial value second gear)

**Initialization**

$$\min_{i_{gb2}\in D} \int_0^{t_f} m_f(i_{g2},\Lambda)dt$$

$$s.t.\ i_{g2} \in [0.2,0.8]$$

$$\min_{c_1(t),\gamma(t)\in U} \int_0^{t_f} m_f(c_1(t),\gamma(t),\Lambda)dt$$

$$s.t. \quad p_b(0) = p_{b,max}$$

$$p_b(t) \in [p_{b,min}, p_{b,max}]$$

$$c_1(t) \subset \{0,1\}$$

$$i_{g1} = 1.412$$

$$p_b(t) = F(p_b(t), c_1(t), t)$$

$$\gamma(t) = \begin{cases} i_{g1} & \text{if} \quad q_s(i_{g2},t) < q_{ref}(t) \\ i_{g2} & \text{if} \quad q_s(i_{g2},t) \geq q_{ref}(t) \end{cases}$$

**Control Design**: Clutch Operation and Gear Shifting
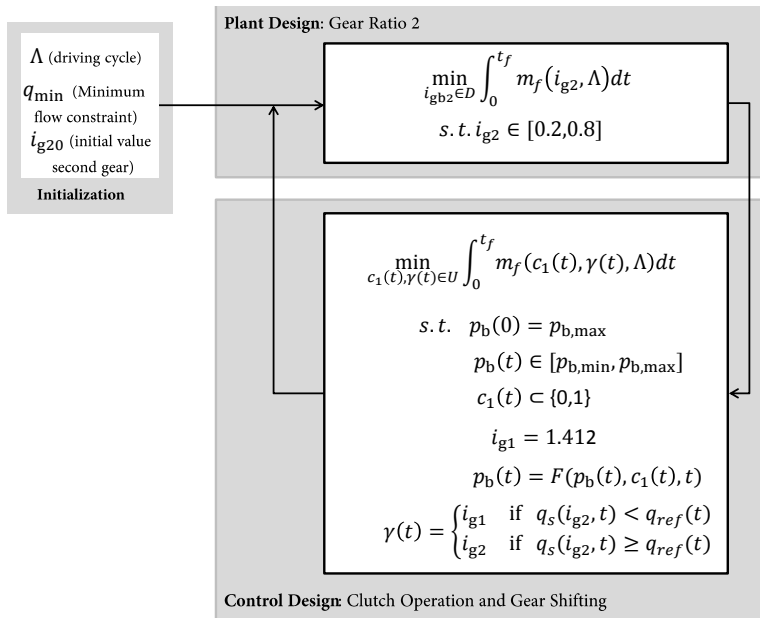
Figure 5.11: Nested optimal design for the 2-speed gearbox and clutch from Fig. 5.10.

value. This behaviour can be explained by: *(i)* when $i_{g2}$ is chosen to small, $i_{g1}$ is selected more frequently to meet the minimum ow constraint; and *(ii)* when $i_{g2}$ is chosen too high the fixed displacement pump delivers more flow than the required minimum flow which increases the fuel consumption.
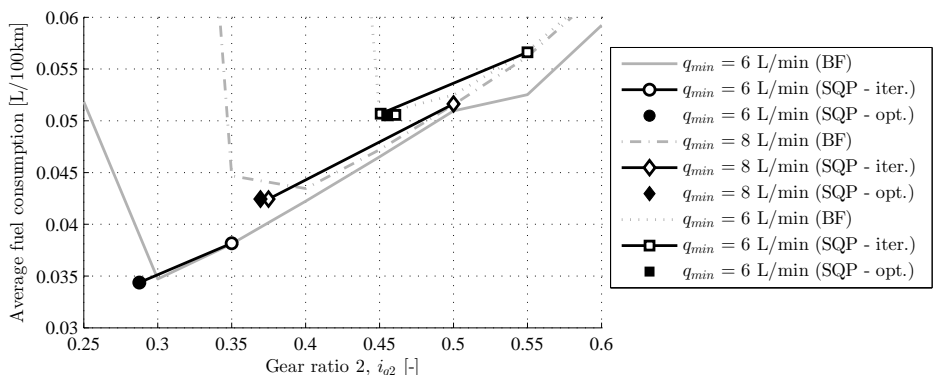


Figure 5.12: Gear design optimization using SQP Optimization and BF Search.

Furthermore, Table 5.3 shows the required number of function evaluations, the optimal ratio for $i_{g2}$ and the resulting fuel consumptions of the combined optimization for the three minimum flow levels.

| Constraint min. flow | Initial value $i_{g20}$ | Optimal value $i_{g2}^*$ | Function evaluations | Combined fuel consumption [L/100 km] [and improvement %] |
|---|---|---|---|---|
| 6 L/min | 0.35 | 0.29 | 19 | 0.0495 [84%] |
| 8 L/min | 0.50 | 0.37 | 30 | 0.0575 [82%] |
| 10 L/min | 0.45 | 0.45 | 28 | 0.0656 [79%] |

Table 5.3: Resulting optimal gear sizing and combined fuel consumption, for different required minimum flows of the nested optimization.

From these results it can be concluded that the potential fuel economy improvement, that can be achieved with the addition of a clutch for the air compressor and two discrete gears for the power steering pump is high (reaching 84% for the most optimistic minimum flow). In this particular case, the low torque demanded by the power steering pump and air compressor makes that the coupling in the combined optimization is small, i.e. the optimal control policy or design of one of these auxiliaries does not influence the optimal solution of the other auxiliary. When the optimization problem is extended to more auxiliaries, the coupling between the auxiliaries should be more evident. So far, the physical implementation of a variable gear or 2-speed gearbox has not been considered. One may envision this implementation to be done in a mechanical way, with a small CVT or gearbox.

## 5.5   Conclusions

Through this chapter the integrated design problem, for sizes and control, of two engine driven auxiliary units has been discussed. This has been implemented in a nested optimization approach using a hybrid algorithm, namely a combination of SQP for the size optimization and DP for optimal control. The optimality of the solutions found by this algorithm is ensured. It was shown that adding a variable gear to the air compressor topology does not improve the fuel consumption on sub-system level or may even make it worse depending on the gear efficiency. However, extending the current power steering and air compressor topologies with two discrete gears and a clutch respectively, can reduce the combined fuel consumption of these auxiliaries significantly. A combined optimization resulted in an improvement of about 84%, depending on the minimum ow of the power steering system.

To come to a system-optimal design, a combined optimization has been performed for an alternative, more flexible topology of the engine driven power steering pump and air compressor. The power steering topology was extended with a 2-speed gearbox. In this topology, the first gear is used for low speed maneuvering, while the second gear is used for highway cruising. It turned out that with this configuration, the fuel consumption could be reduced by about 80% compared to the conventional system. Controllable actuation of a variable displacement pump was proposed as a way to compactly implement such a 2-speed gearbox. The air compressor, as it is currently implemented, introduces drag losses in its idle mode. Although the drag torque is relatively low, it is continuously felt by the engine while the duty cycle of the compressor is only about 5%. The combined optimization showed that adding a clutch between the engine and the air compressor could reduce the fuel consumption of this auxiliary by about 90 %. Due to the low driving torques demanded by the power steering pump and air compressor, the optimal solution that resulted from a combined optimization was equal to the optimal solution resulting from individual optimizations. When more auxiliaries are included in the system-optimization, the coupling between the different auxiliaries may be more evident.

CHAPTER

# SIX

# SYNTHESIS OF REALISTIC DRIVING CYCLES INCLUDING SLOPE INFORMATION

**Abstract /**  This chapter describes a new method to synthesize driving cycles, where not only the velocity is considered, yet also the road slope information of the real-world measured driving cycle. Driven by strict emission regulations and tight fuel targets, hybrid or electric vehicle manufacturers aim to develop new, more energy and cost efficient, powertrains. To enable and facilitate this development, short, yet realistic, driving cycles need to be synthesized. The developed driving cycle should give a good representation of measured driving cycles in terms of velocity, slope, acceleration and so on. Current methods use only velocity and acceleration, and assume a zero road slope. The heavier the vehicle is, the more important the road slope becomes in powertrain prototyping (as with component sizing or control design), hence neglecting it leads to unrealistic, sub-optimal or limited designs. To include the slope, we extend existing methods and propose an approach based on multi-dimensional Markov chains. The validation of the synthesized driving cycle, is based on a statistical analysis (as the average acceleration or maximum velocity) and a frequency analysis. This new method demonstrates the ability of capturing the measured road slope information in the syntesized driving cycle. Furthermore, results show that the proposed method outperforms current methods in terms of accuracy and speed.

# 6.1   Introduction

Designing efficient hybrid electric vehicles (HEVs) with low ownership costs requires detailed feasibility studies before building prototypes. In the design process of a HEV, at least one driving cycle is necessary for evaluating its fuel consumption, emissions and performance. Furthermore, once this driving cycle is known, one can determine the mission of the vehicle, the optimal component sizes and the costs of hybridization. These characteristics make the driving cycle selection an important step in the design of new HEVs [44].

From country to country, or built by various parties, standardized driving cycles are numerous and exist in two forms. *Transient* cycles, such as the VAIL2NREL driving cycle, and *modal* cycles such as the New European Driving Cycle (NEDC), depicted both in Fig. 6.1. The primary difference is that transient cycles involve many velocity variations, typical of on-road driving conditions, whereas modal cycles are a compilation of constant acceleration, deceleration, and possibly constant velocity segments. For example, the NEDC consists of a succession of acceleration and deceleration segments that represent city driving (velocity up to 15 $m/s$) and an acceleration to highway velocity (up to 35 $m/s$). Modal cycles can easily highlight per-segment, vehicle performance criteria (e.g., acceleration or deceleration) and are often used for testing power train components (e.g., emission tests). Yet, since they are not very realistic, in powertrains design, transient cycles are preferred.
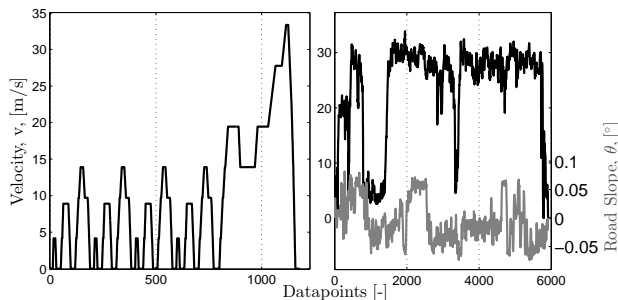


Figure 6.1: Examples of a (left) modal (NEDC), with no slope information, and (right) a transient driving cycle (VAIL2NREL).

Since driving cycles are considerably different, a HEV optimally designed using one cycle, will not be optimally designed with respect to another cycle. Therefore, having a realistic cycle that reflects real-world driving scenarios, is crucial for design. To avoid this drawback (of designs based on a single cycle), in [47–50] several cycles are used and the sensitivity of the design is investigated. Although this is an improved approach for the cycle selection, using two or a very limited amount of cycles, will not reach a

---

See Dieselnet [https://www.dieselnet.com/standards/cycles/].

HEV design robust to all real-life driving scenarios. Moreover, when sizing and control studies are done with optimization algorithms, as Dynamic Programming, long cycles will increase the simulation times significantly.

To decrease the length of several cycles, in [189], micro-trips from several cycles are combined to create a *typical* driving cycle, i.e., one that has certain statistical characteristics similar to the original cycles (percentage of city, highway and suburban driving, average speed and idling time).

In recent years, to improve the quality of the synthesized cycle speed, other methods have been proposed [51–53]. Besides matching the driving cycle statistics, these include also the random nature of a driving cycle. These methods are primely based on Markov Chains and show better results than previous methods. In [54] the authors introduce a two-dimensional Markov chain that considers also information of acceleration. However, no method so far considers information about road slope. This is an important characteristic of the driving cycle, and neglecting it leads to unrealistic HEV designs.

In this chapter, we introduce and compare two cycle synthesis methods, which considers also altitude information. Building upon existing methods we discuss the usability of two-dimensional or three-dimensional Markov chains for cycle generation. Furthermore, we use both statistical and spectral analysis, to identify good cycle candidates. As proven by results, the proposed method can create a new cycle, representing measured cycles well.

The remaining of this chapter is organized as follows. In Section 6.2, existing methods for driving cycle synthesis are explained. Then, in Section 6.3 a detailed description is presented for the used methods, based on single and multi-dimensional stochastic Markov chain. Next, in Section 6.3 two new methods are introduced that also contain road slope information; and, in Section 6.4 results of extensive simulations of the chosen method are discussed. Finally, in Section 6.5, conclusions on the synthesis of driving cycles with road slope information are drawn.

## 6.2   Existing Driving Cycle Synthesis Methods

In recent years several methods were proposed for driving cycle synthesis. Starting from concatenating measured cycles [48–50], to cut-and-clip type of methods [189] and, later on, to Markov Chain based-methods [54, 55], all methodologies have in general the following the structure

**Step 1:**   *Pre-processing* of input (measured) cycles, i.e. segmentation into micro trips [52, 53, 190]

**Step 2:**   *Synthesis* of a new driving cycle, by using rule-based [189] or using Markov Chains [51–54, 56, 191].

**Step 3:** *Validation* of the results, i.e., each generated cycle, by using a statistical, spectral or time domain analysis. Often a combination of multiple criteria is used.

Most often and when needed, this procedure is an iterative one as it will be exemplified also later on. Every existing method to synthesize driving cycles that will be discussed here, uses measured, real world, driving data as input.

Note that, given one measured cycle, $\Lambda_m$,

$$\Lambda_m = \begin{bmatrix} v(t) \\ \theta(t) \end{bmatrix}, \quad \forall\, t \in [0, t_f], \tag{6.1}$$

with $v$ the velocity, $\theta$ the slope of the driving cycle and $t_f$ the final time of the driving cycle, current methods assume

$$\theta(t) = 0, \quad \forall\, t \in [0, t_f]. \tag{6.2}$$

Moreover, as mentioned before, some methods use also the acceleration, $a(t)$, either measured or found by $a = \frac{dv}{dt}$. The first and third steps are not included in all existing driving cycle procedures, whereas the synthesis procedure is always present.

## 6.2.1   Data Preprocessing

Before using the real world driving data for driving cycle synthesis, in several works the data is preprocessed. A first way to do this is by segmenting the velocity values into different classes [51, 54]. For instance, all velocities can be segmented into discrete velocity classes, referred to also bins, with a constant bin width. For example, for a 0.2 m/s (0.72 km/h) bins width, all $v(t) \in [0, 0.2]$ m/s are in the first velocity class, $C^1$, all velocities $v(t) \in [0.2, 0.4]$ m/s are in the second class, $C^2$, and so forth. Thus, prior to the cycle synthesis method, the velocity vector is ordered and defined as

$$v(t) = [\underbrace{[0, ..., 0.2]}_{C^1}, \underbrace{[0.2, ..., 0.4]}_{C^2}, ..., \underbrace{[v_{max} - 0.2, ..., v_{max}]}_{C^N}]. \tag{6.3}$$

A second method to preprocess the measured driving data is to divide the original velocity profile into microtrips. These form different modal events, such as cruising, idle time, acceleration and deceleration, based on velocity and acceleration characteristics [52, 53]. Thus,

$$v(t) = [\underbrace{[v_{1_{min}}, ..., v_{1_{max}}]}_{C^{acceleration}}, \overbrace{\underbrace{[v_{2_{min}}, ..., v_{2_{max}}]}_{C^{deceleration}}}^{\text{Variable bin width}}, ..., \underbrace{[v_{m_{min}}, ..., v_{m_{max}}]}_{C^{cruising}}] \tag{6.4}$$

---

The superscript 1 does not refer to 'C to the power 1', but indicates the first velocity class

Every modal event collection contains microtrips of the original driving cycle, having the same velocity and acceleration characteristics, but can be different in duration (i.e., the bin width is variable). The process of segmenting the original driving cycle into microtrips is usually rule-based (engineering knowledge).

A more elaborated driving condition recognition tool (DCR) is introduced in [53]. In this method several steps are performed prior to the driving cycle synthesis step. Smoothing of the instantaneous acceleration, computed directly from the measured velocity data, was done using Epanechnikov density kernel smoothing algorithm [53]. This was done to eliminate numerical differentiation errors. Next, using statistical values and a neural network, the authors apply data segmentation and classification. The microtrips are glued together, such that parts of the original driving cycle are retained in the synthesized driving cycle.

## 6.2.2   Synthesis Procedure

The different synthesis and compression processes use rule-based, statistical or stochastic methods to synthesize a driving cycle that resembles the original driving cycle. Rule-based methods rely on expert opinion and target at matching a limited number of characteristics from the measured driving cycles [189, 192]. Such a criteria can be represented by the percentages of city, suburban and highway speeds.

Statistical methods aim at matching statistical parameters on velocity and acceleration, such as percentage time in positive acceleration, percentage of standstill time, average velocity. The synthesis procedure of a driving cycle is based on an improvement in matching those parameters, by connecting segments of the original driving cycle. This is done to maintain the same characteristics as in real-world driving [193, 194].

To enhance the probabilities of the driving cycle synthesis procedure (in terms of randomness and choosing an arbitrary length for the synthesized driving cycle) a combination of statistic and stochastic methods for combining different segments of a real world driving cycle is explained in [52, 195]. Stochastic methods use Markov chain theory to capture a model of the input driving cycles and to generate a representative driving cycle. For better results, in [51] and [54] the acceleration is added as an extra dimension for the transition probability matrix (TPM). This TPM is computed from velocity (and acceleration) classes with fixed bin width as described in (6.3), whereas in [52] and [53] the transition probability matrix is computed from the probabilities of segments from the original driving cycle, as described in (6.4). In the latter two works, instead of computing the probabilities of transitions between velocities, the probabilities of transitions between different modal events [52] or microsegments [53] are computed. Modal events are, for example, acceleration, deceleration, cruising, and so on, whereas microsegments are segments of real world driving, separated by consecutive stops. At every time step, instead of using velocity values and combining them to a driving cycle, this method works with segments of the original driving cycle. Therefore, this method generates a driving cycle

which contains parts of the original driving cycle. Yet, it has the big disadvantage that it does not capture the characteristics of the complete measured cycles, as done in [51] and [54].

Thus far, the stochastic method that uses velocity and acceleration classes and generates a purely synthetic driving cycle, from [54,196], has shown better results than other existing methods. Likewise, using stochastically obtained Markov chain driving cycles, in [56] it is shown that one can reach improved vehicle designs at reduced computational costs. These results motivate the incorporation of stochastic driving cycles in HEV optimization studies [56].

### 6.2.3    Post-Processing and Validation

Several different ways to validate the synthesized driving cycle exist. These are based on the comparison of the generated cycle with the input data (measured cycles). One such method is used in [51–53], where the distributions of velocity and optionally, acceleration, within the cycle are analysed.

A second method is to compare statistical parameters of both the measured cycles and the synthesized cycle [52,196]. For instance, these parameters are average velocity, maximal velocity, standard deviation of acceleration, and so on. In [196] an analysis is made on which of these are more crucial for obtaining a good synthesised cycle for HEV design. Ultimately, as done in [51], one can analyse the power spectra resemblance of the velocity (and optionally acceleration), between the original and synthesized driving cycle.

## 6.3    Driving Cycle Synthesis including Slope Information

Motivated by the existing methods and the desire to include altitude information in the synthesized driving cycle, in this work we investigate the applicability of multi-dimensional (multi-states) Markov chains for driving cycle synthesis. In addition, to eliminate the rule-based approach, we apply a post-processing method based on fixed width classes for both velocity and slope. For validation we combine all of the above described methods (e.g., statistical analysis, spectral analysis) to select a candidate cycle, validate the proposed method and analyse the quality of the result.

The desired outcome of a newly developed synthesis procedure is a driving cycle with a velocity, $v(t)$, acceleration, $a(t)$, and road slope profile, $\theta(t)$. These characteristics are all important in control and design studies of hybrid electric vehicles HEVs, with slope being, especially, important for heavier vehicles. To introduce such a methodology one should be aware of the inherited dependency between these parameters and capture this it in the newly developed cycle.

### 6.3.1   Correlation Between Velocity, Acceleration and Slope

The longitudinal dynamics of a vehicle, are given by $m_v \frac{d}{dt} v(t) = F_t - (F_r + F_a + F_g)$, where $F_t$ represents the traction force, $F_r$ represents the rolling resistance force, $F_a$ represents the aerodynamic friction force, $F_g$ represents force loss caused by gravity in non-horizontal driving and $m_v \frac{d}{dt} v(t)$ represents the kinetic force need to achieve desired acceleration $\frac{d}{dt} v(t)$. From this it can be deducted that a change in the road angle, $\theta$, produces a change in $F_g$, which influences the vehicle speed [12].

Considering existing methods [51–53, 196] for driving cycle synthesis, two parallel synthesis processes can be performed, one to synthesize a velocity profile, $\hat{v}(t)$, and one to synthesize a road slope profile, $\hat{\theta}(t)$. An example of the resulting velocity and road slope profile is depicted in Fig. 6.2. This is an undesired, unrealistic output, since in this case there is no dependency between $\hat{v}(t)$ and $\hat{\theta}(t)$. When the road slope is positive (driving uphill), the acceleration will be slower than for a road slope that is zero or even negative (downhill driving). Furthermore, it is very likely that the maximum velocity is reached at $\theta \leq 0$, not for $\theta > 0$. This dependency is obvious in real-life measured cycles, as it will illustrated later on, in our results Section 6.4. Therefore, the velocity profile and road slope profile should be synthesized together, such that their dependency is retained in the synthesized driving cycle.



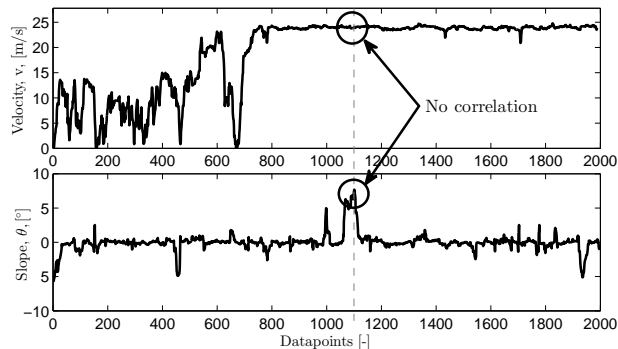Figure 6.2: (Unrealistic) Example of independently synthesized velocity and road slope profile using parallel one-dimensional Markov Chains (one for $v(t)$ and another one for $\theta(t)$)

.

### 6.3.2   Driving Cycle Models based on Discrete Markov Chains

A Markov chain is a random process on a discrete state space for which the Markov property holds. This implies that the probability of an event to occur, given that another

event has occurred, at any future time depends only on its value at the current time. In other words, the future and the past are conditionally independent given the present. The description of the present state at time fully captures all the information that could influence the future step.

**One-dimensional Markov Chain**

As shown in [196] and [55], a driving cycle, $\Lambda_m$, defined in (6.1) can be characterized through a discrete-time Markov chain. Thus, from here onwards, we restrict ourselves to the discrete-time case [197]. For this, the Markov property is defined as follows.

**Definition 2** *Let $\{X_k\}$ be a discrete-time stochastic process which takes its values in a space $S = \{s_1, s_2, ..., s_r\}$. Let $s_j \in S$. If*

$$P\{(X_{k+1} \in s_j)|X_0, X_1, ..., X_k\} = P\{(X_{k+1} \in s_j)|X_k\}, \tag{6.5}$$

*then $\{X_k\}$ is said to be a discrete-time Markov process.*

**Definition 3** *The probability, P, of taking a step from current state $s_i \in S$ to a next state $s_j \in S$, denoted as $P_{ij}$, is*

$$P_{ij} = P(X_{k+1} = s_j \mid X_k = s_i), \tag{6.6}$$

All transition probabilities $P_{ij}$, $\forall\ s_i, s_j \in S$ are captured in a transition probability matrix (TPM), denoted by F. This matrix F has the property that all its entries $P_{ij} \geq 0$ and all its row sum (i.e., all probabilities of leaving a state) are unity,

$$\sum_j P_{ij} = \sum_j P(X_{k+1} = s_j \mid X_k = s_i) = 1 \tag{6.7}$$

The speed vector of a driving cycle, post-processed as in (6.3) or (6.4), will become

$$F = \begin{matrix} & \begin{matrix} v \in C^1 & \cdots & v \in C^N \end{matrix} \\ \begin{matrix} v \in C^1 \\ \vdots \\ v \in C^N \end{matrix} & \begin{pmatrix} & Computed & \\ & from\ v(t) & \\ & of\ \Lambda_m\ (6.1) & \end{pmatrix} \end{matrix} \tag{6.8}$$

We denote this as a *one-dimensional (1D) Markov chain* that models the speed of one or more given cycles. To compute this matrix, in the one dimensional case, the measured velocities of various driving cycles are structured in one vector. Then, a small enough grid is selected (as shown in 6.3) and the transition probability matrix F is computed. The incorporation of acceleration or slope increases the dimensionality of $F$, and will be discussed next. Moreover, the construction of a new cycle, using one or multiple dimensional Markov models will be addressed in Section 6.3.4.

### 6.3.3  Two-Dimensional Markov Chain

Building a driving cycle synthesis method that considers besides velocity, also slope or acceleration, requires a *2D Markov Chain* to be considered. In the 2D case, the states in $F$ are defined by two parameters, for instance $v(t)$ and $\theta(t)$. Thus, every state $s \in S$ is a combination of the velocity class $C_i^v$ and the road slope class $C_i^\theta$. Now $F$ contains the probabilities to go to $C_j^v$ and $C_j^\theta$ at the next time step.

Such a framework is applied in [55, 196] to synthesise a driving cycle considering velocity and acceleration. In many real world driving cycles the acceleration is not measured directly, but obtained from differentiating the measured velocity. Furthermore, real world velocity signals are often measured only every second. This large sampling time leads to an imprecise acceleration signal where specific acceleration information (e.g., the aggressiveness of the driver while driving) is lost. Thus, generating an acceleration profile is not necessary in the driving cycle synthesis method. Motivated by these, in this work we will use a 2D Markov chain based method to capture the velocity and the slope information, rather than the velocity and the acceleration.

Analog to (6.8), to construct $F$, $v(t)$ and $\theta(t)$ from (6.1) are segmented into classes. As motivated in Section 6.2 we assume for these fixed class width, with a predefined number of classes $N$ for slope and $M$ for velocity, defined by $\Delta v = (v_{max} - v_{min})/M$ and $\Delta\theta = (\theta_{max} - \theta_{min})/N$. The subscripts $()_{min}$ and $()_{max}$ represent the minimum and maximum values of these parameters in $\Lambda_{\mathrm{m}}$. The driving cycle now has $M$ velocity classes and $N$ road slope classes. Every road slope value and every velocity value falls in a class $C^v$ and $C^\theta$,

$$
\begin{aligned}
v(t) \in C^v &\in \{C^1, C^2, ..., C^M\},\\
\theta(t) \in C^\theta &\in \{C^1, C^2, ..., C^N\}.
\end{aligned}
\tag{6.9}
$$

The transition probability matrix is a two-dimensional matrix $F \in \mathbb{R}^{M \times N}$, with $M$ rows for the velocity classes and $N$ columns for the road slope classes. Every element of F consists of a $(M \times N)$ matrix containing the probabilities of going from the current state $s_i$ at $t_k$ to the next state $s_j$, at time $t_{k+1}$.

### 6.3.4  Selecting Synthesized Driving Cycle Samples

To synthesize a new driving cycle, $\Lambda_{\mathrm{s}} = [\hat{v}(t) \ \hat{\theta}(t)]^T$, an initial state, $s_i$, and F are used to compute future states $s_j$. To this purpose, a Monte Carlo sampling method [198], based on a Poisson distribution of the probabilities, is used. This Markov Chain Monte Carlo (MCMC) technique has been successfully used in earlier driving cycle synthesis methods [51], as well as in weather forecasting (e.g., wind speed estimation models [199]).

To apply MCMC, the matrix F is transformed into a new matrix T, using two steps. First,

all the probabilities within each element of the matrix F (i.e., $F_{i_v,i_\theta}(j_v, j_\theta)$, $\forall\ i,j$ , are transformed in a vector $\tilde{T}_{i_v,i_\theta} \in \mathbb{R}^{1,M\times N}$ as

$$
\begin{aligned}
\tilde{T}_{i_v,i_\theta} = \Big[ &\big[F_{i_v,i_\theta}(1,1),...,F_{i_v,i_\theta}(M,1)\big]^T \| \\
&\big[F_{i_v,i_\theta}(1,2),...,\ F_{i_v,i_\theta}(M,2)\big]^T \|... \\
\| &\big[F_{i_v,i_\theta}(1,N),...,F_{i_v,i_\theta}(M,N)\big]^T \Big]
\end{aligned}
\tag{6.10}
$$

with $\|$ representing the concatenation of two vectors. This results into a matrix $\tilde{T}$ in which each element is a vector. Then, for each element of $\tilde{T}$, the cumulative sum is determined and the vector is augmented with 0, as

$$
\begin{aligned}
T_{i_v,i_\theta}(q) &= [0,\ \sum_{p=1}^{q} \tilde{T}_{i_v,i_\theta}(p)],\ \forall\ q \in [1,2,...,M\cdot N], \\
&= [0,\ \tilde{T}_{i_v,i_\theta}(1),\ \tilde{T}_{i_v,i_\theta}(1)+\tilde{T}_{i_v,i_\theta}(2),...].
\end{aligned}
\tag{6.11}
$$

By doing this two-step transformation of the matrix F, every element in the newly obtained matrix $T$ is represented by a vector with values starting at 0 and ending at 1. Given the construction from (6.11), it holds that the difference between two consecutive elements of $T_{i_v,i_\theta}$, is equal to the probability of going to this state $s_j$ in $F$. For instance,

$$
F_{i_v,i_\theta}(6,1) = T_{i_v,i_\theta}(6) - T_{i_v,i_\theta}(5).
\tag{6.12}
$$

Therefore, the probability that a transition to $F_{i_v,i_\theta}(6,1)$ occurs, is equal to the probability that a randomly generated number $\mu \in [0,1]$ falls in the interval between $T_{i_v,i_\theta}(5)$ and $T_{i_v,i_\theta}(6)$. In Monte Carlo sampling a repeated random sampling $\mu \in [0,1]$ is selected to generate new samples. When selecting $\mu \in [0,1]$, the first index in the corresponding row of $T_{i_v,i_\theta}$ for which

$$
\mu \le T_{i_v,i_\theta}(z),
\tag{6.13}
$$

holds, is the index which should be selected, i.e., the upper limit of the interval in which $\mu$ falls. In (6.13), $i_v, i_\theta$ stand for the classes ($C_i^v$ and $C_i^\theta$) at the current time $t_k$, and the parameter $z$ indicates the index of the sample which will be selected. Thereafter, the corresponding classes of $j_v$ and $j_\theta$ in the next time step $t_j$, can be derived from this index $z$. For example, given a randomly generated $\mu \cong 0.25$, assume that the corresponding indices of cell $T_{3,7}$ are $T_{3,7}(37)$ and $T_{3,7}(38)$. Therefore, at $t_{k+1}$, $C_j^v$ and $C_j^\theta$ that correspond to this index, $z = 38$, will be chosen. This process, of selecting a sample for driving cycle synthesis, is graphically shown in Fig. 6.3. Converting the index of $T_{i_v,i_\theta}(z)$ into respectively the velocity class, $C_j^v$, and the road slope class, $C_j^\theta$, of the new driving cycle sample, is done by

$$
\begin{aligned}
C_j^v &= T_{i_v,i_\theta}(z) - \lfloor \frac{T_{i_v,i_\theta}(z)}{M} \rfloor \cdot M, \\
C_j^\theta &= \lceil \frac{T_{i_v,i_\theta}(z)}{N} \rceil.
\end{aligned}
\tag{6.14}
$$

---

$F_{i,i}$ is an equivalent representation of $F_{C_i^v,C_i^\theta}$ for a 2D Markov model;

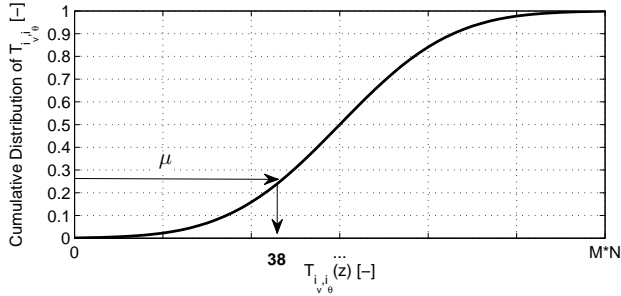For the velocity classes $C_v$, $i,j \in (1,..,M)$, while for the slope classes $C_\theta$, $i,j \in (1,..,N)$.

Figure 6.3: Selection method of driving cycle samples with the use of a random number generator.

**Note**. In (6.14) the operators $\lfloor \ \rfloor$ and $\lceil \ \rceil$ stand for *floor* and *ceil* functions, i.e. $\lfloor \frac{T_{iv,i\theta}(z)}{M} \rfloor = \{\alpha \in \mathbb{Z} \mid \alpha \leq \frac{T_{iv,i\theta}(z)}{M}\}$ and $\lceil \frac{T_{iv,i\theta}(z)}{M} \rceil = \{\beta \in \mathbb{Z} \mid \beta \geq \frac{T_{iv,i\theta}(z)}{M}\}$.

When $C_j^v$ and $C_j^\theta$ are known, the new velocity value $\hat{v}$ and road slope value $\hat{\theta}$ are obtained from taking the average value of the lower and upper limit of the class, assuming a normal distribution within each class,

$$\hat{v} = v_{avg}(\eta), \forall \eta \in C_j^v,$$
$$\hat{\theta} = \theta_{avg}(\eta), \forall \eta \in C_j^\theta. \tag{6.15}$$

This procedure, to select driving cycle samples for drive cycle synthesis, is a step in the cycle synthesis method. This complete method is depicted in Fig. 6.4 for a 2D case, and holds for one or multi-dimensional Markov chains.

In addition to the method presented here for sample selection, updating the probability based on the selected samples, improves the resulting synthesized driving cycle. By doing this, for sufficiently long synthesized driving cycles, the distribution of $\hat{v}(t)$ and $\hat{\theta}(t)$ will approach asymptotically the original distribution. This update is made by substracting the transitions already selected from the transition probability matrix. Once the update is applied, the matrix $T$ from 6.11 is recalculated and the process is re-iterated as shown in Fig. 6.4.

## 6.3.5  Cycle Evaluation and Validation

The initial state of the velocity and the road slope, $s_i$, are selected randomly from the transition probability matrix. In this way the starting point of the newly synthesized driving cycle is always different. The remaining instances are selected as described in Section 6.3.4 and by Fig. 6.4. Due to the stochastic characteristic of the process, the newly created cycle will not always end at a velocity $v = 0\,m/s$. This can pose a problem
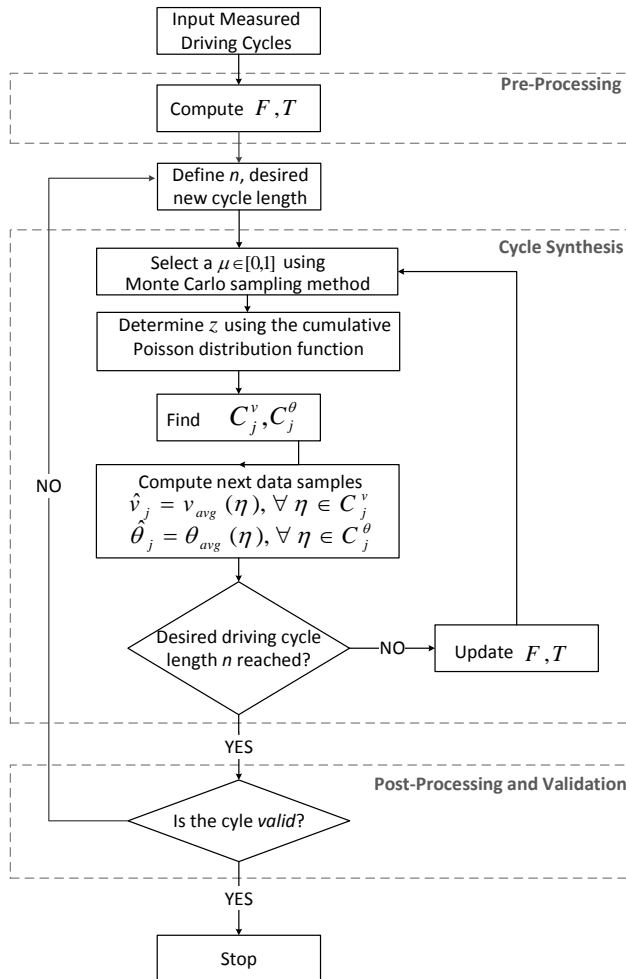
Figure 6.4: Structural outline for the 2D driving cycle synthesis procedure for velocity and slope, using a Monte Carlo sampling method and a cumulative Poisson distribution function.

for hardware testing, as for example on a dynamometer, but should not pose a problem for simulations. Furthermore, the process should be iterated until the synthesized driving cycle is *validated*, i.e., matching the original driving cycle(s) according to predefined requirements on similarity.

The *validation* of a new cycle is often done based on matching *statistical parameters* between the original and the synthesized driving cycle in time domain [52, 53, 55]. Examples include parameters based on velocity (e.g., average velocity, maximal velocity,

and so on) and acceleration. The second criteria is to compare the newly developed cycle to the input data in *frequency domain*. Using the power spectral density, one can conclude if the cycles match in the interest frequency band ($< 0.2$ Hz) [51].

In this work, to validate a newly developed cycle and to keep or reject a solution, we use all the above mentioned methods. The parameters considered are:

| | |
|---|---|
| Mean velocity | $v_a = \frac{1}{n} \sum_{i=1}^{n} v_i$ |
| Standard deviation velocity | $s_v = \sqrt{\frac{1}{n-1} \sum_{i=1}^{n} |v_i - v_a|^2}$ |
| Maximal velocity | $v_{max} = \max_{i=1}^{n}(v_i)$ |
| Mean acceleration | $a_a = \frac{1}{n} \sum_{i=1}^{n} a_i$ |
| Standard deviation positive acc. | $s_a = \sqrt{\frac{1}{n-1} \sum_{i=1}^{n} |a_i - a_a|^2}, \forall a_i > 0$ |
| Maximal acceleration | $a_{max} = \max_{i=1}^{n}(a_i)$ |
| Maximal decceleration | $d_{max} = |\min_{i=1}^{n}(a_i)|, \ \forall a_i < 0$ |

We restrict these parameters of each candidate cycle to match the ones of the measured driving cycle within maximum 10% difference, as used also in the work of Brady et al. [53]. This, in order to guarantee that a particular synthesized cycle satisfactorily represents the input, real-world, driving cycle. In the works of [52, 55] these parameters are used to analyse the synthesised cycle but not in the generation process.

Additionally, as this method considers road slope information, we introduced statistical parameters for road slope as bellow and constrain them to match within a 15% bound.

| | |
|---|---|
| Mean slope | $\theta_a = \frac{1}{n} \sum_{i=1}^{n} \theta_i$ |
| Standard deviation slope | $\theta_a = \sqrt{\frac{1}{n-1} \sum_{i=1}^{n} |\theta_i - \theta_a|^2}$ |
| Maximal slope | $\theta_{max} = \max_{i=1}^{n}(\theta_i)$ |
| Minimal slope | $\theta_{max} = \min_{i=1}^{n}(\theta_i)$ |

Besides these parameters, to compare the 2D method to the 3D method (described in Section 6.3.6), we analyse also computational time. Parameters such as *Percentage of idle* time and *Number of stops* are excluded from our analysis, since they are not present in the available measured cycle.

### 6.3.6   Three-Dimensional Markov Chain

When available, besides the velocity and the slope, one can use the acceleration as an input to the Markov chain. This requires a *3D Markov model*, which can be an extended, more complex form of the two parameter case. To construct the new matrix $F$, the acceleration, $a(t)$, $v(t)$ and $\theta(t)$ information are segmented into classes $C^v$, $C^\theta$, and $C^a$. By choosing the number of classes $M$, $N$ and $O$, the intervals are defined similiar to the 2D case, by $\Delta v = (v_{max} - v_{min})/M$, $\Delta \theta = (\theta_{max} - \theta_{min})/N$ and $\Delta a = \frac{a_{max} - a_{min}}{O}$. The driving cycle now has M velocity classes, N road slope classes, and O acceleration classes. Every velocity, every road slope, and every acceleration falls in a class $C^v$, $C^\theta$, $C^a$ and a transition probability matrix $F \in \mathbb{R}^{M \times N \times O}$ can be build. Moreover, every element of this matrix is composed of a $(M \times N \times O)$ matrix again. Each of these $(M \times N \times O)$ matrices contain the probabilities of going from the curent state $s_i$ at $t_k$ to a next state $s_j$ at $t_{k+1}$. An example of such a matrix is depicted in Fig. 6.5, where the probabilities for leaving a state with classes $C_i^v = 2$, $C_i^\theta = 5$, and $C_i^a = 1$, is shown. This matrix is denoted by $F_{2,5,1}$ and from it one can observe that the probability of staying in the same velocity, road slope and acceleration class, is the highest, namely $F_{2,5,1}(2,5,1) = 0.1538$. The probability of going to $C_j^v = 3$, $C_j^\theta = 4$, and $C_j^a = 2$ is $F_{2,5,1}(3,4,2) = 0.0308$, and the probability of a transition to a state with $C_j^v = 1$, $C_j^\theta = 6$, and $C_j^a = 3$ is $F_{2,5,1}(1,6,3) = 0$.
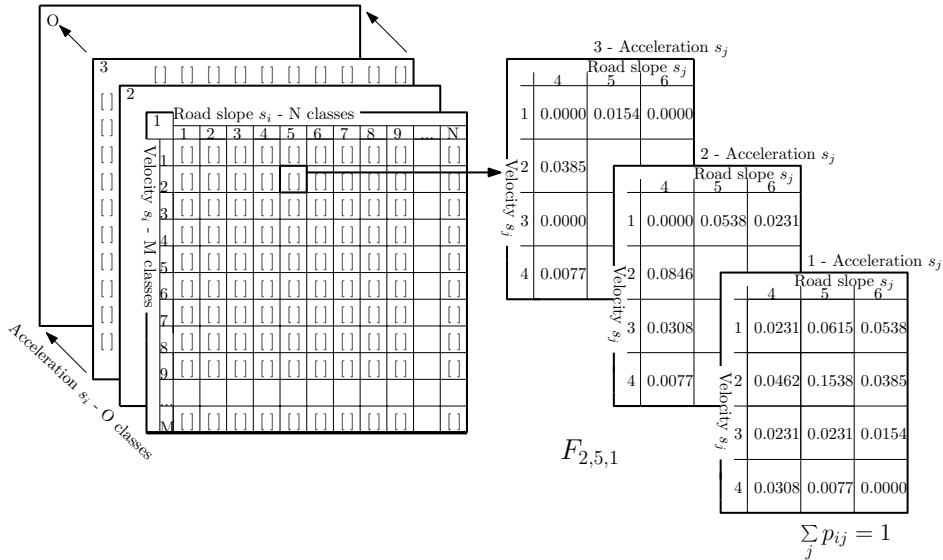
Figure 6.5: Example of three-dimensional transition probability matrix, $F$, from state $s_i$ to $s_j$

To synthesise a new driving cycle, new samples are selected using the procedure explained in Section 6.3.4. Note that the dimensionality of the matrices $F$ and $T$ have

increased, with each elemet of $T \in \mathbb{R}^{1,M \times N \times O}$ being defined as

$$
\begin{aligned}
T_{v_i,\theta_i,a_i} = \Big[ &\big[ F_{v_i,\theta_i,a_i}(1,1,1), ..., F_{v_i,\theta_i,a_i}(M,1,1) \big]^T \| \\
&\big[ F_{v_i,\theta_i,a_i}(1,2,1), ..., F_{v_i,\theta_i,a_i}(M,2,1) \big]^T \|.. \\
&\| \big[ F_{v_i,\theta_i,a_i}(1,N,O), .., F_{v_i,\theta_i,a_i}(M,N,O) \big]^T \Big]
\end{aligned}
\tag{6.16}
$$

Sequentially, the cumulative sum is determined over all these probabilities,

$$
T_{v_i,\theta_i,a_i}(q) = [0, \sum_{p=1}^{q} T_{v_i,\theta_i,a_i}(p)], \forall\, q \in [1,2,...,M \cdot N \cdot O].
\tag{6.17}
$$

By following the process described in Fig. 6.4, the index $z$ is found with the use of a randomly generated number $\mu$, by $\mu \leq T_{v_i,\theta_i,a_i}(z)$. The corresponding classes, with index $z$, of velocity and road slope are found as in (6.14) and for acceleration by

$$
C_j^a = \lceil \frac{T_{i_v,i_\theta,i_a}(z)}{M \cdot N} \rceil.
\tag{6.18}
$$

The procedure is then completed by the steps explained in Section 6.3.4 and Fig. 6.4.

## 6.4   Results

Given measured cycles, to determine which method is most suitable for the construction of a new driving cycle, in this section we compare the *2D Markov Chain* based method and the *3D Markov Chain* based method.

To validate the two proposed methods, one measured driving cycle has been used, which is representative for heavy-duty long-haul routes across Europe (Fig. 6.6). The length of this cycle is 29282 data points that corresponds to 8.1 hours of driving (with a sampling time of 1 second). In this cycle both the road slope and the velocity are measured.

For this analysis, $v(t)$, $\theta(t)$ and $a(t)$ are segmented into 50 classes, hence $M = N = O = 50$. For the particular input cycle this results respectively in class widths of

$$
\Delta v = 0.50 \text{ [m/s]}, \ \Delta\theta = 0.28 \text{ [}^\circ\text{]}, \ \Delta a = 0.072 \text{ [m/s}^2\text{]}.
\tag{6.19}
$$

Next, the desired driving cycle length is chosen to be 4500 data points.

### 6.4.1   2D Method Compared to the 3D Method

In this section the methods described in Section 6.3.3 and Section 6.3.6 are compared as schematically depicted in Fig. 6.7. This is done to highlight the results accuracy and
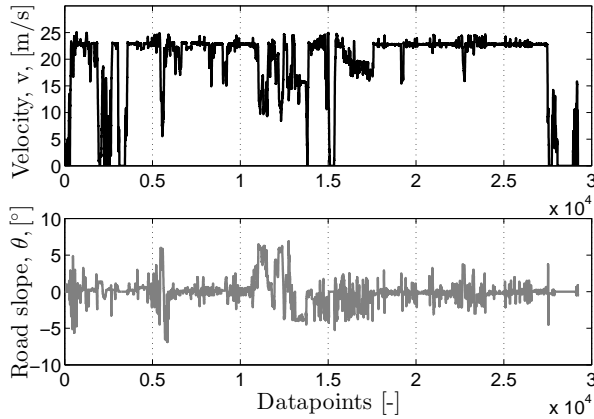
Figure 6.6: Measured driving cycle velocity and speed profiles, in Europe, used as input for the synthesis method.

speed of using one or another method. As explained in Section 6.3, increasing the driving cycle synthesis method, from two to three parameters, also increases the transition probability matrices from being two-dimensional to three-dimensional. This greatly effects both the complexity of calculations and the computation time needed to synthesize a complete new driving cycle. By averaging the results on the computation time and re-
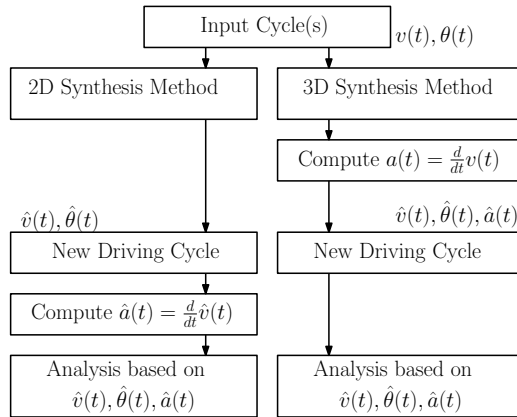


Figure 6.7: Schematic representation of the compared methods.

semblance between the original and the synthesized driving cycle gives a good indication of the performance of both methods. For each of the two methods, the resemblance of the two cycles can be improved when performing more iterations. However, since the process is purely stochastic, there is no guarantee that if a particular cycle generate with one method (after $q$ iterations) is a good candidate, the other method will also output a good cycle in iteration $q$. Therefore, in this sub-section, we use three iterations for

comparing the two methods and after every iteration the results are analysed.

In Table 6.1 the error percentage (for all the parameters introduced in Section 6.3.5) between the measured and the synthesized cycle is shown. From Table 6.1 one can

| Variable Name (Criteria) | 2D Markov chain using $v(t)$ and $\theta(t)$ | 3D Markov chain using $v(t)$, $\theta(t)$ and $a(t)$ |
|---|---|---|
| Mean velocity | 12.66% | 13.04% |
| Standard deviation velocity | 60.71% | 56.18% |
| Maximal velocity | 1.87% | 2.16% |
| Mean slope | 1.58% | 1.50% |
| Standard deviation slope | 12.64% | 16.07% |
| Maximal slope | 5.15% | 7.30% |
| Minimal slope | 16.69% | 17.32% |
| Mean acceleration | 0.015% | 0.08% |
| Standard deviation positive | 24.36% | 44.16% |
| Maximal acceleration | 18.10% | 21.71% |
| Maximal deceleration | 24.18% | 32.57% |
| Computation time | 0.52 seconds | 27.43 seconds |

Table 6.1: Comparison of the 2D and 3D methods using statistical results for velocity, $v(t)$, slope, $\theta(t)$, and acceleration, $a(t)$ with respect to the error percentage.

observe that not all the criteria match the 10% or 15% bounds imposed, such as *Standard deviation velocity*. For that, more iterations need to be done, as it will be exemplified next.

These results show that the 3D method is outperformed in the majority of statistical criteria by the 2D parameter method. Furthermore, the computation time of the 3D method is more than 50 times higher than the computation time of the 2D method. Therefore, when the acceleration is not measured, a 2D method is better and faster in constructing a synthetic driving cycle form measured cycles. To reach this conclusion we performed further and detailed time and frequency domain analysis.

A limitation of the 3D method is given by the number of classes, $M$, $N$ and $O$. With their increase, the matrix T from (6.5) increases significantly, and poses computational challenges (for instance Matlab memory problems). The presence of a measured acceleration signal, with a small enough sampling time, could possibly improve the results of the 3D method.

---

The calculations have been performed by using Matlab R2013a on a 64bit system having an Intel i7-4700MQ processor at 2,40 GHz.

## 6.4.2  Enhanced Performance Analysis for the 2D Method

To evaluate further the 2D proposed method, and to find a *valid* synthetic cycle, the number of road slope classes $N$ and velocity classes $M$ are set to 200 classes. The desired length of the synthesized driving cycle, $n$, is chosen again at $n = 4500$. Given a measured driving cycle of 29282 datapoints (29282 seconds) depicted in Fig. 6.6, this implies that the original driving cycle is reduced in length by approximately a factor of six. In 5433 iterations a *valid* cycle is found as depicted in Fig. 6.8. In this cycle the correlation (interdependency) between the velocity and slope is evidentiated. This is particular important, since neglecting it leads to a generated cycle with a significantly higher power demand for the powertrain.
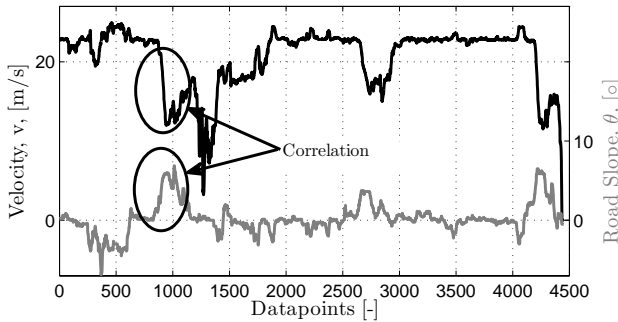


Figure 6.8: The velocity and the road slope of the synthesized driving cycle.

| Validation Criteria | Deviation Values from the Input Cycle |
|---|---|
| Mean velocity | 4.69 % |
| Standard deviation velocity | 9.15 % |
| Maximal velocity | 0.28 % |
| Mean slope | 1.32 % |
| Standard deviation slope | 13.45 % |
| Maximal slope | 0 % |
| Minimal slope | 0 % |
| Mean acceleration | 0.13 % |
| Standard deviation positive acc. | 1.19 % |
| Maximal acceleration | 7.75 % |
| Maximal deceleration | 0.6 % |
| Number of iterations | 5433 |
| Computation time | 104487 seconds |

Table 6.2: Selection of a candidate cycle based on statistical results for velocity, $v(t)$, slope, $\theta(t)$, and acceleration, $a(t)$.

Table 6.2 shows the error percentage between the measured and the synthesized cy-

cle, where all the velocity and acceleration criteria $\leq 10\%$ and all slope related criteria $\leq 15\%$. To compare further the matching of the velocity, the road slope, and the acceleration of the generated and the measured cycle, in Fig. 6.9 - 6.11 the distribution of these is shown. Furthermore, in Fig. 6.12 the power spectra for both the road slope and the velocity are depicted. The results demonstrate the resemblance of the real-life driving cycle with high accuracy.
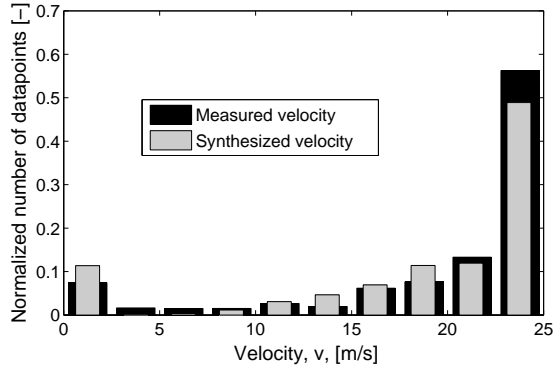


Figure 6.9: Histogram of measured and synthesized velocity using the 2D method and iterative evaluation of candidate cycles.
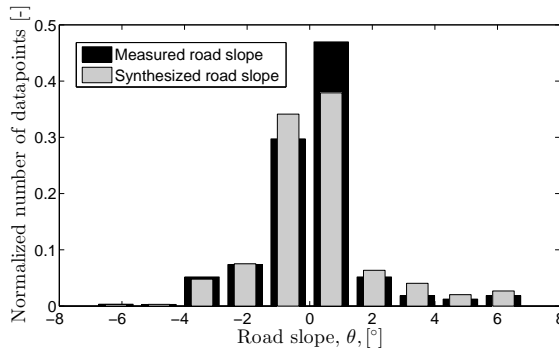


Figure 6.10: Histogram of measured and synthesized road slope using the 2D method and iterative evaluation of candidate cycles.

This resemblance is shown also in Fig. 6.13 and Fig. 6.14, where the current velocity, $v(k)$, and current slope, $\theta(k)$, are depicted and compared with $v(k-10)$ and $\theta(k-10)$ (10 seconds in the past). With increasing time delay, these figures shift from a straight line to a scatter plot between zero and the maximum velocity. The shorter the generated cycle is required to be, the more difficult it is to obey the $\leq 15\%$ slope related criteria. Nonetheless, the length of the desired cycle is not the purpose of this study, and will not be considered here. Increasing the number of classes $M$ and $N$ leads to a better
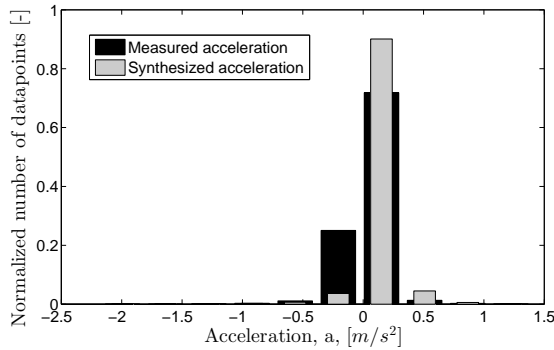
Figure 6.11: Histogram of the acceleration (measured and synthesized) using the 2D method and iterative evaluation of candidate cycles.
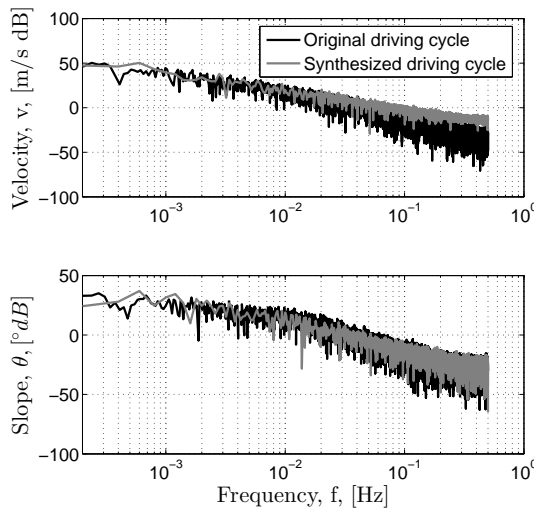


Figure 6.12: Power spectra of the velocity (measured and synthesized) and road slope using the 2D method and iterative evaluation of candidate cycles.

accuracy of the results, yet in the same time increases the computational time. The same trade-off holds for choosing the synthesized driving cycle length $n$ closer to the original driving cycle length. Whereas in this example only one driving cycle is used as input, also multiple driving cycles can be used as input, such that the syntesized driving cycle contains characteristics of every input cycle.

These results demonstrate that the proposed 2D method to generate driving cycles is able to synthesize a good new driving cycle. The outcome of the process is a synthetic driving
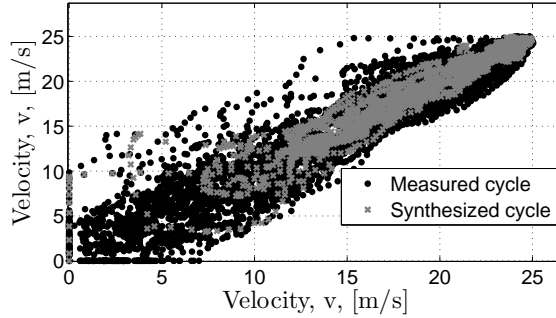
Figure 6.13: Relation between current velocity and velocity 10 seconds in the past, for the measured and synthesized cycle.
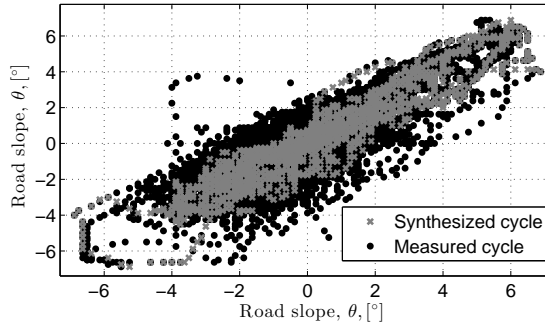


Figure 6.14: Relation between slope and slope 10 seconds in the past, for the measured and synthesized cycle.

cycle that represents its original in terms of time and frequency domain performance criteria. Moreover, the use of acceleration, as a third parameter in the Markov process does not bring a significant improvement in the resemblance, yet increases the computational burden significantly (for a cycle with 1 second sampling time). The high accuracy obtained with the 2D method on the acceleration performance criteria motivates the usage of the 2D method over the 3D method even when better measurement are available (i.e, with lower sampling time).

To further improve the results, the optimal number of velocity and road slope classes *M* and *N* can be found. Moreover, depending on the designer, the choice of the synthesized driving cycle length can be changed.

## 6.5 Conclusions

The possibility of creating a synthetic driving cycle, short and representative of a measured driving cycle, is very important in hybrid or electric vehicle design. By using a synthetic driving cycle, design simulation time can be significantly decreased. Moreover, the characteristics of the driving cycle used immediately influence the size and control parameters of the vehicle. Using a short synthetic cycle, which is representative of more real driving cycles, eliminates the need to iteratively simulate and analyze power train designs for several driving cycles, such as driving in the city or on the highway. Hence, the use of one compact driving cycle that reflects all real-world driving, is preferred above the use of multiple driving cycles or one very long driving cycle.

This work introduces two novel methods to synthesize a driving cycle, required as input in powertrain design studies. Besides the attributes considered so far in literature (i.e., velocity and acceleration), this methods consider also road the slope information from the measured driving cycle. Using Markov chain theory and building upon existing methods (Monte Carlo sampling and the cumulative Poisson distribution function), two methods were introduced and compared using measured data. Both time domain and frequency domain analyses were used to validate the results. In this regard, we show that the proposed two-dimensional method is able to synthesize or compress driving cycles fast and with high accuracy. Moreover, the method is independent of the input cycle length or number, and it is therefore widely applicable. Further work will address the influence of this driving cycle and its specific parameters on the optimal design and control of hybrid electric vehicles (HEV). More insight in the effect of, for example, average velocity or standard deviation of velocity on the component sizes of a HEV, could improve the robustness of HEV design and reduce the effect of cycle beating (where a vehicle is designed based on a driving cycle that does not reflect real-world driving).

# SEVEN

# CONCLUSIONS AND RECOMMENDATIONS

**Abstract /** This chapter reviews and discusses the main conclusions of this thesis. Based on these, recommendations for future developments are given.

## 7.1 Conclusions

The research objective addressed in this thesis was to develop a design methodology that yields an optimal hybrid vehicle with respect to imposed usability conditions and various design targets. To design an optimal system, both the plant and its controller can be varied. Previous approaches in literature have already presented methods and results that addressed this challenge. In the latest and most promising approaches, the hybrid vehicle architecture is fixed and the problem of *plant and controller co-design* results in finding the optimal components sizing and control inputs. Moreover, the driving cycle used to design and evaluate the fuel consumption was singular and region-dependent (such as the NEDC in EU and the EPA in USA). To improve the speed and quality of the design, and to allow the exploration of multiple vehicle configurations (topologies), we formulated and addressed five topics of research:

$O_1$ Identify what are the main challenges in designing hybrid electric vehicles and what interactions between the various design levels influence the optimality of the designed system.

$O_2$ Develop a method of construction and automatic selection of hybrid topologies.

**O$_3$** Investigate the potential of reducing the operational and component costs by powertrain hybridization.

**O$_4$** Analyse the potential benefits of electrification of auxiliary systems present in a vehicle, such as the steering system, the air-conditioning system and so on.

**O$_5$** Build a method to synthesize a short driving cycle representative of real driving cycles, in which the characteristics of speed, acceleration and road altitude variations are accurately captured.

In what follows we will conclude on these topics independently.

**O$_1$: Interaction between the design levels in a HEV**
Chapter 2 highlights four possible levels in the design of a hybrid vehicle: the generation of hybrid architectures, topology optimization, optimal sizing and technology, and optimal control design. This is a multi-level mix-integers optimization problem that is usually non-linear, non-convex and that has more than one optimization target. To solve this, a designer should choose a coordination strategy and search/optimization algorithms. We identified the bi-level nested strategy as the most used one, with Dynamic Programming algorithm often used to find the optimal control inputs. This methodology is suitable and often applied to powertrain sizing and control studies, where the coupling is unidirectional.

**O$_2$: Automatic generation and selection of HEV topologies**
To enable topology optimization studies, in Chapter 3, we presented a methodology to automatically generate (all possible and all feasible) hybrid vehicle topologies. This novel method uses a pre-defined set of components (platform) on which functionality and cost constraints are defined. By using these principles we define and implement a constraint satisfaction problem over finite domains. Solving this problem reduces the enormous original design space of $5.7 \cdot 10^{45}$ possible topologies, to 4779 feasible topologies, all of which are hybrid electric vehicles, with one or two electric machines. Moreover, we analyse the resulted configurations and present trends in HEV development, highlighting the flexibility and modularity of the method. This is an important step in enabling much faster design studies where more cost efficient hybrid vehicles can be found.

**O$_3$: Powertrain components sizing and control**
In Chapter 4, several bi-level optimization algorithms were compared to optimally size and control a parallel hybrid heavy-duty vehicle. These included brute-force, SQP, DIRECT, GA and PSO for component sizing and DP as a control algorithm. The optimization targets considered in this case study were fuel consumption and costs, which were presented for the hybridization and the engine downsizing cases. Results show that brute force search algorithms are too computationally expensive and insufficiently accurate, making optimization algorithms preferable. Moreover, we show using this case study, that only by powertrain hybridization up to 8% of fuel reduction can be achieved on a representative driving cycle, which for long haulage heavy duty trucks is a considerable amount.

Considering the multi-objective fashion of the problem a Pareto trade-off analysis is presented, where fuel and component cost are discussed. All algorithms performed well, however from a computational perspective DIRECT is preferred for non-convex problems and SQP for convex problems. Further work involves increasing the design variables number (e.g., gearbox sizing optimization), the number of topologies used and the application of more driving cycles and/or usage conditions.

**$O_4$: Potential in electrification of auxiliary systems**
The hybridization of a conventional vehicle allows flexibility in the design of the auxiliary units. In Chapter 5, we investigated the fuel consumption of the conventional auxiliary units and the possibilities of hybridization. We proposed several topologies for the power steering system and for the air compressor that can achieve, per-component, up to 80% fuel consumption reduction. Results showed that variable discrete gears and/or clutches, used for auxiliary units bring flexibility for control on-demand and eliminate the high parasitic losses these components have. To arrive at a system optimal design we further investigated the benefits of including more auxiliary units in the same optimization problem. Using SQP and DP, we solved a nested optimization problem, to optimally size the gear ratios and control the clutch operation and gear shifting. Depending on the minimum flow of the power steering system, the results of this case study showed an fuel consumption improvement of 84%, highlighting the benefits of more integrated system-level design.

**$O_5$: Driving cycle synthesis**
To eliminate cycle-beating, powertrain designs are iteratively simulated over multiple driving cycles and the results are analysed, which increases simulation times significantly. Moreover, most available driving cycles do not contain road slope information. In Chapter 6, we introduce a method based on Markov chains, that synthesizes a new driving cycle of a length chosen by the designer. As input, this method requires at least one measured driving cycle. Additional to existing methods, this method synthesizes a driving cycle in which the slope is also considered and is correlated to the velocity profile. Results show that by using the proposed two-dimensional Markov Chain method, one can synthesize or compress driving cycles fast and with high accuracy. The characteristics of the generated cycle match within 10% for the velocity and accelerations and within 15% for the road altitude. Moreover, the method is independent of the input cycle length or number, and it is therefore widely applicable.

## 7.2   Recommendations

This thesis has addressed various topics in the field of optimal design of a hybrid vehicle. Through this study some relevant lines of future research have been identified and are discussed next.

**Algorithms and optimization frameworks for HEV design**
The choice of topologies to be analysed, so far, has been mainly dictated by practical experience rather than by a topology optimization procedure. A computational tractable method for combined topology and component sizing optimization of the plant design is an open research question. Furthermore, using optimization algorithms, to solve different optimization layers, have proven beneficial for design. These could be further used, in more extended coordination methods to include the selection of topologies and technologies. For instance, these extended coordination methods might include: (i) (simultaneous topology and sizing design) alternating with controller design; (ii) controller design nested with respect to simultaneous topology and sizing, (iii) topology alternating with sizing alternating with control; or (iv) simultaneous topology, sizing, and control design.

**Optimal plant and control design for HEVs**
In Chapter 3, a method to find topologies was introduced. It has been shown that, as a result of introducing new components the set of solutions increases significantly, yet no conclusion was drawn on their fuel or cost efficiencies. How to find the optimal topology, in an (more) automatic way, from multiple topologies with a large variety in the components types and numbers, remains an open question. Further, the topology automatic construction and optimization problem creates challenges in the control algorithm development that has to handle various topologies in an automatic way. In this respect, easy-to-use methodologies must be developed, to help developers, and industry in general, to reach better designs in the early steps of HEV development process. These *holistic* design methodologies are crucial for creating market-competitive vehicles, that are suitable for our continuously changing mobility sector.

To reach the optimal system-level design and to make the results more realistic, besides designing the main components of the power train (i.e., battery pack, electric machine and engine), the variation of other sub-components can also be integrated in design studies. Several case studies have been show in Chapter 5 and Appendix A for auxiliary systems, but these should be further extended. One direction here is to investigate the implementability of these novel proposed architectures. Another direction is to integrate more auxiliary units, the transmission or other components in the design study.

**Driving cycles synthesis**
A short realistic cycle can be generated as shown in Chapter 6 and can decrease the simulation times tremendously. Further work should investigate the influence of this driving cycle and its specific parameters on the optimal design and control of a hybrid electric vehicle (HEV). More insight in the effect of, for example, average velocity or standard deviation of velocity on the component sizes of a HEV, could improve the robustness of HEV design and reduce the effect of cycle beating.

# TOPOLOGY OPTIMIZATION STUDIES FOR THE POWER STEERING SYSTEM

## A.1   Optimal Design of Steering Systems

For the truck considered here, in [153] the power consumption of the auxiliary units is presented and can add up to 4% for a long-haul predominant usage. Figure A.1 shows the six possible configurations that have been build for the steering system based on a given set of components (i.e., EM, ICE, planetary gear set, alternator and belts/gears). Each configuration is represented by a certain color/lines characteristics and present the following working principles: (1) combustion engine directly driven Hydraulic Steering (fixed displacement) Pump (H-SP), (2) Electro-Hydraulic Power Steering (EH-PS), (3) power Split Hydraulic Steering Pump (SH-PS), i.e. the combination of H-SP and EH-PS via a planetary gear set, (4) Electro-Hydraulic in combination with a Hydraulic Power Steering (EHH-PS), (5) Electric assisted Hydraulic Power Steering (E-H-PS) and finally (6) Electric Power Steering (E-PS).

In a EHH-PS topology, a H-SP can be combined with a EH-PS to lower the fuel consumption at higher speeds at the expense of fuel consumption at low speeds. To ease the understanding of Figure A.1, the SH-PS topology is depicted in Figure A.4 from Section A.4, which enables the same functionality as the EHH-PS system, but requires only one pump. Introducing a battery pack to supply electric power is also possible, yet this is not considered here as it would increase the design space for the plant and the controller design. For reasons of comparison, in all cases, the electrical power is generated by a
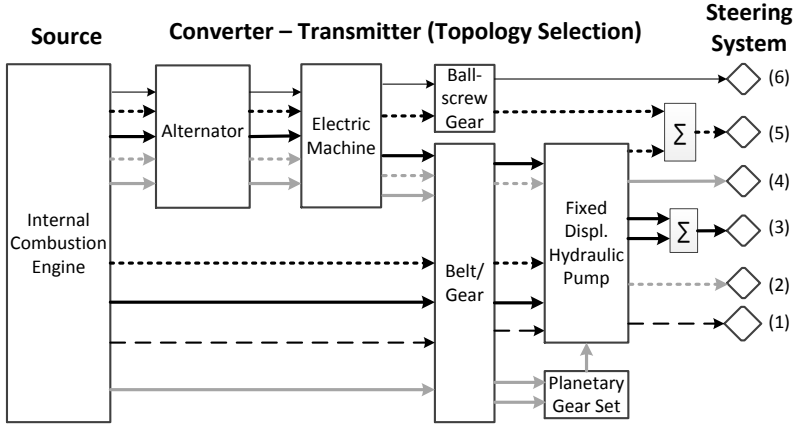
Figure A.1: Overview of the six possible topologies (one per line type) for the steering system

belt driven alternator with a constant efficiency of $\eta_a = 0.70$, for the alternator; and, $\eta_b = 0.80$, for the belt is assumed respectively.

## A.2   Optimization Problem

The objective of each configuration is to minimize the fuel consumption, denoted as $\Phi$, (or produced $CO_2$ emissions) over a representative drive cycle, $\Lambda \subseteq \mathbf{R}^{3 \times n}$, defined as $\Lambda = [s(n) \ d(n) \ v(n) \ c(n)]^T$ and consisting of $n = [1, t_f]$ data points, where $s(\cdot)$ is the slope, $d(\cdot)$ is the distance, $v(\cdot)$ is the speed, $c(n)$ is the curvature and $t_f$ is the final time value of the driving cycle. Next, the sizing and control optimization problem can be defined, in the most general sense, as a co-design problem defined in [200, 201],

$$
\min_{x_c, x_d \subseteq \mathcal{X} \subseteq \mathbf{R}^{1 \times n}} J = \min_{x_c, x_d \subseteq \mathcal{X}} \int_0^{t_f} \Phi_{c,d}(x_c(t), x_d) dt,
$$
$$
s.t. \qquad g_{d,c}(x_c(t), x_d) \leq 0,
$$
$$
h_{d,c}(x_c(t), x_d) = 0. \tag{A.1}
$$

Here $(\cdot)_d$ denotes a parametric sizing variable and $(\cdot)_c$ denotes a control variable. Depending on the topology, the design variables $(x_c, x_d)$, detailed in Table 1, and the objec-

tive to be minimized, $\Phi_{c,d}$, are

$$x_c = \{f_h, f_n\}, \tag{A.2}$$
$$x_d = \{i_1, i_2, P_e, z, l, A\}, \tag{A.3}$$
$$f_{d,c} = \Phi(x_c, x_d) = \dot{m}_f, \tag{A.4}$$
$$f_{d,c} : R^{1xn} \times R^{1xn} \mapsto R^{1xn}, \tag{A.5}$$

with $\dot{m}_f$ the fuel mass flow ratdde.

Table 1. Optimization Design Variables

| Design variable | Symbol | Units |
|---|---|---|
| Fixed gear ratio (ICE-pump) | $i_1$ | $-$ |
| Electric machine rated power | $P_e$ | $kW$ |
| Fixed gear ratio (EM-pump) | $i_2$ | $-$ |
| Fixed gear ratio PGS | $z$ | $-$ |
| Ball-screw lead | $l$ | $m/rev$ |
| Steering house piston area | $A$ | $m^2$ |
| Min. const. flow on highway | $f_h$ | $L/min$ |
| Min. const. flow on national roads | $f_n$ | $L/min$ |

In Table 2 the set of design variables, for each topology, are depicted. The set of inequality constraints, $g_{d,c}$, and equality constraints, $h_{d,c}$, are dictated by the physical properties of the system and they must be defined for each configuration in Figure A.1. An example, for a complex topology is shown in the results section. When $x_c \neq \emptyset$ the output flow ($f_h$ and $f_n$) of the electrically driven pump can be varied. For example, when there is no input at the steering wheel while driving on the highway, the flow can be reduced in order to save energy.

Table 2. Design Variables for each topology

| Variable | $i_1$ | $P_e$ | $i_2$ | $z$ | $l$ | $A$ | $f_h$ | $f_n$ |
|---|---|---|---|---|---|---|---|---|
| Topology 1 | ■ | | | | | | | |
| Topology 2 | | ■ | ■ | | | | ■ | ■ |
| Topology 3 | ■ | ■ | ■ | ■ | | | ■ | ■ |
| Topology 4 | ■ | ■ | ■ | | | | ■ | ■ |
| Topology 5 | ■ | | ■ | | ■ | ■ | | |
| Topology 6 | | ■ | ■ | | ■ | | | |

Ideally, this problem can be solved by a simultaneous optimization problem which, if any, will provide the global optimum value for the control and sizing parameters searched at the cost of high computational time. Here, next, this problem is split into a nested (bi-level) optimization problem, concept defined by [71], where the optimal sizing is solved

by

$$\min_{x_d \subseteq \mathscr{X} \subseteq \mathbf{R}^{1 \times n}} J_d =$$

$$\min_{i_1, i_2, P_e, z, l, A \subseteq \mathscr{X}} \int_0^{t_f} \dot{m}_f(i_1, i_2, P_e, z, l, A) dt, \tag{A.6}$$

$$s.t. \ g_d(i_1, i_2, P_e, z, l, A) \leq 0,$$

$$h_d(i_1, i_2, P_e, z, l, A) = 0,$$

and the control problem is solved by

$$\min_{x_c \subseteq \mathscr{X} \subseteq \mathbf{R}^{1 \times n}} J_c = \min_{f_h, f_n \subseteq \mathscr{X}} \int_0^{t_f} \dot{m}_f(f_h, f_n) dt,$$

$$s.t. \ g_c(f_h, f_n) \leq 0, \tag{A.7}$$

$$h_c(f_h, f_n) = 0.$$

To avoid the optimization algorithm getting stuck in a local minimum, a derivative free optimization algorithm is most suitable for these design problems. The downside of these algorithms is that they generally require (very) large computation times. To overcome the problem of (non)convergence of the global optimal solution, for the sizing problem, we solve (A.6) using a brute-force search over the design vectors. Then, with the same approach, in a nested manner, for each chosen set of $x_d$ the control problem is solved for a discrete grid of $f_h$ and $f_d$. When using a brute-force search method the design space is subdivided into an equidistant grid for each dimension and the objective function is evaluated for all feasible points in this grid. Although this method will not provide as output, the true global minimum, it will enable one to make a comparison between different designs. Moreover, the method is straightforward, suitable for low-dimensional optimization problems where only indicative values are require and represents a good starting method to fully understand the complexity of the problem. Given the high number of design variables, insights on the optimal design problem should be given in a Pareto distribution form. This offers insight into the optimal design set and leaves a certain degree of freedom to the designer as-well.

## A.3   Modeling of Power Steering Topologies

In general, there exist three types of pump models: (i) *empirical* models, based on measured data, are particularly useful when an accurate representation of a particular, existing pump is required, (ii) *physical* models, sometimes less accurate for a particular pump but more uniform, and hence more useful for new pump development, and (iii) *analytical* (or coefficient) models, that can be seen as a combination of the first two. In this latest model type only a limited amount of measurement data is used to determine coefficients that result from physical relations.

Due to limited amount of available data from the real pump, here, the analytical models will be built that include both leakage losses, (caused by the small gaps between the vanes and the housing) and torque losses, $T_l$, (induced by friction). The required, effective torque, $T_e$, and the hydro-mechanical efficiency, $\eta_{hm}$, of the pump are defined by

$$
\begin{align}
T_e &= T_i + T_l, \tag{A.8}\\
\eta_{hm} &= \tfrac{T_i}{T_e}, \tag{A.9}
\end{align}
$$

where $T_i$ is the ideal pump torque, a function of pressure and angular speed. The amount of leakage flow, $q_l$, and friction torque (and therewith volumetric and hydro-mechanical efficiency) depend on operating conditions, i.e.

$$
\begin{align}
q_l &= q_l(\Delta p, \omega, \theta, p, \mu, ...),\\
T_l &= T_l(\Delta p, \omega, \theta, p, \mu, ...), \tag{A.10}
\end{align}
$$

where $\Delta p$ is the pressure difference across the pump, $\theta$ is the operating temperature and $\mu$ is the dynamic viscosity of the fluid.

The hydro-mechanical efficiency, $\eta_{hm}$, and the total efficiency from mechanical to hydraulic power, $\eta_{tot}$, are further deduced from a four-pole notation as

$$
\begin{align}
P_m &= T \cdot \omega \tag{A.11}\\
&= \Delta p \cdot 1/\eta_{hm} \cdot D \cdot \omega, \tag{A.12}\\
\eta_{hm} &= \frac{\Delta p \cdot D}{T}, \tag{A.13}\\
P_h &= \Delta p \cdot q \tag{A.14}\\
&= \Delta p \cdot D \cdot \eta_v \cdot \omega, \tag{A.15}\\
\eta_{tot} &= P_h/P_m \tag{A.16}\\
&= \frac{\Delta p \cdot D \cdot \eta_v \cdot \omega}{\Delta p \cdot \frac{1}{\eta_{hm}} \cdot D \cdot \omega} \tag{A.17}\\
&= \eta_{hm} \cdot \eta_v, \tag{A.18}
\end{align}
$$

where $P_m$ is the mechanical input power, $P_h$ is the hydraulic output power of the pump, $D$ is the instantaneous displacement volume and $\eta_v$ is the volumetric efficiency. Next, this structure, consisting of a volumetric and a hydro-mechanical efficiency, is used to describe the fixed displacement pump for all topologies. Results for modeling and validation of a fixed displacement pump have been shown by the authors in [153].

Mathematical descriptions of these PS systems are build and validated. Scaling of the EM is done using linear scaling. When there are no variables to be controlled, the optimal design problem boils down to a one degree of freedom optimization problem (PSP, E-HPS and EPS topologies).

For each topology, the solution to the design optimization problem depends on the duty cycle of the PS system. Sequentially, the duty cycle is drive cycle dependent and therefore the optimal solution for inner city driving will not always equal the optimal solution

for highway driving. For the results presented here, focused on long-haul usage, a mixed cycle measured on a fully loaded tractor-trailer is used, that combines various road segments, with a predominant (85%) highway driving.

## A.4    Simulation Results

### A.4.1    Variable Flow Control for the Hydraulic Pump

The EH-PS, SH-PS and the EHH-PS topologies enable a controlled oil flow, which means that the output flow of the electrically driven pump, $\phi$, can be varied depending on driving conditions. For example, when there is no input at the steering wheel while driving on the highway, the flow can be reduced in order to save energy. The minimum flow $(f_h, f_n)$ at certain driving conditions is restricted by safety reasons as it takes some time before the pump delivers the required flow and pressure when it is accelerated from a stand-by mode. Since the flow reduction capability is an important benefit of these topologies, it has been included by means of different use cases. In the first three use cases, the flow is varied when driving on highways and national roads as: (flow I) $f_h = 11, f_n = 16$, (flow II) $f_h = 6, f_n = 16$ and (flow III) $f_h = 6, f_n = 11$ . On the drive cycles that are used for the simulations, these flows are sufficient throughout the cycles. The fourth use case serves as a lower bound of what is achievable when the flow could be varied exactly according to the steering wheel input. This use case (flow IV) is applied on all the drive cycles and can be described mathematically as

$$\phi = \left\langle \begin{array}{ll} \phi_r, & \text{for } \phi_r > 6\,L/min; \\ 6\,L/min & \text{for } \phi_r \leq 6\,L/min, \end{array} \right. \tag{A.19}$$

with $\phi_r$ the required flow.

### A.4.2    Pareto Analysis per-Topology

For the first given topology (H-PS), the results for using this method are graphically depicted in Figure A.2, where one can observe that the lowest feasible gear ratio results in the lowest average fuel consumption. As this topology has no control freedom, solving (A.1) boils down to a one degree of freedom optimization problem (A.2), with $x_d = \{i_1\}$ and an active constraints given by

$$q_{min} - D \cdot i_1 \cdot \omega_i + k_l \cdot p_{sh} \leq 0, \tag{A.20}$$

where $q_{min}$ is the minimum flow, $\omega_i$ is the CE idling speed, $p_{sh}$ is the steering house pressure and $k_l$ is the leakage flow coefficient. For this optimization the grid size per dimension is 20 and the simulation time is 15 minutes. The minimum flow at certain

driving conditions is restricted by safety reasons. It is assumed that variable flow can only be applied when driving on highway or national road, since on other roads the steering duty cycle is much higher. When more variables are to be optimized a Pareto
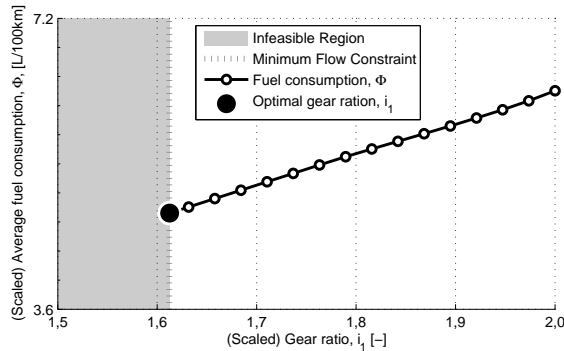


Figure A.2: Pareto front for optimal gear selection in the H-SP Topology

frontier set for the design solutions can be found. This implies that it is impossible to chose for a *more optimal* solution for one design variable without making another design variable worse. Such a result is depicted in Figure A.3 for the second topology, EH-PS. This tradeoff is by itself a result and can help in creating a prediction of how would the fuel consumption change with an increase in the gear ratio or the motor power. For
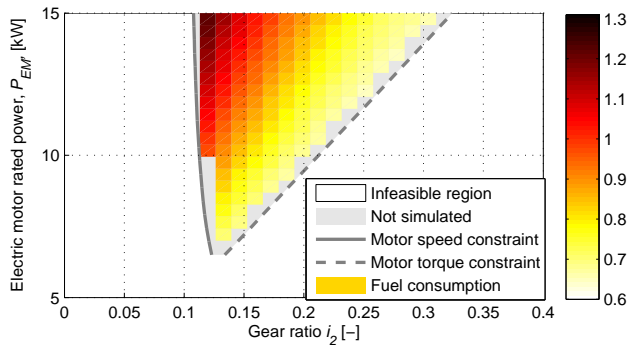


Figure A.3: Optimal size selection of the EH-PS topology with respect to optimal fuel consumption

this case, one could observe that with an increase of EM power also an increase in the gear used is required in order to keep the low fuel consumption. When these results are compared to the fuel consumption of the conventional PS system, it shows that the EH-PS system is only beneficial when variable flow is applied intensively (flow IV). In

more detail, the dual energy conversion reduces the overall efficiency, and the electric motor has to be sized such that it can deliver enough power at the worst case scenario, i.e. high steering pressures, while mostly the required hydraulic pressure is much lower. This implies that the torque demand on the EM is relatively low most of the time and the EM is not operated in its high-efficiency region. The resulting average efficiency of the electric motor/controller is 30% for this use case. For this reason, the hybrid topologies are advantageous solutions as an efficient engine driven pump is combined with variable flow.

A complete sizing example for the optimal design problem can be built for the complex topology SH-PS depicted in Figure A.4, as

$$\min_{i_1,i_2,P_e,z \subseteq \mathscr{X}} \int_0^{t_f} \dot{m}_f(i_1,i_2,P_e,z)dt,$$

$s.t.$

$$q_{min} - D(\frac{z+1}{z}i_1\omega_i - \frac{1}{z}\omega_u i_2) + k_l p_{sh} \leq 0, \qquad (A.21)$$

$$T_r\frac{i_2}{z} - T_u\eta_i\eta_{pgs} \leq 0,$$

$$\frac{(z+1)\omega_c - z\omega_r}{i_2} - \omega_u \leq 0.$$

Here $\omega_u$ is the maximum electric motor angular speed, $T_r$ is the required pump torque, $T_u$
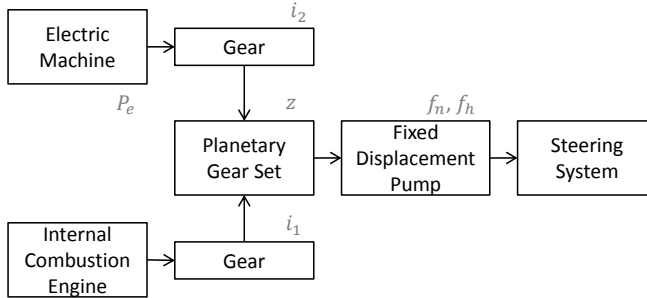


Figure A.4: Schematic representation of the SH-PS topology from Fig. A.1

is the maximum electric motor torque, $\omega_r$ is the required pump speed, $\eta_i$ is the efficiency of the fixed $i_2$ gear and $\eta_{pgs}$ is the efficiency of the planetary gear set. These three constraints define the feasible design space for this topology. Solving (A.21) for $x_d = \{i_1(k),i_2(k),P_e(k),z(k)\}$, where $k$ is the number of grid points per dimension yields $x_d = \{0.38\ 0.34\ 4.8\ 7.6\}$. This subset of the attainable set is called a *Pareto set* and consists of *Pareto optimal points*. A point $x_{d_\chi} \subseteq \mathscr{X}$ is Pareto optimal if and only if there is no other $x_d \subseteq \mathscr{X}$ such that $x_d < x_{d_\chi}$, in this case with an extra (equality) constraint that fixes the planetary gear ratio. From this Pareto plot, one can conclude that there is a

range of planetary gear ratio's within the attainable set $\mathscr{X}$ resulting in about the same fuel consumption. Therefore the planetary gear set can be chosen according to secondary aspects, such as availability or packaging restrictions. Because of the large flexibility in
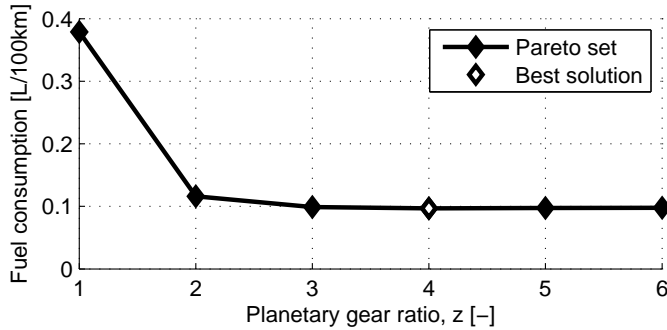


Figure A.5: Pareto graph for the optimal planetary gear ratio, z, in the SH-PS topology

gear combinations it is not known what combinations are likely to result in a low fuel consumption. Therefore, the design space of the planetary gear set was chosen according to constructional (in)feasibility.

### A.4.3 Comparison of the Six Topologies

The comparison of these 6 topologies for all defined oil flows and the optimal set $x_{d_\chi} \subseteq \mathscr{X}$ is depicted in Figure A.6. When variable flow is applied intensively on all roads (use case IV), the fuel consumption of the EHH-PS may even be reduced by up to 80% compared to the conventional system. The simulation time to simulate one complex topology (e.g., SH-PS) goes up to 7 hours and 30 minutes. The benefit of E-PS, enabling true steering on demand, makes this solution very attractive for passenger cars but cannot overcome the arising issues when E-PS is applied to heavier vehicles. First, the required power to drive the electric motor has to be delivered by the battery and second, the the electric motor has to be powerful enough to steer the wheels at vehicle standstill. This would require a very high torque output and might also bring a weight increase when compared with its hydraulic counterpart. The brute-force search showed that the analyzed E-PS topology is not feasible for a conventional truck, having a 24 V battery. An E-H-PS could be a good alternative, combining the benefits of 'power on demand' with the conventional hydraulic steering system. The resulting benefit of this topology is not impressive since the of the pump is still sized for the worst case scenario. Another benefit of E-H-PS topology is that the piston area of the steering house can be reduced, such that less oil flow is required. Compared to the H-SP topology, the average fuel consumption has been reduced by 15% with the use of a 2.4 kW motor.
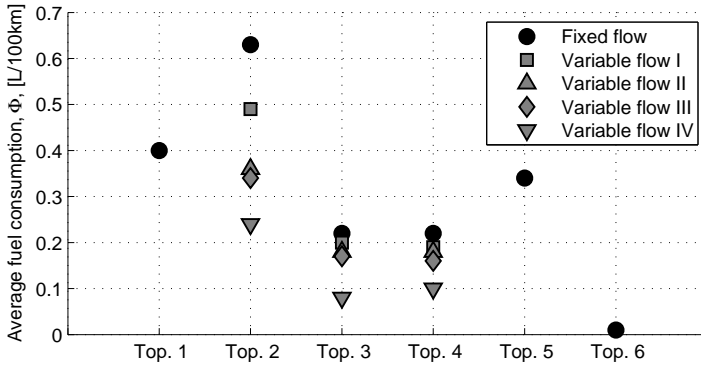
Figure A.6: Influence of the minimum flow for different topologies

From Figure A.6 one can conclude that, for all topologies, lowering the minimum flow improves the fuel efficiency. The topologies and the approach shown here offer both insights on the functionality of the system and enable the visualisation of trade-offs between choosing one or another value (see Figures A.2, A.3 and A.5) for different parameters explained in Table 1. The results show that, depending on the duty cycle, complex topologies can reduce fuel consumption by more than 80% when compared with conventional, hydraulic steering systems. Moreover, they can also enable functions as start/stop and zero emission driving. These benefits are achieved also due to the possibility to control the oil flow and they can be improved with the decrease of the minimum constant flow.

[1] S. Chu and A. Majumdar. Opportunities and challenges for a sustainable energy future. *Nature*, 488:294–303, 2012.

[2] J.G.J. Olivier, G.Janssens-Maenhout, M. Muntean, and J.A.H.W. Peters. Trends in Global $CO_2$ Emissions: 2014 Report, 2014.

[3] K. Holmberg, P. Andersson, N.-O.Nylund, K. Mäkelä, and A. Erdemir. Global energy consumption due to friction in trucks and buses. *Tribology International*, 78:94–114, 2014.

[4] J. Yang. Potential applications of thermoelectric waste heat recovery in the automotive industry. In *24th International Conference on Thermoelectrics*, pages 170–174, 2005.

[5] E. Feru, F. Willems, C. Rojer, B. de Jager, and M. Steinbuch. Heat exchanger modeling and identification for control of Waste Heat Recovery systems in diesel engines. In *American Control Conference*, pages 2860–2865, 2013.

[6] A. Emadi, K. Rajashekara, S.S. Williamson, and S.M. Lukic. Topological overview of hybrid electric and fuel cell vehicular power system architectures and configurations. *IEEE Transactions on Vehicular Technology*, 54(3):763–770, 2005.

[7] M. Ehsani, Y. Gao, and J.M. Miller. Hybrid Electric Vehicles: Architecture and Motor Drives. *Proceedings of the IEEE*, 95(4):719–728, 2007.

[8] D.W. Gao, C. Mi, and A. Emadi. Modeling and Simulation of Electric and Hybrid Vehicles. *Proceedings of the IEEE*, 95(4):729–745, 2007.

[9] C.C. Chan. The State of the Art of Electric and Hybrid Vehicles. *Proceedings of the IEEE*, 90(2):247–275, 2002.

[10] C.C. Chan. The state of the art of electric, hybrid, and fuel cell vehicles. *Proceedings of the IEEE*, 95(4):704–718, 2007.

[11] C.C. Chan, A. Bouscayrol, and K. Chen. Electric, hybrid, and fuel-cell vehicles: Architectures and modeling. *IEEE Transactions on Vehicular Technology*, 59(2):589–598, 2010.

[12] L. Guzzella and A. Sciarretta. *Vehicle Propulsion Systems - Introduction to Modeling and Optimization, Second Edition*. Springer Berlin Heidelberg New York, 2007.

[13] M. Ehsani, Y. Gao, and A. Emadi. *Modern Electric, Hybrid Electric, and Fuel Cell Vehicles: Fundamentals, Theory, and Design, Second Edition*. CRC Press, Taylor & Francis Group, 2009.

[14] C. Mi, M.A. Masrur, and D.W. Gao. *Hybrid Electric Vehicles: Principles and Applications with Practical Perspectives*. John Wiley & Sons, Ltd, 2011.

[15] G. Ulsoy, H. Peng, and M. Çakmakci. *Automotive Control Systems*. Cambridge University Press, 2014.

[16] E. Silvas, E.A. Backx, T. Hofman, H. Voets, and M. Steinbuch. Design of Power Steering Systems for Heavy-Duty Long-Haul Vehicles. In *19th IFAC World Congress*, pages 3930–3935, 2014.

[17] T.J. Barlow, S. Latham, I.S. McCrae, and P.G. Boulter. *A reference book of driving cycles for use in the measurement of road vehicle emissions : version 3*. Bracknell : IHS, 2009.

[18] K.B. Wipke, M.R. Cuddy, and S.D. Burch. ADVISOR 2.1: a user-friendly advanced powertrain simulation using a combined backward/forward approach. *IEEE Transactions on Vehicular Technology*, 48(6):1751–1761, 1999.

[19] N.J. Schouten, M.A. Salman, and N.A. Kheir. Fuzzy Logic Control for Parallel Hybrid Vehicles. *IEEE Transactions On Control Systems Technology*, 10(3):460–468, 2002.

[20] N.J. Schouten, M.A. Salman, and N.A. Kheir. Energy management strategies for parallel hybrid vehicles using fuzzy logic. *Control Engineering Practice*, 11(2):117–117, 2003.

[21] B.M. Baumann, G. Washington, B.C. Glenn, and G Rizzoni. Mechatronic design and control of hybrid electric vehicles. *IEEE/ASME Transactions on Mechatronics*, 5(1):58–72, 2000.

[22] V. Johnson, K. Wipke, and D. Rausen. Hev control strategy for real-time optimization of fuel economy and emissions. In *SAE, Paper no. 2000-01-1543*, 2000.

[23] G. Pagenelli, T. Guerra, S. Delprat, J. Satin, E. Combes, and M. Delhom. Simulation and assessement of power control strategies for parallel car. *Institution of Mechanical Engineers, Part D: J. Automobile Eng.*, 214:705–718, 2000.

[24] A. Sciarretta, M. Back, and L. Guzzella. Optimal Control of Parallel Hybrid Electric Vehicles. *IEEE Transactions On Control Systems Technology*, 12(3):352–363, 2004.

[25] T. Hofman. *Framework for Combined Control and Design Optimization of Hybrid Vehicle Propulsion Systems*. PhD thesis, Eindhoven University of Technology, 2007.

[26] C. Musardo, G. Rizzoni, Y. Guezennec, and B. Staccia. A-ECMS: An Adaptive Algorithm for Hybrid Electric Vehicle Energy Management. *European Journal of Control*, 11:509–524, 2005.

[27] N. Kim, S. Cha, and H. Peng. Optimal Control of Hybrid Electric Vehicles Based on Pontryagin's Minimum Principle. *IEEE Transactions on Control Systems Technology*, 19(5):1279–1287, 2011.

[28] N. Kim, S. Won Cha, and H. Peng. Optimal equivalent fuel consumption for hybrid electric vehicles. *IEEE Transactions on Control Systems Technology*, 20(3):817–825, 2012.

[29] S.J. Moura, H. K. Fathy, D. S. Callaway, and J. L. Stein. A Stochastic Optimal Control Approch for Power Management in Plug-in Hybrid Electric Vehicles. *IEEE Transactions on Control Systems Technology*, 19(3):545–555, 2010.

[30] T. Leroy, J. Malaize, and G. Corde. Towards real-time optimal energy management of HEV powertrains using stochastic dynamic programming. In *IEEE Vehicle Power and Propulsion Conference*, pages 383–388, 2012.

[31] E.D. Tate, J.W. Grizzle, and H. Peng. SP-SDP for Fuel Consumption and Tailpipe Emissions Minimization in an EVT Hybrid. *IEEE Transactions on Control Systems Technology*, 18(3):673–687, 2010.

[32] J. Liu and H. Peng. Modeling and Control of a Power-Split Hybrid Vehicle. *IEEE Transactions on Control Systems Technology*, 16(6):1242–1251, 2008.

[33] L. Johannesson, M. Asbogard, and B. Egardt. Assessing the Potential of Predictive Control for Hybrid Vehicle Powertrains Using Stochastic Dynamic Programming. *IEEE Transactions on Intelligent Transportation Systems*, 8(1):71–83, 2007.

[34] S. Di Cairano, D. Bernardini, A. Bemporad, and I.V. Kolmanovsky. Stochastic MPC with Learning for Driver-Predictive Vehicle Control and its Application to HEV Energy Management. *IEEE Transactions on Control Systems Technology*, 22(3):1018–1031, 2014.

[35] V. Ngo, T. Hofman, M. Steinbuch, and A. Serrarens. Predictive gear shift control for a parallel Hybrid Electric Vehicle. In *IEEE Vehicle Power and Propulsion Conference*, pages 1–6, 2011.

[36] M. Koot, J.T.B.A. Kessels, B. de Jager, W.P.M.H Heemels, P.P.J. van den Bosch, and M. Steinbuch. Energy management strategies for vehicular electric power systems. *IEEE Transactions on Vehicular Technology*, 54(3):771–782, 2005.

[37] F.R. Salmasi. Control Strategies for Hybrid Electric Vehicles: Evolution, Classification, Comparison, and Future Trends. *IEEE Transactions on Vehicular Technology*, 56(5):2393–2404, 2007.

[38] B. Ganji and A. Z. Kouzani. A Study on Look-Ahead Control and Energy Management Strategies in Hybrid Electric Vehicles. In *8th IEEE International Conference on Control and Automation*, pages 388–392, 2010.

[39] A. Sciarretta and L. Guzzella. Control of Hybrid Electric Vehicles. *IEEE Control Systems Magazine*, 27(2):60–70, 2007.

[40] S.G. Wirasingha and A. Emadi. Classification and Review of Control Strategies for Plug-In Hybrid Electric Vehicles. *IEEE Transactions on Vehicular Technology*, 60(1):111–122, 2011.

[41] O. Grondin, l. Thibault, and C. Quérel. Energy Management Strategy for Diesel Hybrid Electric Vehicle. *Oil Gas Science and Technology - Rev. IFP Energies Nouvelles*, 70(1):125–141, 2015.

[42] R.M. Patil, Z. Filipi, and H.K. Fathy. Comparison of Supervisory Control Strategies for Series Plug-in Hybrid Electric Vehicle Powertrains Through Dynamic Programming. *IEEE Transactions on Control Systems Technology*, 22(2):502–509, 2014.

[43] A. Sciarretta, L. Serrao, P.C. Dewangan, P. Tona, E.N.D. Bergshoeff, C. Bordons, L. Charmpa, P. Elbert, L. Eriksson, T. Hofman, M. Hubacher, P. Isenegger, F. Lacandia, A. Laveau, H. Li, D. Marcos, T. Nüesch, S. Onori, P. Pisu, J. Rios, E. Silvas, M. Sivertsson, L. Tribioli, A.-J. van der Hoeven, and M. Wu. A control benchmark on the energy management of a plug-in hybrid electric vehicle. *Control Engineering Practice*, 29:287–298, 2014.

[44] E. Silvas, E. Bergshoeff, T. Hofman, and M. Steinbuch. Comparison of Bi-Level Optimization Frameworks for Sizing and Control of a Hybrid Electric Vehicle. In *IEEE Vehicle Power and Propulsion Conference*, pages 1–6, 2014.

[45] E. Silvas, K. Hereijgers, H. Peng, T. Hofman, and M. Steinbuch. Synthesis of Realistic Driving Cycles with High Accuracy and Computational Speed, Including Slope Information. *Submitted for journal publication; In review.*, -:–, 2015.

[46] P. Kågeson. Cycle-Beating and the EU Test Cycle for Cars. *European Federation for Transport and Environment*, 98:1–10, 1998.

[47] M. Pourabdollah, A. Grauers, and B. Egardt. Effect of Driving patterns on Components sizing of a Series PHEV. In *IFAC Symposium on Advances in Automotive Control*, pages 17–22, 2013.

[48] S. Stockar, V. Marano, M. Canova, G. Rizzoni, and L. Guzzella. Energy-Optimal Control of Plug-in Hybrid Electric Vehicles for Real-World Driving Cycles. *IEEE Transactions on Vehicular Technology*, 60(7):2949–2962, 2011.

[49] Z. Wang, G. Xu, W. Li, and Y. Xu. Driving Load Forecasting Using Cascade Neural Networks. In *Lecture Notes in Computer Science: Volume Advances in Neural Networks*, volume 4493, pages 988–997. Springer, 2007.

[50] A.A. Abdelsalam and S. Cui. A Fuzzy Logic Global Power Management Strategy for Hybrid Electric Vehicles Based on a Permanent Magnet Electric Variable Transmission. *Energies*, 5(4):1175–1198, 2012.

[51] E. Tazelaar, J. Bruinsma, P.A. Veenhuizen, and P.P.J. van den Bosch. Driving cycle characterization and generation, for design and control of fuel cell buses. *World Electric Vehicle Journal*, 3:1, 2009.

[52] J. Lin and D.A. Niemeier. An exploratory analysis comparing a stochastic driving cycle to California's regulatory cycle. *Atmospheric Environment*, 36(38):5759–5770, 2002.

[53] J. Brady and M. O'Mahony. The Development of a Driving Cycle for the Greater Dublin Area Using Large Database of Driving Data with a Stochastic and Statistical Methodology. In *Proceedings of Irish Transport Research Network*, pages 1–23, 2013.

[54] T.-K. Lee, B. Adornato, and Z.S. Filipi. Synthesis of Real-World Driving Cycles and Their Use for Estimating PHEV Energy Consumption and Charging Opportunities: Case Study for Midwest/U.S. *IEEE Transactions on Vehicular Technology*, 60(9):4153–4163, 2011.

[55] T.-K. Lee and Z.S. Filipi. Impact of Model-Based Lithium-Ion Battery Control Strategy on Battery Sizing and Fuel Economy in Heavy-Duty HEVs. *SAE Int. J. Commer. Veh.*, 4(1):198–209, 2011.

[56] B.M. Geller and T.H. Bradley. Analyzing Drive Cycles for Hybrid Electric Vehicle Simulation and Optimization. *ASME. J. Mech. Des., No. MD-14-1227*, 137(4):1–14, 2015.

[57] R. Trigui, E. Vinot, and M. Boujelben. Offline Optimization for Components Sizing and Analysis of a Plug-in Hybrid Urban Microbus. In *IEEE Vehicle Power and Propulsion Conference*, pages 382–387, 2009.

[58] E. Vinot, R. Trigui, B. Jeanneret, J. Scordia, and F. Badin. HEVs Comparison and Components sizing Using Dynamic Programming. In *IEEE Vehicle Power and Propulsion Conference*, pages 314–321, 2007.

[59] S.M. Lukic and A. Emadi. Effects of drivetrain hybridization on fuel economy and dynamic performance of parallel hybrid electric vehicles. *IEEE Transactions on Vehicular Technology*, 53(2):385–389, 2004.

[60] O. Sundstrom, L. Guzzella, and P. Soltic. Optimal Hybridization in Two Parallel Hybrid Electric Vehicles using Dynamic Programming. In *The International Federation of Automatic Control World Congress*, pages 4642–4647, 2008.

[61] S. Ebbesen, P. Elbert, and L. Guzzella. Engine Downsizing and Electric Hybridization Under Consideration of Cost and Drivability. *Oil & Gas Science and Technology Rev. IFP Energies nouvelles*, 68:109 – 116, 2013.

[62] T. Hofman, S. Ebbesen, and L. Guzzella. Topology Optimization for Hybrid Electric Vehicles With Automated Transmissions. *IEEE Transactions on Vehicular Technology*, 6:2442–2451, 2012.

[63] G. Rousseau, D. Sinoquet, A. Sciarretta, and Y. Milhau. Design Optimisation and Optimal Control for Hybrid Vehicles. In *International Conference on Engineering Optimization*, volume 12(1-2), pages 199–213, 2008.

[64] W. Gao and C. Mi. Hybrid vehicle design using global optimisation algorithms. *Int. J. Electric and Hybrid Vehicles*, 1(1):57–70, 2007.

[65] D.-G. Li, Y. Zou, X.-S. Hu, and F.-C Sun. Optimal sizing and control strategy design for heavy hybrid electric truck. In *Vehicle Power and Propulsion Conference (VPPC), 2012 IEEE*, pages 1100–1106, 2012.

[66] A. Shojaei, D. Strickland, D. Scott, M. Tucker, G. Kirkpatrick, B. Price, S. Luke, and J. Richmond. Powertrain optimisation in a hybrid electric bus. In *IEEE Vehicle Power and Propulsion Conference*, pages 857–862, 2012.

[67] C. Desai and S. S. Williamson. Optimal design of a parallel hybrid electric vehicle using multi-objective genetic algorithms. In *IEEE Vehicle Power and Propulsion Conference*, pages 871–876, 2009.

[68] T. Nüesch, T. Ott, S. Ebbesen, and L. Guzzella. Cost and fuel-optimal selection of HEV topologies using Particle Swarm Optimization and Dynamic Programming. In *American Control Conference*, pages 1302–1307, 2012.

[69] B.A. Skinner, P. R. Palmer, and G. T. Parks. Multi-objective Design Optimisation of Submarine Electric Drive Systems. In *IEEE Electric Ship Technologies Symposium*, pages 65–71, 2007.

[70] X. Zhang, C.-T. Li, D. Kum, and H. Peng. Prius$^+$ and Volt$^-$: Configuration Analysis of Power-Split Hybrid Vehicles With a Single Planetary Gear. *IEEE Transactions on Vehicular Technology*, 61(8):3544–3552, 2012.

[71] H.K. Fathy, J. A. Reyer, P.Y. Papalambros, and A. Galip Ulsog. On the Coupling between the Plant and Controller Optimization Problems. In *American Control Conference*, pages 1864–1869, 2001.

[72] J.T. Allison and D.R. Herber. Multidisciplinary Design Optimization of Dynamic Engineering Systems. *American Institute of Aeronautics and Astronautics Journal*, 52(4):691–710, 2014.

[73] W.-W. Xiong and C.-L. Yin. Design of series-parallel hybrid electric propulsion systems and application in city transit bus. *Journal of World Scientific and Engineering Academy and Society*, 8(5):578–590, 2009.

[74] J. Kang, W. Choi, S. Hong, J. Park, and H. Kim. Control strategy for dual-mode power split HEV considering transmission efficiency. In *IEEE Vehicle Power and Propulsion Conference*, pages 1–6, 2011.

[75] N.-D. Kim, J.-M. Kim, and H.-S. Kim. Control strategy for a dual-mode electromechanical, infinitely variable transmission for hybrid electric vehicles. *Proceedings of the Institution of Mechanical Engineers, Part D: Journal of Automobile Engineering*, 222:1587–1601, 2008.

[76] E. Nordlund and C. Sadarangani. The four-quadrant energy transducer. In *Industry Applications Conference*, volume 1, pages 390 – 397, 2002.

[77] P. Zheng, R. Liu, P. Thelin, E. Nordlund, and C. Sadarangani. Research on the Cooling System of a 4QT Prototype Machine Used for HEV. *IEEE Transactions on Energy Conversion*, 23(1):61–67, 2008.

[78] Y. Cheng, R. Trigui, C. Espanet, A. Bouscayrol, and S. Cui. Specifications and Design of a PM Electric Variable Transmission for Toyota Prius II. *IEEE Transactions on Vehicular Technology*, 60(9):4106–4114, Nov 2011.

[79] S. Dewenter, A. Binder, and M. Strauch. Simulation model for a serial hybrid bus and impact of energy management on fuel consumption. In *IEEE Vehicle Power and Propulsion Conference*, pages 863–868, 2012.

[80] P. Elbert, T. Nuesch, A. Ritter, N. Murgovski, and L. Guzzella. Engine On/Off Control for the Energy Management of a Serial Hybrid Electric Bus via Convex Optimization. *IEEE Transactions on Vehicular Technology*, 63(8):3549–3559, Oct 2014.

[81] M. Kim, Y.-J. Sohn, W.-Y. Lee, and C.-S. Kim. Fuzzy control based engine sizing optimization for a fuel cell/battery hybrid mini-bus. *Journal of Power Sources*, 178(2):706 – 710, 2008.

[82] I. Aharon and A. Kuperman. Topological Overview of Powertrains for Battery-Powered Vehicles With Range Extenders. *IEEE Transactions on Power Electronics*, 26(3):868–876, 2011.

[83] A. Del Pizzo, R.M. Polito, R. Rizzo, and P. Tricoli. Design criteria of on-board propulsion for hybrid electric boats. In *XIX International Conference on Electrical Machines*, pages 1–6, 2010.

[84] T. Ogawa, H. Kanno, T. Soeda, and Y. Sugiyama. Environmental evaluation of a diesel hybrid shunting locomotive. In *Electrical Systems for Aircraft, Railway and Ship Propulsion*, pages 1–6, 2012.

[85] A. Rassolkin and H. Hoimoja. Power quality application of hybrid drivetrain. In *Electrical Systems for Aircraft, Railway and Ship Propulsion*, pages 1–4, 2012.

[86] J. Baert, S. Jemei, D. Chamagne, D. Hissel, S. Hibon, and D. Hegy. Energetic macroscopic representation of a hybrid electric locomotive and experimental characterization of Nickel-Cadmium battery cells. In *15th European Conference on Power Electronics and Applications*, pages 1–10, 2013.

[87] C. Mayet, J. Pouget, A. Bouscayrol, and W. Lhomme. Influence of an Energy Storage System on the Energy Consumption of a Diesel-Electric Locomotive. *IEEE Transactions on Vehicular Technology*, 63(3):1032–1040, 2014.

[88] R. Hayeri, A. Taghavi, and M. Durali. Preliminary design of a series Hybrid Pneumatic powertrain for a city car. In *IEEE Vehicle Power and Propulsion Conference*, pages 1–6, 2010.

[89] J. Liu. *Modeling, Configuration and Control Optimization of Power-Split Hybrid Vehicle*. PhD thesis, The University of Michigan, 2007.

[90] T. Hofman, M. Steinbuch, R. van Druten, and A.F.A. Serrarens. Design of CVT-Based Hybrid Passenger Cars. *IEEE Transactions on Vehicular Technology*, 58(2):572–587, 2009.

[91] Z. Chen, C.C. Mi, B. Xia, and C. You. Energy management of power-split plug-in hybrid electric vehicles based on simulated annealing and Pontryagin's minimum principle. *Journal of Power Sources*, 272:160–168, 2014.

[92] Z.Q. Zhu and D. Howe. Electrical Machines and Drives for Electric, Hybrid, and Fuel Cell Vehicles. *Proceedings of the IEEE*, 95(4):746–765, 2007.

[93] A. F. Burke. Batteries and Ultracapacitors for Electric, Hybrid, and Fuel Cell Vehicles. *Proceedings of the IEEE*, 95(4):806–820, 2007.

[94] S.M. Lukic, J. Cao, R.C. Bansal, F. Rodriguez, and A. Emadi. Energy Storage Systems for Automotive Applications. *IEEE Transactions on Industrial Electronics*, 55(6):2258–2267, 2008.

[95] R.T. Doucette and M.D. McCulloch. A comparison of high-speed flywheels, batteries, and ultracapacitors on the bases of cost and fuel economy as the energy storage system in a fuel cell based hybrid electric vehicle. *Journal of Power Sources*, 196(3):1163 – 1170, 2011.

[96] Z. Song, H. Hofmann, J. Li, X. Han, X. Zhang, and M. Ouyang. A comparison study of different semi-active hybrid energy storage system topologies for electric vehicles. *Journal of Power Sources*, 274(0):400–411, 2015.

[97] Y. He, M. Chowdhury, Y. Ma, and P. Pisu. Merging mobility and energy vision with hybrid electric vehicles and vehicle infrastructure integration. *Energy Policy*, 41:599–609, 2012.

[98] N. Murgovski, L.M. Johannesson, and B. Egardt. Optimal Battery Dimensioning and Control of a CVT PHEV Powertrain. *IEEE Transactions on Vehicular Technology*, 63(5):2151–2161, 2014.

[99] T.H. Bradley and A.A. Frank. Design, demonstrations and sustainability impact assessments for plug-in hybrid electric vehicles. *Renewable and Sustainable Energy Reviews*, 13(1):115–128, 2009.

[100] T. Lee and Z. Filipi. Real-World Driving Pattern Recognition for Adaptive HEV Supervisory Control: Based on Representative Driving Cycles in Midwestern US. In *SAE Technical Paper*, pages 2012–01–1020, 2012.

[101] R. Patil, Z. Filipi, and H. Fathy. Computationally Efficient Combined Design and Control Optimization using a Coupling Measure. In *IFAC Symposium on Mechatronic Systems*, pages 144–151, 2010.

[102] P.Y. Papalambros and N.F. Michelena. Trends and chanllenges in system design optimization. In *Int. Workshop on Multidisciplinary Design Optimization*, 2000.

[103] S.B. Ebbesen. *Optimal Sizing and Control of Hybrid Electric Vehicles*. PhD thesis, ETH Zurich, 2012.

[104] X. Wu, B. Cao, J. Wen, and Z. Wang. Application of Particle Swarm Optimization for component sizes in parallel Hybrid Electric Vehicles. In *IEEE World Congress on Evolutionary Computation*, pages 2874–2878, 2008.

[105] S. Tosserams. *Distributed Optimization for Systems Design - An Augmented Lagrangian Coordination Method*. PhD thesis, Technische Universiteit Eindhoven, 2008.

[106] S. Tosserams, L.F.P. Etman, and J.E. Rooda. A classification of methods for distributed system optimization based on formulation structure. *Structural and Multidisciplinary Optimization*, 39(5):503–517, 2009.

[107] E. Silvas, T. Hofman, A. Serebrenik, and M. Steinbuch. Functional and Cost-Based Automatic Generator for Hybrid Vehicles Topologies. *IEEE/ASME Transactions on Mechatronics*, 20(4):1561–1572, 2014.

[108] Krzysztof Apt. *Principles of Constraint Programming*. Cambridge University Press, 2009.

[109] A. E. Bayrak, Y. Ren, and P.Y. Papalambros. Design of Hybrid-Electric Vehicle Arhitectures using Auto-Generation of Feasible Driving Modes. In *Proceedings of the ASME 2013 International Design Engineering Technical Conferences, ASME*, pages 1–9, 2013.

[110] A.E. Bayrak, Y. Ren, and P.Y. Papalambros. Optimal Dual-Mode Hybrid Electric Vehicle Powertrain Architecture Design for a Variety of Loading Scenarios. In *International Conference on Advanced Vehicle Technologies, ASME*, pages 1–8, 2014.

[111] X. Zhang, H. Peng, J. Sun, and S. Li. Automated modeling and Mode Screening for Exhaustive Search of Double-Planetary-Gear Power Split Hybrid Powetrain. In *ASME Dynamic Systems and Control Conference*, pages 1–8, 2014.

[112] Z. Pan, X. Zhang, E. Silvas, H. Peng, and N. Ravi. Modelling and Optimization of All-Wheel-Drive Hybrid Powertrain for Pick-up Trucks. In *ASME Annual Dynamic Systems and Control Conference*, pages 1–8, 2015.

[113] R.S. Sharp and H. Peng. Vehicle dynamics applications of optimal control theory. *Vehicle System Dynamics*, 49(7):1073–1111, 2011.

[114] M. Shams-Zahraei, A.Z. Kouzani, S. Kutter, and B. Bäker. Integrated thermal and energy management of plug-in hybrid electric vehicles. *Journal of Power Sources*, 216:237–248, 2012.

[115] T. Hofman, M. Steinbuch, R.M. van Druten, and A.F.A. Serrarens. Hybrid component specification optimisation for a medium-duty hybrid electric truck. *Int. J. Heavy Vehicle Systems*, 15, Nos. 2/3/4:356–392, 2008.

[116] E. Tazelaar, Y. Shen, P.A. Veenhuizen, T. Hofman, and P.P.J. van den Bosch. Sizing Stack and Battery of a Fuel Cell Hybrid Distribution Truck. *Oil Gas Science and Technology - Rev. IFP Energies Nouvelles*, 67(4):563–573, 2012.

[117] E. Vinot, R. Trigui, Yuan Cheng, C. Espanet, A. Bouscayrol, and V. Reinbold. Improvement of an EVT-Based HEV Using Dynamic Programming. *IEEE Transactions on Vehicular Technology*, 63(1):40–50, 2014.

[118] T.H. Cormen, C.E. Leiserson, R.L. Rivest, and C. Stein. *Introduction to Algorithms, Third Edition*. The MIT Press, 3rd edition, 2009.

[119] Y. Zou, F. Sun, X. Hu, L. Guzzella, and H. Peng. Combined Optimal Sizing and Control for a Hybrid Tracked Vehicle. *Energies*, 5:4697–4710, 2012.

[120] S. Koziel and L. Leifsson. *Surrogate-Based Modeling and Optimization Applications in Engineering*. Springer-Verlag New York, 2013.

[121] G. Lei, T. Wang, Y. Guo, J. Zhu, and S. Wang. System-Level Design Optimization Methods for Electrical Drive Systems: Deterministic Approach. *IEEE Transactions on Industrial Electronics*, 61(12):6591–6602, 2014.

[122] N. Kang, M. Kokkolaras, P.Y. Papalambros, S. Yoo, W. Na, J. Park, and D. Featherman. Optimal design of commercial vehicle systems using analytical target cascading. *Structural and Multidisciplinary Optimization*, 50(6):1–12, 2014.

[123] N. Kang, M. Kokkolaras, and P.Y. Papalambros. Solving multiobjective optimization problems using quasi-separable MDO formulations and analytical target cascading. *Structural and Multidisciplinary Optimization*, 50(5):849–859, 2014.

[124] C.-C. Lin, H. Peng, J.W. Grizzle, and J.-M. Kang. Power management strategy for a parallel hybrid electric truck. *IEEE Transactions on Control Systems Technology*, 11(6):839–849, 2003.

[125] P. Tulpule, V. Marano, and G. Rizzoni. Energy management for plug-in hybrid electric vehicles using equivalent consumption minimisation strategy. *International Journal of Electric and Hybrid Vehicles*, 2(4):329–350, 2010.

[126] O. Sundstrom, L. Guzzella, and L.P. Soltic. Torque-Assist Hybrid Electric Powertrain Sizing: From Optimal Control Towards a Sizing Law. *IEEE Transactions on Control Systems Technology*, 18(4):837–849, 2010.

[127] D. Assanis, G. Delagrammatikas, R. Fellini, Z. Filipi, J. Liedtke, N. Michelena, P. Papalambros, D. Reyes, D. Rosenbaum, A. Sales, and M. Sasena. Optimization Approach to Hybrid Electric Propulsion System Design. *Mechanics of Structures and Machines: An International Journal*, 27(4):393–421, 1999.

[128] K. Wipke, T. Markel, and D. Nelson. Optimizing Energy Management Strategy and Degree of Hybridization for a Hydrogen Fuel Cell SUV. In *Electric Vehicle Symposium*, pages 1–12, 2001.

[129] R. Fellini, N. Michelena, P. Papalambros, and M. Sasena. Optimal design of automotive hybrid powertrain systems. In *EcoDesign '99: First International Symposium On Environmentally Conscious Design and Inverse Manufacturing*, pages 400–405, 1999.

[130] W. Gao and S.K. Porandla. Design Optimization of a Parallel Hybrid Electric Powertrain. In *IEEE Vehicle Power and Propulsion Conference*, pages 1–6, 2005.

[131] R. Shankar, J. Marco, and F. Assadian. The Novel Application of Optimization and Charge Blended Energy Management Control for Component Downsizing within a Plug-in Hybrid Electric Vehicle. *Energies*, 5(12):4892–4923, 2012.

[132] L. Wu, Y. Wang, X. Yuan, and Z. Chen. Multiobjective Optimization of HEV Fuel Economy and Emissions Using the Self-Adaptive Differential Evolution Algorithm. *IEEE Transactions on Vehicular Technology*, 60(6):2458–2470, 2011.

[133] V. Paladini, T. Donateo, A. de Risi, and D. Laforgia. Super-capacitors fuel-cell hybrid electric vehicle optimization and control strategy development. *Energy Conversion and Management*, 48(11):3001–3008, 2007.

[134] B.A. Skinner, G.T. Parks, and P.R. Palmer. Comparison of Submarine Drive Topologies Using Multiobjective Genetic Algorithms. *IEEE Transactions on Vehicular Technology*, 58(1):57–68, 2009.

[135] S. Ebbesen, C. Dönitz, and L. Guzzella. Particle swarm optimisation for hybrid electric drivetrain sizing. *Int. J. of Vehicle Design*, 58, Nos. 2/3/4:181–199, 2012.

[136] M. Pourabdollah, E. Silvas, N. Murgovski, M. Steinbuch, and B. Egardt. Optimal Sizing of a Series PHEV: Comparison between Convex Optimization and Particle Swarm Optimization. In *IFAC Workshop on Engine and Powertrain Control, Simulation and Modeling*, pages 1–8, 2015.

[137] N. Murgovski, L. Johannesson, J. Sjöberg, and B. Egardt. Component Sizing of a Plug-in Hybrid Electric Powertrain via Complex Optimization. *Mechatronics*, 22(1):219–245, 2011.

[138] N. Murgovski, L. Johannesson, J. Hellgren, B. Egardt, and J. Sjberg. Convex optimization of charging infrastructure design and component sizing of a plug-in series HEV powertrain. In *18th IFAC World Congress*, pages 13052–13057, 2011.

[139] X. Hu, N. Murgovski, L.M. Johannesson, and B. Egardt. Comparison of Three Electrochemical Energy Buffers Applied to a Hybrid Bus Powertrain With Simultaneous Optimal Sizing and Energy Management. *IEEE Transactions on Intelligent Transportation Systems*, 15(3):1193–1205, 2014.

[140] B. Egardt, N. Murgovski, M. Pourabdollah, and L. Johannesson Mardh. Electromobility Studies Based on Convex Optimization: Design and Control Issues Regarding Vehicle Electrification. *IEEE Control Systems*, 34(2):32–49, 2014.

[141] M. Pourabdollah, N. Murgovski, A. Grauers, and B. Egardt. Optimal Sizing of a Parallel PHEV Powertrain. *IEEE Transactions on Vehicular Technology*, 62(6):2469–2480, 2013.

[142] D.R. Jones, C.D. Perttunen, and B.E. Stuckman. Lipscitzian Optimization Without the Lipschitz Constant. *Journal of Optimization Theory and Application*, 79(1):157–181, 2003.

[143] M. Montazeri-Gh, A. Poursamad, and B. Ghalichi. Application of genetic algorithm for optimization of control strategy in parallel hybrid electric vehicles. *Journal of the Franklin Institute*, 343(4-5):420–435, 2006.

[144] B. Zhang, Z. Chen, C. Mi, and Y.L. Murphey. Multi-objective parameter optimization of a series hybrid electric vehicle using evolutionary algorithms. In *IEEE Vehicle Power and Propulsion Conference*, pages 921–925, 2009.

[145] S. Kirkpatrick, C. D. Gelatt, and M. P. Vecchi. Optimization by simulated annealing. *Science*, 220(4598):671–680, 1983.

[146] N. Murgovski. *Optimal Powertrain Dimensioning and Potential Assessment of Hybrid Electric Vehicles*. PhD thesis, Chalmers University of Technology, 2012.

[147] X. Hu, N. Murgovski, L.M. Johannesson, and B. Egardt. Optimal Dimensioning and Power Management of a Fuel Cell/Battery Hybrid Bus via Convex Programming. *IEEE/ASME Transactions on Mechatronics*, 20(1):457–468, 2015.

[148] R. Fellini, N. Michelena, P. Papalambros, and M. Sasena. Optimal Design of Automotive Hybrid Powertrain Systems. In *IEEE First International Symposium on Environmentally Conscious Design and Inverse Manufacturing*, pages 400–405, 1999.

[149] R. Patil, B. Adornato, and Z. Filipi. Design Optimization of a Series Plug-in Hybrid Electric Vehicle for Real-World Driving Conditions. *SAE Int. J. Engines*, 3(1):655–665, 2010.

[150] T.-K. Lee, Z. Bareket, T. Gordon, and Z.S. Filipi. Stochastic Modeling for Studies of Real-World PHEV Usage: Driving Schedule and Daily Temporal Distributions. *IEEE Transactions on Vehicular Technology*, 61(4):1493–1502, 2012.

[151] S. Tosserams, M. Kokkolars, L. F. P. Etman, and J. E. Rooda. A Nonhierarchical Formulation of Analytical Target Cascading. *Journal of Mechanical Design*, 132(5):051002–1/13, 2010.

[152] J.R.R.A. Martins and A.B. Lambe. Multidisciplinary Design Optimization: A Survey of Architectures. *AIAA Journal*, 51(9):2049–2075, 2013.

[153] E. Silvas, O. Turan, T. Hofman, and M. Steinbuch. Modeling for Control and Optimal Design of a Power Steering Pump and an Air Conditioning Compressor Used in Heavy Duty Trucks. In *IEEE Vehicle Power and Propulsion Conference*, pages 1–6, 2013.

[154] E. Silvas, E.A. Backx, H. Voets, T. Hofman, and M. Steinbuch. Topology Design and Size Optimization of Auxiliary Units : A Case Study for Steering Systems. In *FISITA World Automotive Congress*, pages 1–7, 2014.

[155] E. Silvas, T. Hofman, and M. Steinbuch. Review of Optimal Design Strategies for Hybrid Electric Vehicles. In *IFAC Workshop on Engine and Powertrain Control, Simulation and Modeling*, volume 1(3), pages 57–74, 2012.

[156] M. Ehsani. 20 - conventional fuel/hybrid electric vehicles. In *Alternative Fuels and Advanced Vehicle Technologies for Improved Environmental Performance*, pages 632–654. Woodhead Publishing, 2014.

[157] G. Rizzoni, L. Guzzella, and B.M. Baumann. Unified modeling of hybrid electric vehicle drivetrains. *IEEE/ASME Transactions on Mechatronics*, 4(3):246–257, Sep 1999.

[158] T. Hofman, R.M. van Druten, A.F.A. Serrarens, and J. van Baalen. A Fundamental Case Study on the IMA and Prius Drivetrain Concepts. In *Int. Battery, Hybrid and Fuel Cell Electric Vehicle Symposium & Exposition*, pages 1–12, 2005.

[159] J. Liu and H. Peng. A systematic design approach for two planetary gear split hybrid vehicles. *Vehicle System Dynamics: International Journal of Vehicle Mechanics and Mobility*, 48(11):1395–1412, 2010.

[160] S.F. Alyaqout, P.Y. Papalambros, and A.G. Ulsoy. Combined Robust Design and Robust Control of an Electric DC Motor. *IEEE/ASME Transactions on Mechatronics*, 16(3):574–582, 2011.

[161] S. Rothgang, T. Baumhöfer, H. van Hoek, T. Lange, R.W. De Doncker, and D. Uwe Sauer. Modular battery design for reliable, flexible and multi-technology energy storage systems. *Applied Energy*, 137(0):931–937, 2015.

[162] G. Mohan, F. Assadian, and S. Longo. An optimization framework for comparative analysis of multiple vehicle powertrains. *Energies*, 6:5507–5537, 2013.

[163] B. Wang, M. Xu, and L. Yang. Study on the economic and environmental benefits of different EV powertrain topologies. *Energy Conversion and Management*, 86:916–926, 2014.

[164] C.-H. Hsu and J.-J. Hsu. Epicyclic gear trains for automotive automatic transmissions. *Proceedings of the Institution of Mechanical Engineers. Part D: J. of Automobile Engineering*, 214(5):523–532, 2000.

[165] A. Swantner and M.I. Campbell. Topological and parametric optimization of gear trains. *Engineering Optimization*, 44(11):1351–1368, 2012.

[166] P. Nuzzo, H. Xu, N. Ozay, J.B. Finn, A.L. Sangiovanni-Vincentelli, R.M. Murray, A. Donze, and S.A. Seshia. A contract-based methodology for aircraft electric power system design. *IEEE Access*, 2:1–25, 2014.

[167] A. Sangiovanni-Vincentelli. Quo vadis, SLD? Reasoning about Trends and Challenges of System-Level Design. *Proceedings of the IEEE*, 95(3):467–506, 2007.

[168] S. Dasgupta, C. Papadimitriou, and U. Vazirani. *Algorithms*. McGraw-Hill, 2008.

[169] S.C. Brailsford, C.N. Potts, and B.M. Smith. Constraint satisfaction problems: Algorithms and applications. *European J. of Operations Research*, 199(3):557–581, 1999.

[170] A. Pinto, A. Bonivento, .L. Sangiovanni-Vincentelli, R. Passerone, and M. Sgroi. System Level Design Paradigms: Platform-based Design and Communication Synthesis. *ACM Transactions on Design Automation of Electronic Systems*, 11(3):537–563, 2004.

[171] K. Keutzer, A.R. Newton, J.M. Rabaey, and A. Sangiovanni-Vincentelli. System-level design: orthogonalization of concerns and platform-based design. *IEEE Transactions on Computer-Aided Design of Integrated Circuits and Systems*, 19(12):1523–1543, 2000.

[172] J. Wielemaker, T. Schrijvers, M. Triska, and T. Lager. SWI-Prolog. *Theory and Practice of Logic Programming*, 12(1-2):67–96, 2012.

[173] T. Katražnik. Analytical framework for analyzing the energy conversion efficiency of different hybrid electric vehicle topologies. *Energy Conversion and Management*, 50(8):1924–1938, 2009.

[174] O. Sundstrom, D. Ambuhl, and L. Guzzella. On Implementation of Dynamic Programming for Optimal Control Problems with Final State Constraints. In *IFP International Conference Advances in Hybrid Powertrains*, volume 65(1), pages 91–102, 2010.

[175] T. Donateo, L. Serrao, and G. Rizzoni. A Two-step Optimization Method for the Preliminary Design of a Hybrid Electric Vehicle. *International Journal of Electric and Hybrid Vehicles*, 1(2):142–165, 2008.

[176] O. Sundstrom. *Optimal Control and Design of Hybrid-Electric Vehicles*. PhD thesis, ETH Zurich, 2009.

[177] S.S. Williamson, A. Khaligh, S. C. Oh, and A. Emadi. Impact of Energy Storage Device Selection on the Overall Drive Train Efficiency and Performance of Heavy-Duty Hybrid Vehicles. In *IEEE Vehicle Power and Propulsion Conference*, pages 1–10, 2005.

[178] E. Bideaux, J. La-te, A. Derkaoui, W. Marquis-Favre, S. Scavarda, and Guillemard F. Design of a hybrid vehicle powertrain using an inverse methodology. In *In Power Transmission and Motion Control*, 2005.

[179] S. Nelson, M. Parkinson, and P. Papalambros. Multicriteria Optimization in Product Platform Design. In *Proceedings of the ASME Design Engineering Technical Conferences*, pages DETC99/DAC–8676, 1999.

[180] M. Kluger and J. Harris. Fuel Economy Benefits of Electric and Hydraulic off-engine Accessories. In *SAE Technical Paper 2007-01-0268*, pages 1–6, 2007.

[181] N. Pettersson and K.H. Johansson. Modelling and control of auxiliary loads in heavy vehicles. *Int. Journal of Control*, 79(5):479–495, 2006.

[182] Board on Energy and Environmental Systems. *Technologies and Approaches to Reducing the Fuel Consumption of Medium-and Heavy-Duty Vehicles*. Washington, DC: The National Academies Press, 2010.

[183] C.-J. Brodrick, T.E. Lipman, M. Farshchi, N.P. Lutsey, H.A. Dwyer, D. Sperling, S.W. Gouse Iii, D.B. Harris, and F.G. King. Evaluation of Fuel Cell Auxiliary Power Units for Heavy-Duty Diesel Trucks. *Transportation Research Part D: Transport and Environment*, 7(4):303–315, 2002.

[184] F. Stodolsky, L. Gaines, and A. Vyas. Analysis of Technology Options to Reduce the Fuel Consumption of Idling Trucks. Technical report, Argonne National Lab., IL (US), 2000.

[185] C. P. Sonchal and A. V. Kulkarni. Energy Efficient Hydraulic Power Assisted Steering System ($E^2$HPAS). In *SAE International 2012-01-0976*, 2012.

[186] W. Yu and D. Williams. Energy Saving Analysis of Power Steering System by Varying Flow Design. In *SAE Technical Paper 2007-01-4216*, 2007.

[187] E.A. Backx. Optimal Design of Heavy-Duty Truck Auxiliaries. CST 2014.005, Eindhoven University of Technology, 2014.

[188] SAE J1343. Information Relating to Duty Cycles and Average Power Requirements of Truck and Bus Engine Accessories. In *SAE International*, pages 1–7, 2000.

[189] Z. Zou, S. Davis, K. Beaty, M. O'Keefe, T. Hendricks, R. Rehn, S. Weissner, and V.K. Sharma. A New Composite Drive Cycle for Heavy-Duty Hybrid Electric Class 4-6 Vehicles. In *SAE Technical Paper 2004-01-1052*, 2004.

[190] V. Larsson, L. Johannesson Mårdh, B. Egardt, and S. Karlsson. Commuter Route Optimized Energy Management of Hybrid Electric Vehicles. *IEEE Transactions on Intelligent Transportation Systems*, 15(3):1145–1154, 2014.

[191] P. Nyberg, E. Frisk, and L. Nielsen. Generation of Equivalent Driving Cycles Using Markov Chains and Mean Tractive Force Components. In *IFAC World Congress*, pages 8787–8792, 2014.

[192] M Montazeri-Gh and M Naghizadeh. Development of car drive cycle for simulation of emissions and fuel economy. In *Proceedings of 15th European simulation symposium*, 2003.

[193] G. Amirjamshidi and M.J. Roorda. Development of Simulated Driving Cycles: Case study of the Toronto Waterfront Area. In *TRB Annual Meeting*, volume 69, pages 1–16, 2013.

[194] S.H. Kamble, T.V. Mathew, and G.K. Sharma. Development of real-world driving cycle: Case study of Pune, India. *Transportation Research Part D: Transport and Environment*, 14(2):132–140, 2009.

[195] Z. Dai, D. Niemeier, and D. Eisinger. Driving cycles: a new cycle-building method that better represents real-world emissions. Technical report, Department of Civil and Environmental Engineering, University of California, Davis, 2008.

[196] T.-K. Lee and Z.S. Filipi. Synthesis of real-world driving cycles using stochastic process and statistical methodology. *Int. J. Vehicle Design*, 57(1):17–36, 2011.

[197] C.M. Grinstead and J. Laurie Snell. *Introduction to Probability*. American Mathematical Society, 1997.

[198] C. Andrieu, N. De Freitas, A. Doucet, and M.I. Jordan. An introduction to MCMC for machine learning. *Machine Learning*, 50(1-2):5–43, 2003.

[199] S. Karatepe and K. W. Corscadden. Wind Speed Estimation: Incorporating Seasonal Data Using Markov Chain Models. *ISRN Renewable Energy*, 2013:1–9, 2013.

[200] J.A. Reyer, H.K. Fathy, , P.Y. Papalambros, and A. Galip Ulsoy. Comparison of Combined Embodiment Design and Control Optimization Strategies Using Optimality Conditions. In *ASME Design Engineering Technical Conference and Computers and Information in Engineering Conference*, pages 1–10, 2001.

[201] J.A. Reyer and P.Y. Papalambros. Combined Optimal Design and Control With Application to an Electric DC Motor. *Journal of Mechanical Design*, 124:183–191, 2002.

# ACKNOWLEDGEMENTS

Four years. They went fast and brought with them new people, places, friends, emotions, satisfactions, new knowledges and changes of character. Looking back, it has been a great period of time. For this experience to happen, I had the direct or indirect support of many special people, to whom I owe words of appreciation and gratitude.

I start by thanking my promotor, without whom this project would not have been possible. Maarten Steinbuch, thank you for everything, and everything means a lot. For the opportunities offered during both my master and my PhD studies. Your way of thinking, quick and focused, which always manages to find the weak points of each hypothesis, helped me a lot with my own decisions. Our conversations, started with a translation of emotions into a stomachache, took me each time a step forward. I continue with Theo Hofman, my co-promoter, who was by my side in every step of this project. Theo, thank you for your guidance, for letting me define my own research paths and for supporting me in all research directions I wanted to go.

For segments of this thesis, I was fortunate to collaborate with different inspiring people. All these collaborations have resulted in joint publications, visits and progress. Alexander Serebrenik, from the MDSE Group of Mathematics and Computer Science Department, thank you for your patience, critical eye and willingness to bring closer our fields of work. Pascal Etman, from our CST Group; thank you for the very constructive discussions and review of my work. Nikolce Murgovski and Mitra Pourabdollah, from Chalmers University of Technology in Sweden, I thank you for the visit you've made to our group and the time we spent together at conferences. Our fruitful collaboration for a short period of time was very pleasant.

Part of my PhD study I've spent at the University of Michigan in Ann Arbor, MI, USA. I am grateful to Huei Peng for this great opportunity, for hosting me in his group and for our collaboration. Many thanks go also to the PhD students form the Vehicle Dynamics Laboratory, Ziheng Pan, Yuxiao Chen, Su-Yang Shieh, Ding Zhao, Xiaowu Zhang, Shaobing Xu, Steven Karamihas, Wubing Qin, Jin Ge, Chaozhe He, Tianyou Guo and Linjun Zhang. Thank you for our discussions, joint work and for showing me a good

time in Ann Arbor. I would also like to thank Mihaela Banu for inviting me to give a talk at her group, in Michigan, and to Alparslan Emrah Bayrak, form the Optimal Design Laboratory, for our lunch talks on topology synthesis. My apartment colleagues, my host and the friends I made during my stay in US, Ana Pamela Torres Ocampo, Elsje Pienaar and Kathryn Luczek, thank you for the wonderful times.

I extend my sincere gratitude to the members of my reading committee. Huei Peng from University of Michigan, Bo Egardt from Chalmers University of Technology, Hans Hellendoorn from Delft University of Technology, Henk Voets from DAF Trucks and Mark van den Brand from Eindhoven University of Technology, thank you for reviewing this dissertation and for taking part in my promotion.

I would also like to thank the Dutch automotive research program HTAS (High Tech Automotive Systems) for the financial support of my project, and to our industrial partner, DAF Trucks N.V., for the collaboration. Special words of gratitude go to Henk Voets. Thank you for being as a second copromotor and for always encouraging me to see 'the bigger picture' of the problem at hand. Loek Van Seeters, thank you for hosting me in your group and for valuable advices. Mark Nievelstein, Rudolf Huisman, Guus Arts, John Kessels, Coco Jongerius and Bram de Jong, thank you for the technical expertise and feedback provided in various parts of the project. Jos van Heck, thank you for reading thoroughly and providing me constructive feedback on Chapter 6 of the thesis. To the other PhD researchers in this project, Thinh Pham, Vital van Reeven and Yanja Dajsuren, many thanks for sharing helpful tips and emotions throughout the project.

During this PhD, I supervised five master students, for their internship and master thesis, which brought me a different kind of work satisfaction. Ömer Turan, Frank Rams, Eric Backx, Erik Bergshoeff and Kobus Hereijgers, thank you for our collaboration and your contributions to the results presented in this thesis. Togheter with Erik, I also thank Aart-Jan van der Hoeven for their work in the TU/e team, with which we won the second place at the IFAC Workshop on Engine and Powertrain Control Simulation and Modeling, in Paris, 2012. I am grateful and appreciate the help of Antonio Sciarretta, from IFP France, to include our work from this competition in a joint journal publication.

For their day by day support, enjoyable moments and for helping me understand a new kind of normality, I thank my colleagues from our -1 floor. Especially, I want to thank my long-term or short-term office mates Gillis Hommen, Shenhai Ran, Vital van Reeven, Alejandro Iván Morales Medina, Ignacio González Alonso and Jurgen van Zundert, for all the good times we had and their unconditional support. Sava Marinkov, Irmak Aladağlı, Elise Moers, Robbert van Herpen, Rick van der Maas, Annemiek van der Maas, Tom van der Sande and Rolf Gaasbeek, thank you for outside-of-work activities, your efforts of learn Romanian dances at parties and our entertaining discussions. Also very important, I thank Petra Aspers and Geertje Janssen-Dols, for all the administrative work and pleasant chats we had. To all the ladies in the WISE (Women in Science) network, no one mentioned no one forgotten, thank you for the experiences we shared and for having me in the Board. Thanks also to the organizers and members of the Graduate School Student Council, for having me as part of their team.

I am very thankful to my supervisors from my master internship and thesis, Marc Van de Wal, Wouter Aangenent and Rob Hoogendijk, for all they taught me. The one year period that I spent at ASML Research was an intensive learning process, a springboard for the beginning of this PhD. Also part of my graduate school, I thank to my (past) colleagues with which I occasionally keep in touch, Sultan Imangaliyev and Marc Janssens.

For my friends, those people that you can call at any time, thank you for the brilliant moments spent together. In each place where I'm *a local*, be that in Bucharest, at my parents, grandparents or here in the Netherlands, friends have been always there for me. Irina, Ron, Cosmina, Andrei, Iulia, Sebi, Diana, Gix, Mădă, Gabi, Silviu, Turcu, Cristina and all the ones not explicitly mentioned here, thank you for your friendship.

For my family, the voice of reason, where help is unconditional and support is unbounded, there aren't enough words to thank them. Many thanks to my parents, Virgil and Despina, for raising me to who I am today and to my sisters, Elena and Maria, for always being by my side. My grandparents, Angela and Dumitru, thank you for being as parents to me. Dec and Alex, thank you for all the support and good times over the years. Finally, to my partner, Andrei, thank you for making my life so beautiful and meaningful.

*Emilia Silvaş*
*Eindhoven, November 2015*

# CURRICULUM VITAE

Emilia Silvaş was born on September 10$^{th}$, 1986 in Novaci, Romania.

| | |
|---|---|
| 2001-2005 | High School Preda Buzescu, Valcea, Romania. Class of Informatics. |
| 2005-2009 | B.Sc. in Automatic Control and Computer Science at Polytechnic University of Bucharest, Romania. Specialization in Intelligent Systems Control; graduation project on 'A Neuro-Fuzzy Controller for an Inverted Pendulum'. |
| 2009-2011 | M.Sc. in Systems and Control at Eindhoven University of Technology, The Netherlands. Specialization in Control Systems Technology Group. Member of the Educational Committee for this Master Program. |
| 2010-2011 | Internship and Graduation Thesis at ASML Mechatronics Research, Veldhoven, The Netherlands, on 'Decoupling and Modal Control of a 6 Degrees of Freedom Motion System'. |
| 2011-2015 | Ph.D. Candidate in the Control Systems Technology Group at Eindhoven University of Technology, The Netherlands. Collaboration with DAF Trucks N.V.. Member of the University Graduate School Student Council and Board member of the WISE Network. |
| 2012 | 2$^{nd}$ place at Plug-in Hybrid Electric Vehicle Benchmark Competition; building a control algorithm for the Chevrolet Volt. IFAC Workshop on Engine and Powertrain Control Simulation and Modeling, Paris, France. |
| 2015 | Visiting Scholar in the Vehicle Dynamics Lab, Department of Mechanical Engineering, at University of Michigan, Ann Arbor, MI, United States. |

**The Stone Age did not end because we ran out of stones..**
Inspiration - Charles Darwin, *On the Origin of Species*

..we found better solutions.

*Integrated Optimal Design for Hybrid Electric Vehicles*
Thesis by Emilia Silvaş

This thesis explores the *design* of hybrid electric vehicles to reach more energy and cost efficient concepts. Examples of heavy-duty trucks are used to demonstrate the benefits of using new methods for: *synthesizing* hybrid electric architectures; showing the hybridization and engine downsizing potential; electrify auxiliary units (such as steering system, air compressors); and, create *realistic* speed and altitude profiles (driving cycles).

TU/e